Scuola di Ingegneria Industriale e dell'Informazione
Corso di Laurea Magistrale in Ingegneria Fisica

X-ray emission intensity ratios detection for fast chemical characterization

Thesis advisor:
Giacomo Claudio Ghiringhelli
Research supervisor:
Pieter Glatzel

Candidate:
Serena Graziano

Anno Accademico 2020/2021

Abstract

Many advancements have been made in the last 25 years in the field of the inner-shell spectroscopies. These spectroscopies are element and site specific and for this reason they are used to probe the chemical structure of matter. The inner-shell spectroscopies involve an incoming X-ray photon which interacts with a given analyte and creates a core-hole, leaving the system in an excited state. At this point the system can decay emitting a photon. The kind of spectroscopy that records the intensity of these emitted X-ray photons as a function of the emitted energy is called X-ray emission spectroscopy (XES) and is chemically sensitive. In particular K_α (2p $\rightarrow$1s) and K_β (3p$\rightarrow$1s) emission lines have a shape that depends on the analyte's oxidation (+2, +3, +4 and mixed-valence), spin state (high spin/low spin and mixed-spin), local coordination (octahedral, tetrahedral) and ligands. K-emission spectroscopy is useful to study compounds containing 3d transition metals since it is strongly sensitive to the metal 3d states. Both K_α and K_β emission lines are sensitive to the spin state of the transition metal since these lines are shaped respectively by the 2p-3d and 3p-3d exchange interactions, which confer them an indirect sensitivity to the net 3d shell spin. Since the 3p-3d interaction is stronger than the 2p-3d, usually it is preferable to measure the K_β emission lines (and not the K_α ones) for spin-state determination studies. In order to recognize the differences between analytes in different chemical states it is usually recorded the whole X-ray emission spectra of the compound under study.
In this work, it will be studied and analyzed a new method to distinguish between different compounds using X-ray emission spectroscopy (XES). This technique should allow to quickly identify and discern different chemical species because it does not require the acquisition of the full XES spectrum. In particular, it consists in measuring the emitted intensity from a compound at only two specific emission energies and then in computing the ratio of these two values (this quantity will be called intensity ratio). It is then possible to associate to each compound an intensity ratio that, at those given energies, is characteristic to that specific compound. The fundamental idea is to find the two emission energies at which the spectra must be sampled in order to obtain, for different compounds, intensity ratios that are distinguishable. In principle, if the correct two emission energies are considered, it should be possible to recognize in which chemical environment (electronic structure, spin state, oxidation state and local coordination) is a certain analyte just by looking at its intensity ratio.
In particular in this work different iron bearing compounds have been analyzed in order to verify the validity and limits of this method.

Sommario

Negli ultimi 25 anni ci sono stati molti progressi nell'ambito delle spettroscopie di elettroni interni. Queste spettroscopie sono usate per sondare la struttura chimica della materia poichè sono specifiche dell'elemento e del sito. Le spettroscopie di elettroni interni coinvolgono un raggio X che interagisce con un certo analita creando una lacuna, il sistema viene lasciato in uno stato eccitato. A questo punto il sistema può decadere emettendo un fotone. La spettroscopia che analizza l'intensità di questi fotoni emessi in funzione dell'energia è chiamata spettroscopia a emissione di raggi X (XES) ed è sensibile chimicamente. In particolare le linee di emissione K_α (2p $\rightarrow$1s) e K_β (3p$\rightarrow$1s) hanno una forma che dipende dall'ossidazione dell'analita (+2, +3, +4 e valenza mista), dal suo stato di spin (high/ low o spin misto), dalla sua coordinazione locale (ottaedrica,tetraedrica) e dai suoi ligandi. Le linee di emissione K sono utili per studiare composti che contengono metalli di transizione 3d poichè sono molto sensibili agli stati 3d. Sia le linee di emissione K_α che quelle K_β sono sensibili allo stato di spin dei metalli di transizione poichè la loro forma è dovuta rispettivamente all'interazione di scambio tra gli elettroni 2p-3d e 3p-3d, questo permette di avere una sensibilità indiretta allo spin degli elttroni 3d. Dato che l'interazione 3p-3d è più forte di quella 2p-3d, di solito è meglio misurare le linee di emissione K_β (e non quelle K_α) per determinare lo stato di spin. In genere per riconoscere le differenze di un analita in stati chimici diversi è necessario registrare lo spettro completo di emissione del composto in analisi.
In questo lavoro verrà studiato e analizzato un nuovo metodo per distinguere diversi composti usando la spectroscopia di emissione di raggi X (XES). Questo metodo permette di identificare e distinguere diverse specie chimiche molto velocemente perchè non c'è bisogno di acquisire lo spettro di emissione di raggi X (XES) completo. In particolare consiste nel misurare l'intensità emessa da un composto a solamente due energie di emissione e nel ricavare il rapporto tra questi due valori (questa quantità verrà chiamata intensity ratio). E' poi possibile associare a ogni composto un intensity ratio che, a quelle energie, è caratteristico di un certo composto. L'idea fondamentale è quella di trovare due energie di emissione a cui gli spettri possano essere campionati in modo da ottenere, per composti diversi, intensity ratio distinguibili. In teoria, se le due giuste energie di emissione fossero considerate, dovrebbe essere possibile riconoscere in quale ambiente chimico (struttura elettronica, stato di spin, stato di ossidazione e coordinazione locale) è un certo analita solamente guardando il suo intensity ratio.
In particolare in questo lavoro sono stati analizzati diversi composti contenenti ferro in modo da verificare la validità e i limiti di questo metodo.

Contents

Chapter 1

Experimental techniques

This chapter is devoted to explaining how X-rays are produced in synchrotron facilities and the physical principles that are exploited. In particular the focus will be given to the ESRF (European Synchrotron Radiation Facility) that is situated in Grenoble and to the beamline ID26 that is where the experimental data of this thesis were collected.

1.1 Synchrotron radiation

A charged particle that is accelerated always emits an electromagnetic radiation [1], this phenomenon can be understood by considering the conservation of energy principle. In particular a charge travelling along a circular path is always subject to an acceleration perpendicular to its velocity, for this reason it emits an electromagnetic radiation. This radiation is called synchrotron radiation. In order to force the charged particles, that in general are electrons or positrons, to curve and to follow a circular trajectory it is necessary to apply a magnetic field [2].
This kind of radiation presents the following characteristics:

- a broad spectrum (from microwaves to hard X-rays) and so the possibility to select the suitable wavelength for a certain purpose;
- a high flux of photons that allows fast experiments;
- a high brilliance, given by the fact that the photon beam is highly collimated;
- a high stability;
- a pulsed time structure;
- it is polarized.

The first observation of a synchrotron radiation took place in 1947 at the General Electric Research Laboratory in the USA, and it was quickly clear that this kind of radiation was a very intense and extremely versatile source of X-rays [3] and it did not constitute only an unwanted effect, since it is a loss in the radiation, as it was though at first but it could be used for experiments. For this reason in the 60s scientists started developing first generation synchrotron facilities with the aim to study the production of synchrotron radiation from accelerated electrons

in storage rings. This first attempt was not so performing because the output obtained was very limited. In the 80s first generation facilities were upgraded to second generation ones [4] and in the 90s third generation storage rings started to be built; these synchrotron facilities present a brilliance that is approximately 10^{12} times higher than the early lab based sources, a considerable spatial coherence and a very collimated beam. The ESRF, that started being operative in 1994, has been the first facility of this kind ever built in the whole world, nowadays all synchrotron facilities belong to this third generation apart from the ESRF itself that, after a long shutdown of 20 months in 2019/2020, has been converted into an EBS (Extremely Brilliant Source) facility that can reach a coherence and brilliance 100 times higher than the previous generation [5]. In Figure 1.1 it is showed the brilliance that has been achieved in the years for different kinds of synchrotron facilities, in the picture it is given a particular importance to the case of ESRF, that has been the first facility to be of third and then of fourth generation.

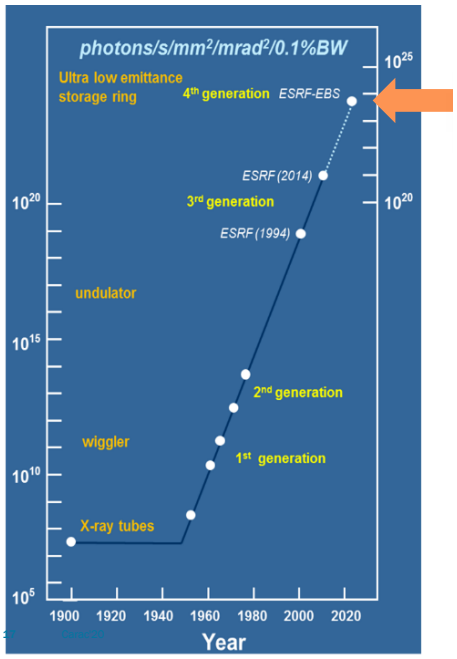

Figure 1.1: Evolution in the years of brilliance in synchrotron facilities [5].

1.2 European Synchrotron Radiation Facility

In this section the main features and components of the ESRF will be explained and the modifications implemented to convert the synchrotron facility from third into fourth generation will be pointed out.
The structure of the synchrotron is depicted in Figure 1.2: there is an electron gun that, every 50 ms, emits electrons packed in bunches, the electrons produced are first accelerated in a linear accelerator called linac (linear accelerator) and then in a circular accelerator called booster ring, that has a circumference of 300 m, until they reach a speed close to the one of light and an energy of 6 GeV. At this point the electrons are ready to be injected, this action happens only few times a day,

in the storage ring, that has a circumference of 844 m, where they are kept in circulation for many hours. The long circular tube in which the electrons circulate is maintained at very low pressure, around 10^{-9} mbar, in order to have Ultra High Vacuum (UHV) and avoid in this way scattering events with gas residual [6]. In this conditions electrons can circulate in the storage ring for an average time up to 60h, time during which they can emit, tangentially to the ring, the synchrotron radiation that will be used in the different beamlines to carry out experiments. Inside

Figure 1.2: Schematic picture of a synchrotron facility [7].

the storage and the booster ring there are several RF (radiofrequency) cavities that are necessary for the proper functioning of the synchrotron. Each cavity contains electromagnetic fields oscillating at a given frequency, that is around 352 MHz for the ESRF storage ring and 3GHz for the booster one [8], these cavities provide the electrons passing through them with enough energy to compensate the energy lost with the emission of the radiation and in this way the electrons are pushed forward along their orbit. It is extremely important to tune all the cavities at the same radiofrequency in order to avoid decelerations and oscillations of the electrons around unstable trajectories. As already said, the electrons are organised into packets called *bunches* whose length is mainly determined by the RF system; the radiofrequency of the cavities determines the filling mode of the storage ring, namely the number of bunches that circulate in the ring at the same time.
It is necessary now to explain in more detail the structure of the storage ring and its main components: the ring is not perfectly circular but it presents 32 straight and 32 curved sections in alternating order, the curved sections contain bending magnets and the straight parts contain focusing magnets and insertion devices. The bending magnets (BM) force the electrons to curve and to follow a circular orbit, due to this deflection the electrons emit a continuous spectrum of x-rays (from microwaves to hard X-rays) tangentially to the orbit of the electrons (see Figure 1.3). The focusing magnets are composed by quadrupole magnets, that are used to focus the beam and to maintain the electrons into a circular trajectory, and by sextupole magnets, that are necessary to correct chromatic aberrations of the beam that are due to the presence of electrons with energy slightly different from the desired energy (6 GeV). The insertion devices (ID) are magnetic structures composed by a complex

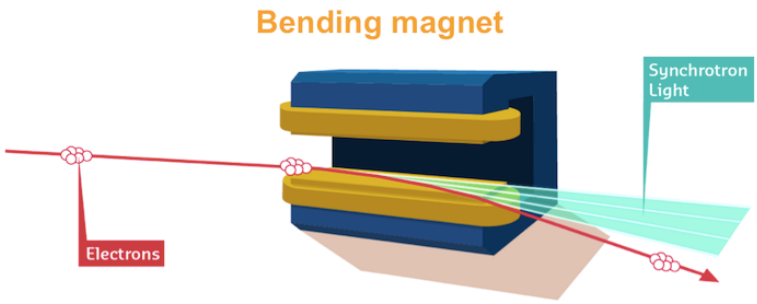

Figure 1.3: Synchrotron radiation emitted from a bunch of electrons passing through a bending magnet [6].

array of small magnets with alternating polarization which force the electrons, that feel a sinusoidally varying magnetic field B, to follow a wavy trajectory in the horizontal plane in addition to their forward motion (see Figure 1.4); at each bend a radiation is emitted and it can interfere with the radiations emitted from other consequent bends, giving as a result a very focused radiation. Within this class of devices it is possible to distinguish two objects with similar structure but different properties: undulators and wigglers. What differentiates these two devices is the deflection parameter K: a *wiggler* has $K >> 1$, it has a big oscillation amplitude (a large deviation angle) and for this reason the radiation emitted from each bend does not interfere much with other radiations but it is summed incoherently generating a broad spectrum similar to that of the bending magnets, while an *undulator* has $K \leq 1$, it has a small oscillation amplitude (a small deviation angle) and so the radiation emitted at each bend will interfere coherently with the other emitted radiations and an ultra-bright, or very focused, and quasi-monochromatic light is obtained. This radiation is more focused than that coming from a bending magnet and the photons emitted in this way are concentrated at certain energies, by changing the gap between the magnetic poles it is possible to tune the wavelength of the emitted X-rays and so the respective energy.

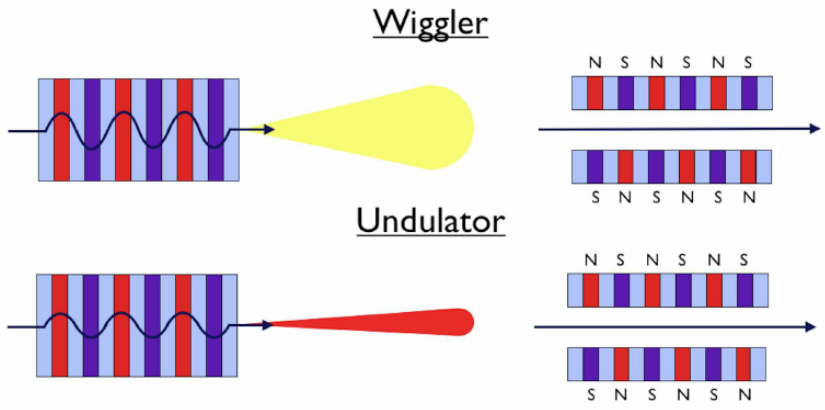

Figure 1.4: **Left**: top view of the radiation from a wiggler (top) and from an undulator (bottom). **Right**: side view of the radiation from a wiggler (top) and from an undulator (bottom) [9].

The beamlines that use the radiation emitted by Bending Magnets to carry out experiments are denominated with the acronym BM while the ones that use the radiation from Insertion Devices are called ID.

This is the general description of a synchrotron and specifically of the ESRF. As already depicted before, this facility has recently been upgraded and it can currently be considered as an extremely brilliant source (EBS) facility, the main difference is given by the presence of a more complex magnetic lattice in the storage ring (see Figure 1.5), there is an increase of the number of bending and focusing magnets. This modification allows a reduction of the horizontal emittance, or spread of the electron beam, by a factor of 30; this new design is able to guide and focus the electrons in order to produce an X-ray beam 100 times more brilliant and coherent than before.

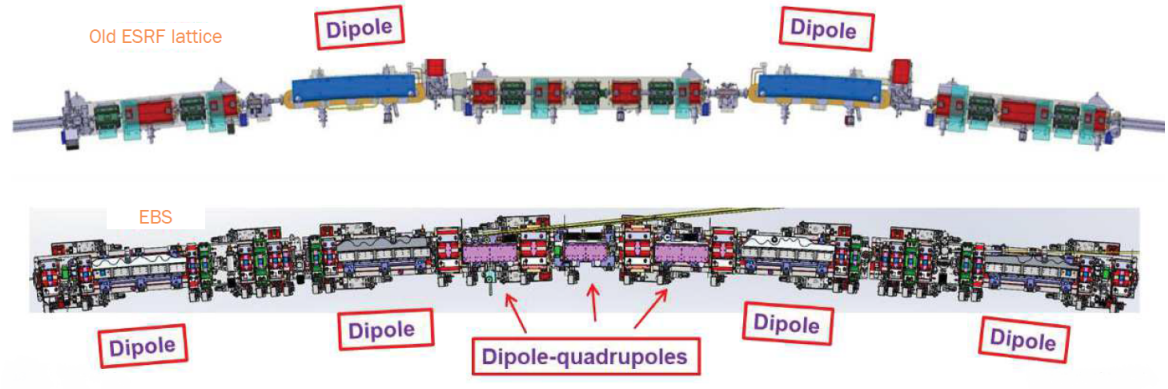

Figure 1.5: Comparison between the magnetic lattice in the case of third (top) and fourth (bottom) generation ESRF [5].

1.3 ID26 beamline

1.3.1 Beamline layout

ID26 is an insertion device beamline (see Figure 1.6 for the detailed structure), it has a 5 m long straight section where three undulators are present, two have a length of the period of the alternating magnetic fields of 35 mm, i.e. there are 46 periods, while the third undulator has magnets that can be rotated in order to change the period length between 35 mm and 27 mm. Using this configuration of insertion devises it is possible to obtain a X-ray beam with energy from 2.4 keV, when the fundamental harmonic is used, up to 30 keV if the fifth harmonic is exploited; moreover this beam presents a very high photon flux and brilliance that allow measurements in very diluted samples. After the undulators there is a set of vertical slits, used to reduce the power of the white beam that thereafter reaches the Horizontal Defecting Mirror (HDM1). The HDM1 is a water-cooled flat silicon mirror used to deflect away from the storage ring the white beam coming from the undulators in order to protect all the following optical components from the heat load. After the HDM1 there is again a set of horizontal slits and then the beam

passes through a monochromator that selects the required wavelength and energy, that can be calculated using the Bragg's law, in order to obtain a monochromatic beam; in particular a cryogenically cooled monochromator with two reflecting Si crystals (Si[311] with reflection range from 4.37 keV to 43.4 keV and Si[111] from 2.28 keV to 22.69 keV) is used. The beam is then focused independently on the horizontal and vertical direction thanks to two mirrors (HFM2, VFM3) that are in a Kirkpatrick-Baez configuration. These two mirrors work in total reflection and reject specific harmonics depending on their coating, that can be made of Pt, Si or Pd. The spot size that is typically achieved after the focusing process is of 500 µm (horizontally) × 100 µm (vertically). In general it is possible to monitor the incoming flux of photons by measuring the scattering of some kapton or plastic foils (I00, I01, I02) that can be inserted on the path. Instead, to calibrate the energy it is possible to substitute these foils with metallic ones and measure their absorption. Finally there are a fast shutter, Al attenuators and other slits in order to regulate the incoming power on the sample. There are two experimental hutches that are indicated in Figure 1.6 as EH1 and EH2, the most used is the second one because it contains the X-ray emission spectrometer that can be exploited to study different kinds of spectroscopy.

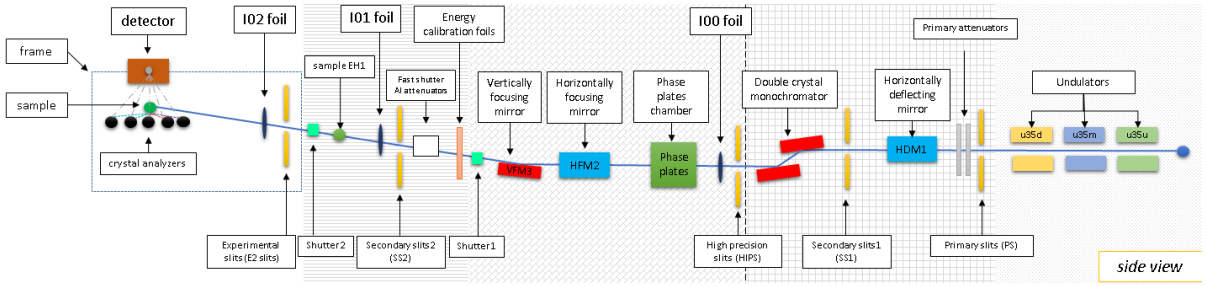

Figure 1.6: Scheme of beamline ID26 [10].

1.3.2 X-ray emission spectrometer

The spectrometer that is present at ID26 is a multi-crystal Johann-type spectrometer for X-ray emission spectroscopy [11]. In X-ray emission spectroscopy (XES) the X-rays that are emitted from the sample, whose atoms have previously undergone a core hole creation event, are detected. The energy of the emitted X-rays is around a fluorescence line or an absorption edge. An instrument for XES allows high energy resolution X-ray fluorescence spectroscopy (e.g. K_β spectroscopy), resonant X-ray emission spectroscopy (RXES), resonant inelastic X-ray scattering (RIXS) and high energy resolution fluorescence detected (HERFD) X-ray absorption spectroscopy [12], [13].
If the hard X-ray regime is considered, as it happens at ID26, in order to analyze the emitted X-rays, instruments based on perfect crystal Bragg optics are generally used. Common geometries are Rowland or von Hámos, where the basic physical principle used is X-ray diffraction. In particular the spectrometer that is mounted at the beamline is based on the concept of Rowland circle, that is a point-to-point focusing geometry, where the idea is that of maintaining on a circle the three components: the sample, the detector and the crystal (see Figure 1.7). The sample is placed

in a point of the circle that for convention is identified as the origin of the system $(0, 0, 0)$, in this point the incoming X-ray beam impinges on the sample. This point is kept always fixed and it is a reference for the other components which instead can move on the circumference of the Rowland circle. The X-rays, that are emitted from the sample, reach the crystal analyzer and they are diffracted, for simplicity the crystal is kept exactly in front of the sample at $(x, 0, 0)$; the angle that is formed between the emitted rays and the central plane of the crystal and then between the diffracted rays and again the central plane is called Bragg angle (θ_B) and is directly connected with the emitted energy. The crystal analyzer has a spherical shape with

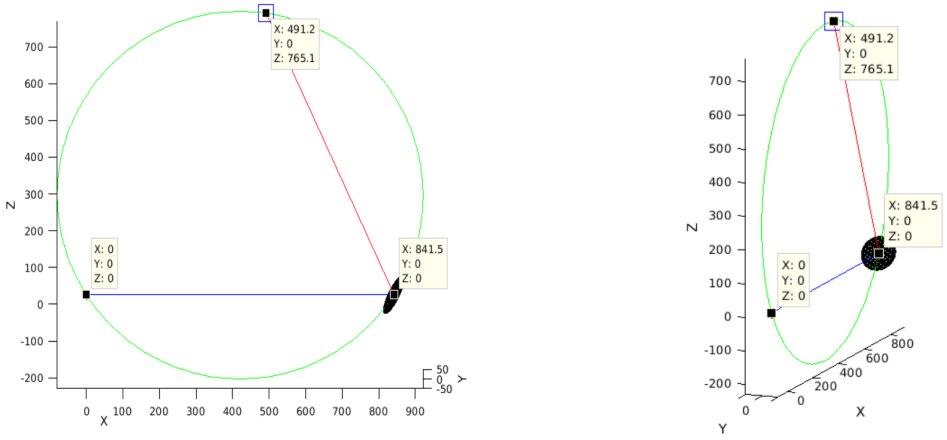

Figure 1.7: Rowland circle with one crystal analyzer and Bragg angle $\theta_B = 57.3°$; at position $(0, 0, 0)$ there is the sample, at $(x, 0, 0)$ the crystal analyzer and at $(x, 0, z)$ the detector. These images are computed using a ray tracing MATLAB program. **Left**: Lateral view of the Rowland circle. **Right**: tilted view of the Rowland circle.

Johann geometry (see Figure 1.8), which is achieved by bending the crystal to a radius $R_P = 2R$ where R is the radius of the Rowland circle and thanks to this the crystal planes will be parallel to the circle itself. The problem of this configuration is that only the central point of the crystal is in contact with the Rowland circle and so there are some aberrations that however can be neglected if the crystal surface is not too large.

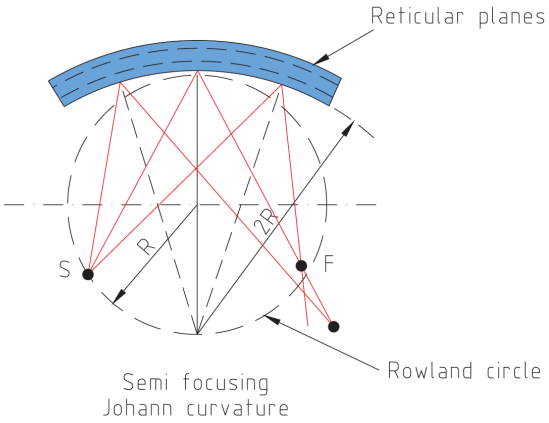

Figure 1.8: Johann geometry [14]

In practice one must choose the element to analyze and then the fluorescence line (emission energy) to be measured, and from the fluorescence line it is possible to calculate the Bragg angle. Indeed it happens that when changing the fluorescence line the Rowland circle rotates around the sample and so the Bragg angle, the crystal's and detector's position will change accordingly (see Figure 1.9). The important characteristic of this configuration is that the Bragg angle is the same from any point on the circle. The fundamental law that is valid and allows to connect

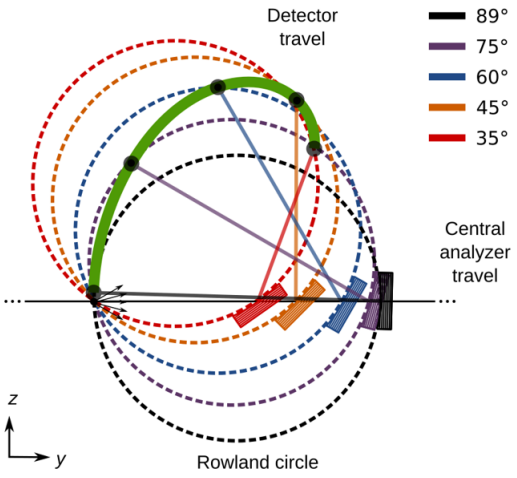

Figure 1.9: Rotation of the Rowland circle and travel of the detector based on the changing of the emission energy [11].

the Bragg angle to the emission energy is the Bragg's law

$$n\lambda = 2dsin\theta_B.$$

In this equation n is an integer number, λ is the wavelength of the emitted X-ray that is inversely proportional to the emitted energy ($\lambda = hc/E$ where $c = c_0$, with c_0 speed of light because the X-rays are waves, and h is the Planck constant). Moreover d is the lattice spacing:

$$d = \frac{a}{\sqrt{h^2 + k^2 + l^2}}$$

where a is the lattice parameter and h, k, l are the Miller indices. In the end there is θ_B that is the Bragg angle that depends on the fluorescence line and on the atomic number of the atoms and on the specific electronic transition that is being considered. In particular the Bragg angle is directly connected to the emission energy by the formula:

$$\theta_B = arcsin\left(\frac{hc}{2dE}\right)$$

thanks to this expression the exact angle at which there is diffraction for a certain emission energy can be retrieved.
It is useful to use more than one crystal analyzer in order to cover a larger solid angle [11] and in particular the spectrometer at ID26 has 5 crystal analyzers (see Figure 1.10) that can be moved independently by tilting their surface or moving them closer to the source. The central crystal is exactly in front of the sample and

the others are shifted with respect to the origin along the y axis by the quantities in mm $(-240, -120, 0, 120, 240)$. For each crystal there is a different Rowland circle that always intersects with the others at the source position and, only if all crystals have the same Bragg angle, at the detector position. It is important to stress the fact that any ray diffracted from the 5 crystals will arrive in a certain point in which $y = 0$ so of coordinates $(x, 0, z)$.

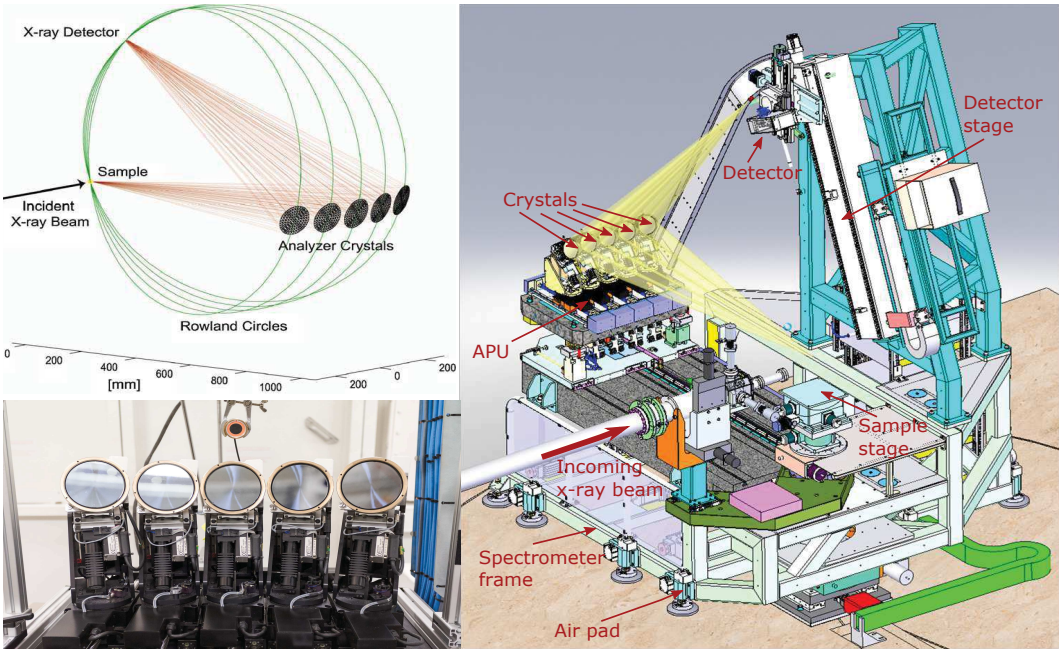

Figure 1.10: **Left**: (top) ray tracing sketch of a 5 crystals Rowland geometry and (bottom) the Bragg crystals mounted at ID26. **Right**: scheme of the high resolution X-rays emission spectrometer present at the beamline ID26 [15].

1.3.3 Detector

A fundamental component of the spectrometer is the detector, different kinds of detectors can be used depending on the experiment that must be done.

Avalanche Photodiode (APD)

At ID26 the detector that is mainly mounted is a Silicon Avalanche Photodiode (APD), that is a single element detector [11]. It is a highly sensitive semiconductor photodiode that exploits the photoelectric effect to convert light into electricity. The most important characteristics of such detector is first of all the fact that it has a fast response, roughly of 10 ns, so it is very linear up to very high count rates (around 10 MHz) because the dead time, that is the time that is necessary to wait in order to have a ready detector after the arrival of a photon, is very short since it responds so fast, and secondly it is a device that is very easy to use because it is a complete hard-software system [16].

Maxipix

For the experiment that has been performed in this thesis a detector called Maxipix was used. The Maxipix is a fast readout (with a readout dead time of less than 300 microseconds), photon-counting pixel detector, it has been developed by ESRF and it is based on the Medipix2 [17], that is a readout chip developed by CERN. This device is a fast noise-free X-ray area detector with high spatial and temporal resolution, it is formed by 256 x 256 pixels where each pixel has size of 55µm x 55µm (see Figure 1.11).

Figure 1.11: The maxipix is a fast read-out, photon-counting detector.

Chapter 2

The case study

The aim of this study is to find a fast way to distinguish between compounds containing the same analyte in different chemical states. In order to do this it is employed the X-ray spectroscopy and in particular the non-resonant X-ray emission spectroscopy that is a technique that has a high chemical sensitivity.

2.1 X-ray emission spectroscopy (XES)

In X-ray emission spectroscopy a core electron is removed by exciting the system with the proper energy and then an electron from an outer shell immediately ($\tau \approx 10^{-15}s$ [18]) fills the core-hole, at this point an electron (Auger emission) or a X-ray photon (X-ray fluorescence emission) is emitted. This work will deal in particular with the X-ray fluorescence emission. Depending now on the core-hole that is created it is possible to have different fluorescence lines: if the core-hole is in 1s they are called K-fluorescence lines while if the core-hole is in 2s or 2p they are called L-fluorescence lines. The focus will be given to K-fluorescence lines because the yield, that represents the probability of a core-hole to be filled by a radiative process (in competition with non-radiative processes as Auger), is higher than the case of L-fluorescence lines [19]. There are many K-emission lines depending on the shell from which the electron decays to fill the 1s core-hole. In Figure 2.1 all the possible K-emission lines with their relative spectral shape are shown.
The K_α lines are the most intense and they arise from the transitions $2p \rightarrow 1s$. The spin orbit interaction, that is the interaction of the electron spin with its own orbital moment, splits the 2p level in two levels ($2p_{3/2}$ and $2p_{1/2}$), separated by 10 eV, and for this reason there are two fluorescence lines: K_{α_1} (from $2p_{3/2} \rightarrow 1s$) and K_{α_2} (from $2p_{1/2} \rightarrow 1s$). The exchange interaction, that is the electron-electron interaction due to wavefunctions exchange symmetry, between the 2p electrons and the valence (3d) electrons is the reason why the spectra are sensitive to the valence shell. It happens that in K_α lines the predominant interaction is the spin orbit interaction; the exchange interaction is not enough to resolve splittings in the single K_{α_1} and K_{α_2}. Moreover, the spin-polarized nature is hidden within the single peaks, leading to a slight asymmetry [20, 21, 22].
The K_β main lines, also called core to core (CTC) K_β lines, arise from the transitions $3p \rightarrow 1s$ and are approximately 8 times weaker than the K_α lines. The spin orbit interaction splits the 3p level in two but only by less than 1 eV and so no K_{β_1} and K_{β_3} splitting is observed [23]. As in K_α lines the exchange interaction between

the 3p electrons and the valence (3d) electrons is the reason why the spectra are sensitive to the valence shell. In K_β lines the predominant term is the exchange interaction. In particular there are two mechanisms that influence the spectral shape of the K_β lines: the screening of the core-hole potential and the exchange interaction between 3p and 3d electrons. The K_β spectrum is composed by a main peak $K_{\beta_{1,3}}$ and a shoulder $K_{\beta'}$ that has a complete spin-polarized origin [24].
The K_β satellites arise from the transitions of the valence states into 1s and for this reason they are called valence to core (VTC) K_β lines, they are approximately 500 times weaker than the K_β lines.
It is important to notice that the K_β lines are more sensitive than the K_α lines to the spin state of the compound because of the strong interaction between 3p and 3d electrons (while the interaction between 2p and 3d electrons is weaker) [25]. On the other hand the K_α lines have a higher intensity with respect to the K_β and so it is possible to extract more or less the same amount of information from both lines.

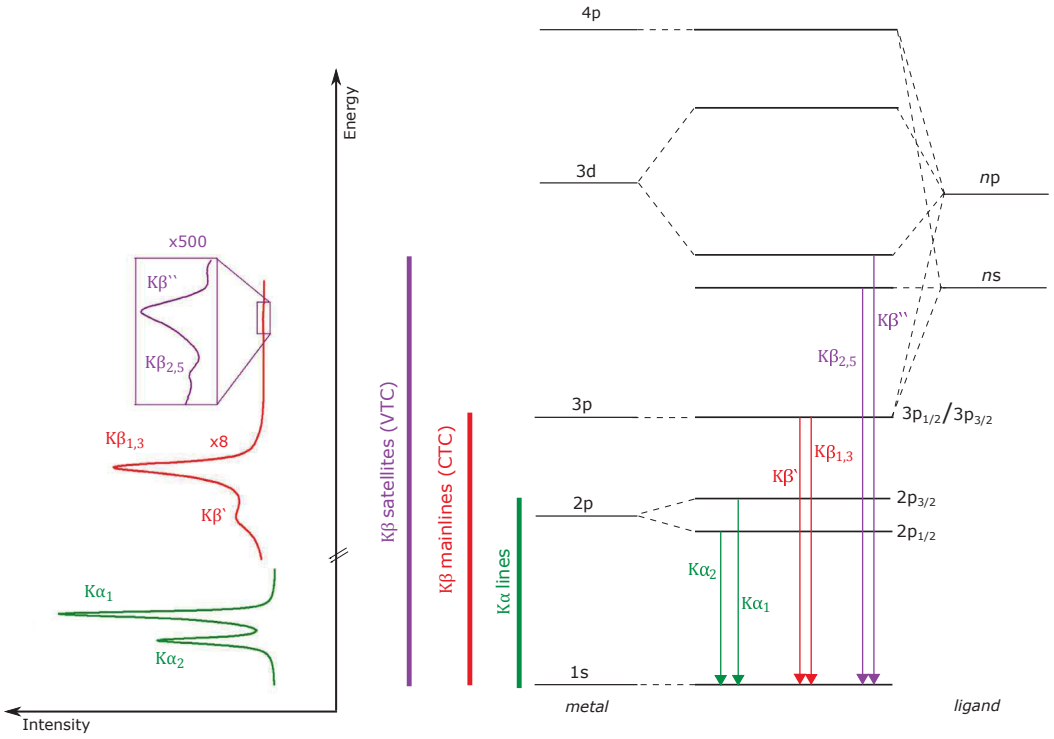

Figure 2.1: **Left**: Spectral shape of the different K-fluorescence lines. **Right**: One electron picture of the different K-emission lines [26].

2.2 Two energies X-ray emission spectroscopy

In general, in order to quantify the spectral differences between dissimilar compounds, it is necessary to measure the full K_α or K_β emission spectra and then compare and analyze the differences. Another way to identify the chemical state of a compound and to detect chemical shifts in the spectra has been studied in this thesis.
The method that is proposed in the following pages is an innovative way to identify and distinguish different chemical species in a very fast way, it consists in measuring the emitted intensity from a compound at only two specific emission energies, without recording the whole spectrum, and then in computing the ratio of these two values (this quantity will be called intensity ratio). In this way it is possible to simplify some quantities thanks to the division of the two intensities; in particular the ratio will be independent on the incoming photon flux, the absorber concentration and any absorption effect in and around the sample. Furthermore, the signal will be quasi background free for point-to-point focusing spectrometers. Obviously, the information content is lower than in a full XAS or XES spectrum but likely sufficient for many purposes. The spectra are sensitive to any change of the spin state and of the chemical environment around the analyte ion, even though these spectral changes might be very small.
In particular the K_α and K_β emission lines can be analyzed because no monochromatic incident beam is required to record the non-resonant emission lines (this approach can use any X-ray source including the free electron lasers).

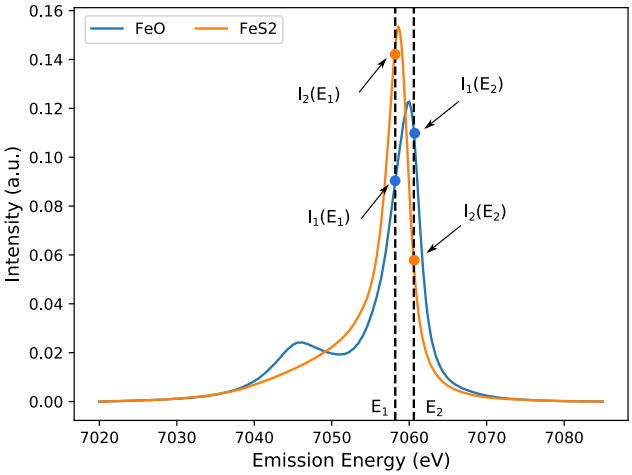

Figure 2.2: K_β emissions lines (the intensity is normalized to the area below the curve) of the iron bearing compounds FeO and FeS_2. The dashed lines indicate the two energies at which the spectra should be sampled in order to compute the intensity ratio of each compound.

In order to better understand this technique, it is possible to look at the example in Figure 2.2 where the K_β spectra of two iron bearing compounds are plotted. As can be seen from the graph, the two spectra are different since iron is in two different chemical environments. In particular iron in FeO is in a high spin state (this can

be recognized by the presence of the $K_{\beta'}$ shoulder) while iron in FeS_2 is in a low spin configuration. The method proposed in this work attempts to distinguish the presence of an analyte (in our case iron) in different chemical environments just by sampling the spectra at two energies (E_1 and E_2 in Figure). At this point it is possible to associate to each compound an intensity ratio that, at those given energies, is characteristic to that specific compound; in particular for the example in Figure the two intensity ratios are given by the following formulas:

$$ratio_{FeO} = \frac{I_1(E_2)}{I_1(E_1)}$$

$$ratio_{FeS_2} = \frac{I_2(E_2)}{I_2(E_1)}$$

As can be seen, the ratio depends on the energies at which the spectra are sampled. In order to maximize the contrast between the intensity ratios

$$contrast = ratio_{FeO} - ratio_{FeS_2}$$

and thus be able to recognize the presence of the analyte in different chemical environments, it is necessary to sample the spectra at the right emission energies.
It is fundamental now to find the two emission energies (E_1, E_2) at which the spectrometer should be tuned in order to obtain intensity ratios that have a high enough contrast and that allow to clearly recognize in which chemical environment (electronic structure, spin state, oxidation state and local coordination) is a certain analyte.
The crystal analyzers of the multi-analyzer XES spectrometer (see 1.3.2) are tuned to two different emission energies (two crystals to an energy and the other three to the other one); the rays diffracted by the crystals will impinge on the detector in a certain position depending on the emission energy at which the crystals are tuned, the fact that they are tuned at two different energies will give two spots on the surface of the detector and from these spots the intensities corresponding to those emission energies are recorded.

2.2.1 Code implementation

So for the purpose of finding the two emission energies (at which the spectra will be sampled), that allow to discriminate between different chemical environments of an analyte, a Python code was implemented. In order to test the code the data that had been recorded in 2016 at the beamline by Sara Lafuerza[1] were used. The data files report the measured K_α and K_β spectra of different Fe compounds and these data consist in two vectors where the first one contains the values of the emission energies and the second one the corresponding intensities (see Figure 2.3 for the K_β emission spectrum of FeO where the intensity is normalized to the area below the curve). The first important step, that must be done before proceeding with the analysis, is to verify that the energy range of all spectra under consideration is the same. This ensures that the intensity vectors of different spectra have the same dimension and are associated to the same energies. Each intensity vector contains

[1]Sara Lafuerza is a former scientist at ID26

n elements (each element of the vector will be called I_j with $j = 1, 2, ..., n$). At this point it is possible to get rid of the energy axis and consider just the associated intensity vectors.

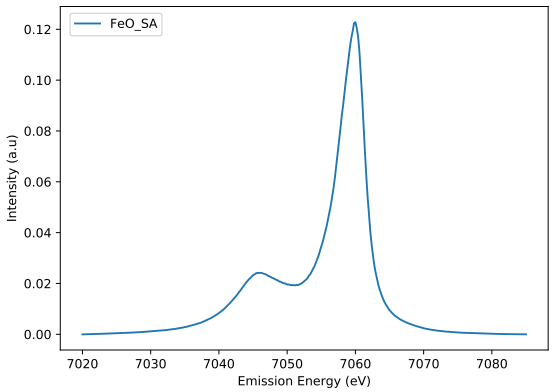

Figure 2.3: K_β emission line of FeO, in this case the plotted intensity is normalized to the area below the curve.

It is possible now to generate (for each spectrum) a matrix such that the elements of the first row are given by the division of the first intensity value I_1 by all other intensity points I_1, I_2, ..., I_n, the second row contains the division of the second intensity value I_2 by all the others I_1, I_2, ..., I_n and so on until the last row that contains the division of the last intensity value I_n by all the others I_1, I_2, ..., I_n. In the end the matrix associated to a certain spectrum is composed by all possible ratios between different intensity values. This is the matrix that represents the quantity of interest in such case:

$$RATIO = \begin{pmatrix} \frac{I_1}{I_1} & \frac{I_1}{I_2} & \dots & \frac{I_1}{I_n} \\ \frac{I_2}{I_1} & \frac{I_2}{I_2} & \dots & \frac{I_2}{I_n} \\ \vdots & \vdots & \ddots & \vdots \\ \frac{I_n}{I_1} & \frac{I_n}{I_2} & \dots & \frac{I_n}{I_n} \end{pmatrix}$$

It will be calculated now for each element of the RATIO matrix an error using the usual error propagation formula since in this kind of measurements the noise has a Poisson statistics:

$$e_f = \sqrt{\left(\frac{\partial f}{\partial x}\right)^2 e_x^2 + \left(\frac{\partial f}{\partial y}\right)^2 e_y^2 + \left(\frac{\partial f}{\partial z}\right)^2 e_z^2 + ...}$$

In this case f represents each element of the RATIO matrix , x, y, z the variables and e_x, e_y, e_z their errors.
For instance if the following element $f = I_2/I_1$ of the RATIO matrix is considered, the error associated can be calculated as follows:

$$e_{I_2/I_1} = \sqrt{\left(\frac{1}{I_1}\right)^2 I_2 + \left(\frac{I_2}{I_1^2}\right)^2 I_1}$$

where the variables are $x = I_2$ and $y = I_1$ while their errors are $e_{I_2} = \sqrt{I_2}$, $e_{I_1} = \sqrt{I_1}$, that are the square root of the absolute number of counts.
By computing for each element of the RATIO matrix the error, it is possible to obtain the associated NOISE matrix. The signal to noise matrix is simply given by the elementwise division between the absolute value of the RATIO matrix and the corresponding NOISE matrix which elements are calculated thanks to the previous formula.

2.2.2 Two compounds

In order to find the two energies at which different compounds have distinguishable intensity ratio it is necessary first to start studying what happens when two compounds are compared (in Figure 2.4 it is plotted the K_β spectrum of FeO compared to the spectrum of FeS_2.). At this point, it is necessary to associate to each com-

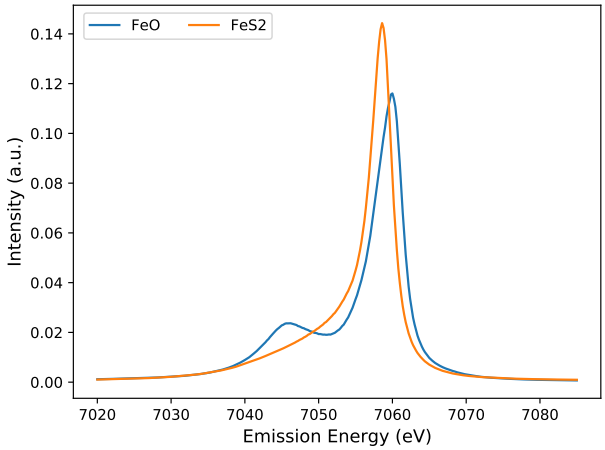

Figure 2.4: K_β emission spectra of FeO (iron is in high spin state) and FeS_2 (iron is in low spin state) with intensity normalized to the area of their respective curves.

pound a RATIO matrix computed as shown before: so called RATIO1 for the first compound and RATIO2 for the second one. In this case the relevant quantity that must be studied is the difference between the RATIO matrices of the two compounds because in this matrix all the possible intensity ratio contrasts (see 2.2) of the two compounds are present:

$$DELTA = RATIO1 - RATIO2$$

$$DELTA = \begin{pmatrix} \frac{I'_1}{I'_1} & \frac{I'_1}{I'_2} & \cdots & \frac{I'_1}{I'_n} \\ \frac{I'_2}{I'_1} & \frac{I'_2}{I'_2} & \cdots & \frac{I'_2}{I'_n} \\ \vdots & \vdots & \ddots & \vdots \\ \frac{I'_n}{I'_1} & \frac{I'_n}{I'_2} & \cdots & \frac{I'_n}{I'_n} \end{pmatrix} - \begin{pmatrix} \frac{I''_1}{I''_1} & \frac{I''_1}{I''_2} & \cdots & \frac{I''_1}{I''_n} \\ \frac{I''_2}{I''_1} & \frac{I''_2}{I''_2} & \cdots & \frac{I''_2}{I''_n} \\ \vdots & \vdots & \ddots & \vdots \\ \frac{I''_n}{I''_1} & \frac{I''_n}{I''_2} & \cdots & \frac{I''_n}{I''_n} \end{pmatrix} = \begin{pmatrix} \frac{I'_1}{I'_1} - \frac{I''_1}{I''_1} & \frac{I'_1}{I'_2} - \frac{I''_1}{I''_2} & \cdots & \frac{I'_1}{I'_n} - \frac{I''_1}{I''_n} \\ \frac{I'_2}{I'_1} - \frac{I''_2}{I''_1} & \frac{I'_2}{I'_2} - \frac{I''_2}{I''_2} & \cdots & \frac{I'_2}{I'_n} - \frac{I''_2}{I''_n} \\ \vdots & \vdots & \ddots & \vdots \\ \frac{I'_n}{I'_1} - \frac{I''_n}{I''_1} & \frac{I'_n}{I'_2} - \frac{I''_n}{I''_2} & \cdots & \frac{I'_n}{I'_n} - \frac{I''_n}{I''_n} \end{pmatrix}$$

where I'_1, I'_2, ...,I'_n are the intensities of the first compound while I''_1, I''_2, ...,I''_n are

the intensities of the second compound. Ideally, in order to recognize the different chemical environments of iron, it is necessary to find, in the DELTA matrix, where the contrast between intensity ratios is maximized. In any case it is not sufficient to just analyze the DELTA matrix since an associated noise matrix must be taken into account. The noise matrix is again calculated with the error propagation formula previously explained but in this case the signal is the difference between the RATIO matrices. The error associated to each element of this DELTA matrix is the sum of the errors associated to each element of the matrices RATIO1 and RATIO2; for example for one element of the signal matrix $f = I'_2/I'_1 - I''_2/I''_1$:

$$e_{I'_2/I'_1 - I''_2/I''_1} = \sqrt{\left(\frac{1}{I'_1}\right)^2 I'_2 + \left(\frac{I'_2}{I'^2_1}\right)^2 I'_1 + \left(\frac{1}{I''_1}\right)^2 I''_2 + \left(\frac{I''_2}{I''^2_1}\right)^2 I''_1}$$

By computing the error for each element of the DELTA matrix it is possible to obtain the associated noise matrix. The signal to noise matrix is obtained dividing elementwise the absolute value of the DELTA matrix by the associated NOISE matrix. At this point it is possible to select in this last signal to noise matrix where the contrast is larger (i.e. the maximum element of the matrix) and from the indices of this element retrieve the corresponding emission energies at which it is better to set the spectrometer. The signal to noise matrix is symmetric and so it is possible to select half of it without losing information, the terms that are zero are put equal to Nan (Not a number) and a contour plot, that has on both axes the emission energy is plotted like in Figure 2.5. This Figure shows the signal to noise relative to all possible emission energy pairs for the specific case of a high spin and low spin compound; there is a color bar that indicates the magnitude of the signal to noise, in particular the yellow denotes the largest signal to noise and so the largest contrast between intensity ratios. An important consideration is that the signal to

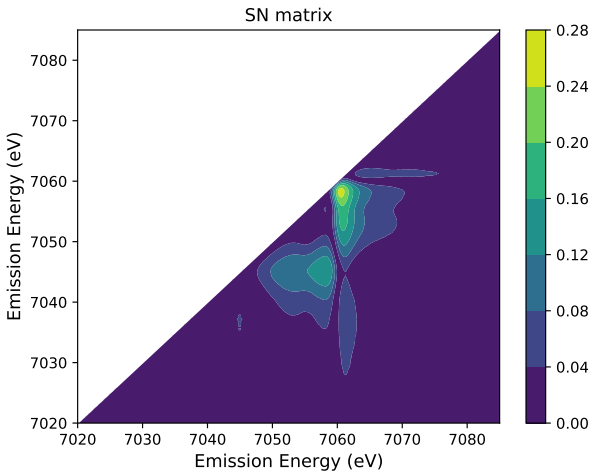

Figure 2.5: Countour plot of the signal to noise matrix given by the combination of K_β emission spectra of FeO (high spin) and FeS_2 (low spin).

noise matrix, that has been calculated and plotted, could give the incorrect signal to noise value because in a real measurement some combinations of energy will give points on the detector that are too close and so partially superimposed, due to the fact that each ray arriving on the detector has a certain spot size ($\sim 2mm$). If

the crystals are tuned at two Bragg angles (see 1.3.2), that correspond to two energies that are too close, the two foci on the detector will be indistinguishable. In particular, by using the Bragg's law, it is possible to calculate the arrival position on the detector of two different emission energies and retrieve the minimum energy separation between two emission energies required to have a distance between their positions on the detector equal to 2mm.
It turns out that for K_α with crystal analyzers such as Ge[440] the energies must be separated at least by 2 eV and for K_β with Ge[620] by 1.4 eV. After calculating this separation parameter, a new signal to noise matrix must be created; it is still a triangular matrix but it has the main and other subdiagonals equal to zero because, depending on the separation parameter, some energy combinations have to be deleted because they involve two energies that are too close (see Figure 2.6 **Left**). Indeed, each element of the main diagonal is given by two energies that have the same value and the first subdiagonals have elements given by the combination of very close energies; by putting these elements equal to zero, these combinations, that would not be measurable because they do not give different foci on the detector, will not be considered.

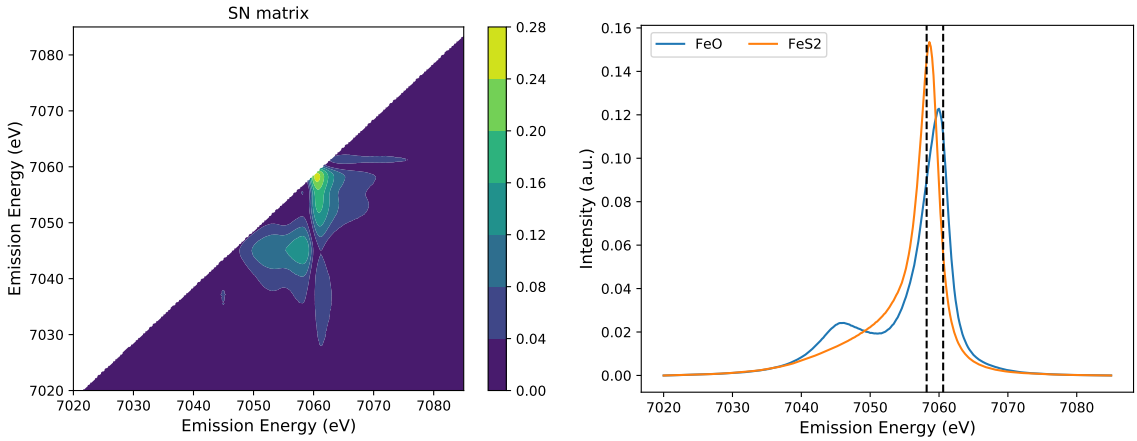

Figure 2.6: **Left**: Countour plot of the signal to noise matrix given by the combination of K_β emission spectra of FeO (high spin) and FeS2 (low spin). In this plot the signal to noise matrix has the main diagonal and some sub diagonals removed in order to take into account only energy combinations that give distinguishable spots on the detector. **Right**: K_β emission spectra of FeO (high spin) and FeS_2 (low spin) with two lines that identify the best two energies that give the maximum signal to noise (i.e. maximum contrast).

At this point it is possible to identify in this last correct matrix where the maximum signal to noise is present and, by retrieving the indices of its position, find at which energies it is associated. To have a visual idea of which energies give the higher signal to noise, that corresponds to the situation with better contrast between the two compounds, two lines at the right energies and intersecting the spectra can be plotted like in Figure 2.6 **Right**.

If two emission lines are too similar (that means that the spectral differences are very small), the contrast between the intensity ratios will be again very small. It is possible to obtain a high enough signal to noise (where the signal is the contrast between intensity ratios and the noise is the error associated to this contrast and

depends inversely on the square root of the total counts) by reducing the error on the contrast, to do this it is necessary to count for a longer time.
If instead two compounds have quite different emission lines (as the case in Figure 2.6 **Right**), the signal to noise will be very high even with very low counts.

2.2.3 More compounds

It is possible now to consider how to deal with more than two compounds and how to identify the two emission energies that should allow to distinguish between as many chemical environments of a certain analyte as possible. In this situation it is necessary to retrieve for each pair of different compounds their signal to noise matrix and then sum up all these matrices in one total signal to noise matrix, where it is possible to identify the maximum. The identification of this element allows to find which are the two emission energies that should give the maximum contrast for as many considered compounds as possible.
For example if there are three compounds it is firstly necessary to calculate for each one, starting from their measured spectra, the RATIO matrix already seen above, getting the three matrices RATIO1, RATIO2 and RATIO3. The following step is to consider all possible combinations between the three compounds and generate three signal to noise matrices (SN1, SN2 and SN3) where the signal is given by RATIO1-RATIO2, RATIO1-RATIO3 and RATIO2-RATIO3 and the noise is calculated with the error propagation formula. In the end the three signal to noise matrices (SN1, SN2 and SN3) are summed up and the highest value inside this last matrix (SUM MATRIX) identifies the two emission energies that give the best compromise to obtain three distinguishable intensity ratios for the three different compounds (see Figure 2.7 for an example of the three SNs matrices and the SUM MATRIX). Surely this method works when two compounds are compared but when more compounds are considered a problem arises: the two emission energies found are the ones that correspond to the peak value in the SUM MATRIX but not necessary to a peak in all the single matrices SNs. If this happens it will not be possible to distinguish between the compounds relative to that SN matrix but only between the compounds which SN matrix gave a quite high signal to noise (high contrast between intensity ratios) at those two energies.
Further studies could be done to find a better way to select the best energy compromise when more than two compounds are compared.

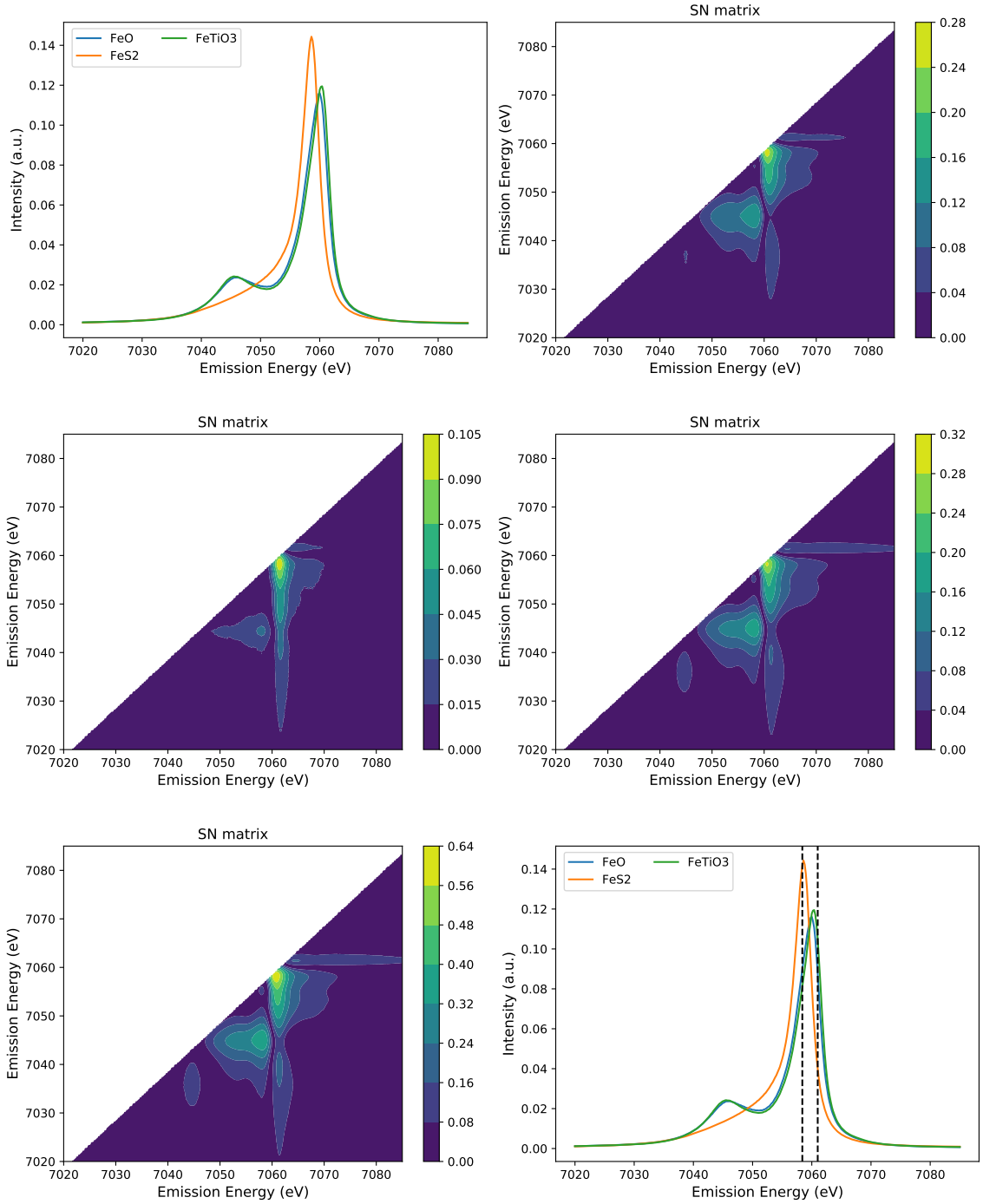

Figure 2.7: **Top Left**: K_β normalized emission spectra of FeO (high spin), FeS_2 (low spin) and $FeTiO_3$ (high spin). **Top Right**: Contour plot of the signal to noise matrix (SN1) given by the combination of K_β emission spectra of FeO and FeS_2. **Middle Left**: Contour plot of the signal to noise matrix (SN2) given by the combination of K_β emission spectra of FeO and $FeTiO_3$. **Middle Right**: Contour plot of the signal to noise matrix (SN3) given by the combination of K_β emission spectra of FeS_2 and $FeTiO_3$. **Bottom Left**: Contour plot of the total signal to noise matrix (SUM MATRIX) given by the sum of the single signal to noise matrices. **Bottom Right**: K_β emission spectra of FeO (high spin), FeS_2 (low spin) and $FeTiO_3$ (high spin) with two lines that identify the best two energies that give the maximum signal to noise in the SUM MATRIX.

Chapter 3

Experimental Results and Data Analysis

3.1 Samples

The K_α and K_β lines of many iron bearing minerals have been analyzed and compared. In particular the compounds that have been studied are embedded inside a circular block of resin (see Figure 3.1) with a diameter of 25mm, this whole sample is called Astimex mineral standard[1] and contains 53 between natural minerals and synthetic compounds (see Table 3.1). Between all these minerals there are 18 that contain iron, some of them in very scarse quantity or with just traces of it, they are highlighted in light blue in Figure 3.1 (**Right**) and indicated with an asterisk in Table 3.1.

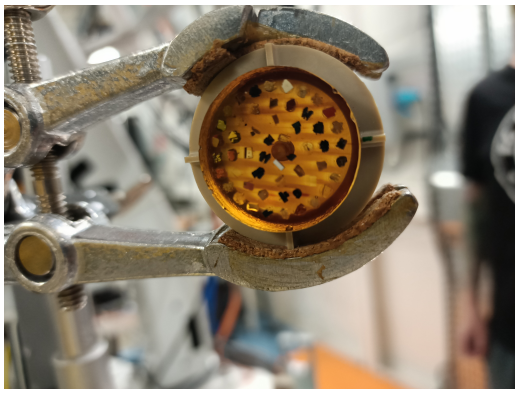

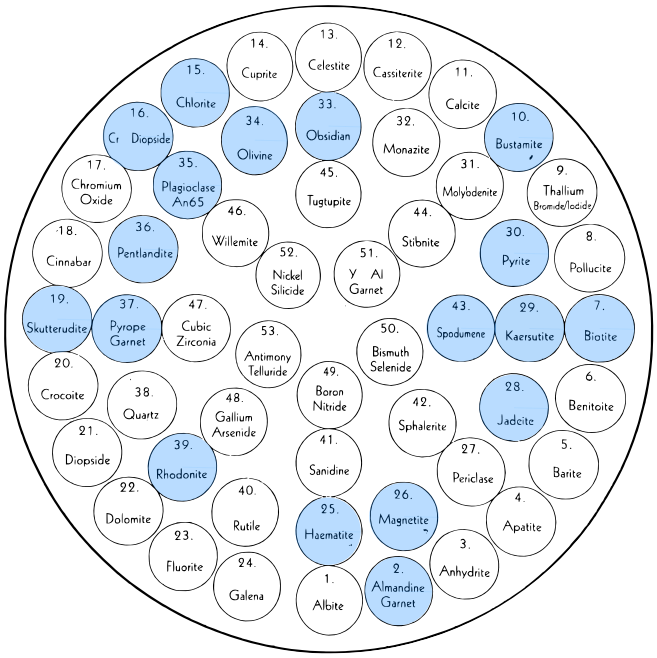

Figure 3.1: **Left**: Picture of the Astimex mineral standard. **Right**: Scheme of the Astimex mineral standard, the minerals highlighted in light blue contain iron or traces of it in different percentages.

[1]This sample has kindly been supplied by the beamline ID21 for the duration of the experiment.

No.	Compound	Chemical formula	No.	Compound	Chemical formula
1	Albite	NaAlSi3O8	28	Jadeite*	NaAlSi2O6
2	Almandine Garnet*	Fe3Al2Si3O12	29	Kaersutite*	Ca2Na(MgFe)4Ti,Si6Al2O22(OH)2
3	Anhydrite	CaSO4	30	Pyrite*	FeS2
4	Apatite	Ca5(PO4)3F	31	Molybdenite	MoS2
5	Barite	BaSO4	32	Monazite	(Ce,La,Y,Th)PO4
6	Benitoite	BaTiSi3O9	33	Obsidian*	Na,K,Al,Fe silicate glass
7	Biotite*	K(Fe,Mg)3AlSi3O10(OH)2	34	Olivine*	(MgFe)2SiO4
8	Pollucite	CsSi2AlO6	35	Plagioclase*	(Ca,Na)Al(Al,Si)Si2O8
9	Thallium Bromide	TlBr	36	Pentlandite*	(Fe,Ni)9S8
10	Bustamite*	(Mn,Ca)SiO3	37	Pyrope Garnet*	Mg3Al2Si3O12
11	Calcite	CaCO3	38	Quartz	SiO2
12	Cassiterite	SnO2	39	Rhodonite*	(Mn,Fe,Mg,Ca)SiO3
13	Celestite	SrSO4	40	Rutile	TiO2
14	Cuprite	Cu2O	41	Sanidine	(K,Na)AlSi3O8
15	Chlorite*	Mg6AlSi3O10(OH)8	42	Sphalerite	ZnS
16	Chrome Diopside*	(Mg,Cr)CaSi2O6	43	Spodumene*	LiAlSi2O6
17	Chromium Oxide	Cr2O3	44	Stibnite	Sb2S3
18	Cinnabar	HgS	45	Tugtupite	Na4AlBeSi4O12Cl
19	Skutterudite*	(Co,Ni)As3-x	46	Willemite	(ZnMn)2SiO4
20	Crocoite	PbCrO4	47	Cubic Zirconia	ZrO2
21	Diopside	MgCaSi2O6	48	Gallium Arsenide	GaAs
22	Dolomite	MgCa(CO3)2	49	Boron Nitride	BN
23	Fluorite	CaF2	50	Bismuth Selenide	Bi2Se3
24	Galena	PbS	51	Yttrium Al Garnet	Y3Al5O12
25	Hematite*	Fe2O3	52	Nickel Silicide	Ni2Si
26	Magnetite*	Fe3O4	53	Antimony Telluride	Sb2Te3
27	Periclase	MgO			

Table 3.1: This is the list of minerals contained inside the Astimex standard, the asterisk indicates materials that contain or may contain traces of iron.

3.2 Experimental setup

The sample was mounted on a support inside the experimental hutch EH2, that is the one containing the emission spectrometer, and its surface was rotated by 45° with respect to the incoming X-rays beam and to the spectrometer, in this way the beam can hit the sample and the light, emitted after the decaying processes occurring inside the material, can now reach the Bragg crystals and then the detector (see Figure 3.2). In order to have a higher transmission of light there is, within the Bragg crystals, the detector and the sample, a plastic bag filled with helium. The

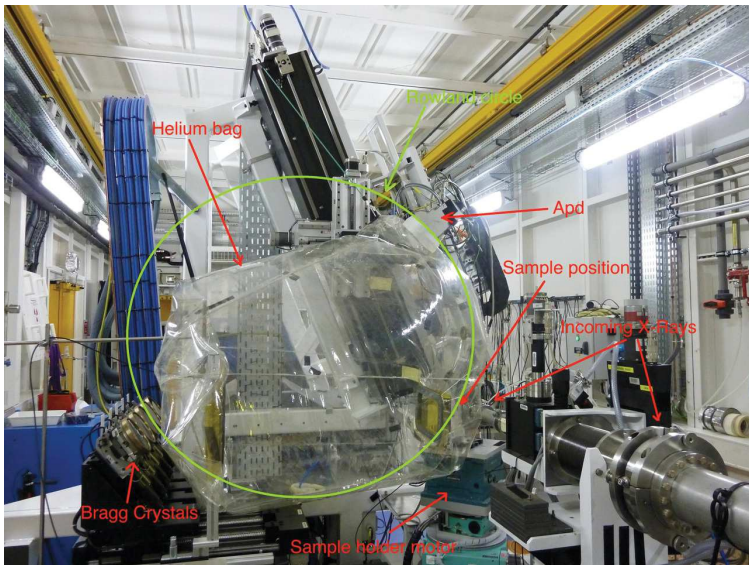

Figure 3.2: X-Rays emission spectrometer at ID26, the Rowland circle is highlighted in green [27].

incoming beam was set around 7.2 keV that is slightly above the iron K edge binding energy (1.112 keV) in order to remove the 1s core electrons of iron; to get this energy it is necessary to use a monochromator with Si[111] reflecting crystals because, as already said in sub chapter 1.3.1, this configuration can provide a reflection range from 2.28 keV to 22.69 keV. For the measurement of K_β line the five Bragg crystals of the spectrometer that are used are all Ge[620] while for the measurement of K_α line they are all Ge[440].
Moreover the beam that impinges on the sample has a vertical size of 0.1 mm and an horizontal size of 0.22 mm, dimensions determined by a slit located at the exit of the beam.

3.3 X-ray emission spectroscopy measurements

For this part of the experiment, that consists in recording the spectra of the compounds, it was used an APD as detector. The synchrotron mode during the experiment was 16 bunch filling mode where there are 16 highly populated and equally spaced bunches travelling inside the ring at the same time, the filling occurs every 5 minutes. With this modality the risk is to have saturation at the APD because

there are too many photons very close in time impinging on the detector. A dead time correction is applied in order to take into account this problem and retrieve good intensity values at the detector.

3.3.1 Identification of the minerals position

The first measurement that has been performed had the aim to identify on the resin block the positions of the minerals that contained iron; in order to recognize these elements the spectrometer was set in such a way to record at the detector only the intensity at the emission energy 7.059 keV, that is the energy where the peak of the iron K_β line occurs. Then the sample was moved horizontally (along the y direction) and vertically (along z direction) in order to scan each point and retrieve at the detector the corresponding intensity. In this way it is possible to recognize minerals that have high iron concentration because they will have higher intensity at the detector. In Figure 3.3 these minerals appear in yellow, while the orange ones are less concentrated in iron or are materials that have a K_β maximum peak close to the iron one (in this case there is still a good signal). The purple ones do not contain Fe and so they give no intensity at iron K_β peak energy, that is the energy on which the spectrometer is sitting. It is possible to notice from the picture that some minerals do not contain iron because they are purple but they have orange edges, this is probably due to the fact that the block of resin had been drilled with an iron bearing material in order to create the holes to insert the minerals and some iron remains are present. For clarity and simplification of notation the Fe bearing minerals have been denominated from S1 to S18 as shown in Figure 3.3 and indicated in Table 3.2.

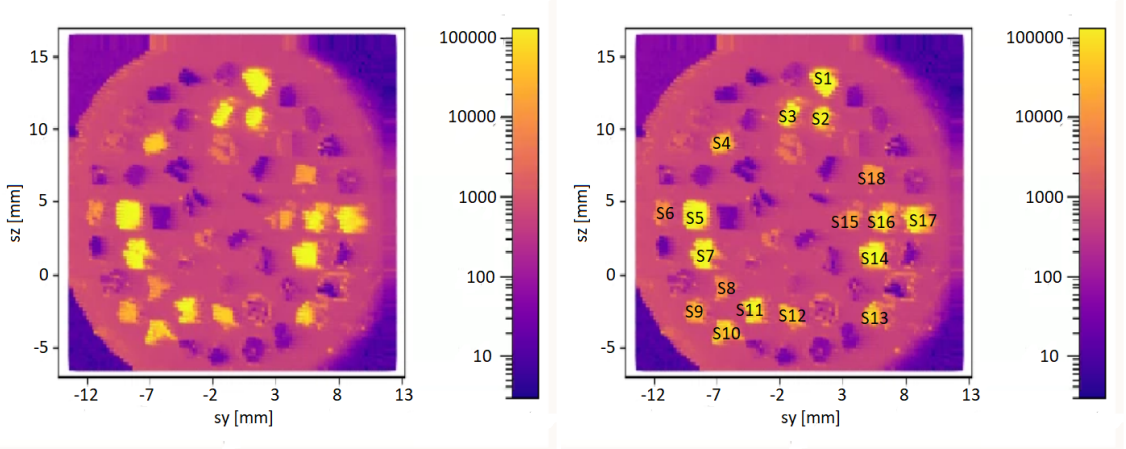

Figure 3.3: **Left**: Scan of the Astimex standard at the emission energy 7.059 keV, that is the iron K_β peak energy. It is the scan of the sample along y and z directions, the colour indicates the intensity at the detector in each point of the sample where yellow is the largest intensity and purple is lower intensity. **Right**: This is the same image but where the different iron bearing minerals have been indicated with their denomination from S1 to S18.

Compound	**Identification**
Almandite Garnet	S1
Magnetite	S2
Haematite	S3
Rhodonite	S4
Pyrope Garnet	S5
Skutterudite	S6
Pentlandite	S7
Plagioclase An65	S8
Diopside	S9
Chlorite	S10
Olivine	S11
Obsidian	S12
Bustamite	S13
Pyrite	S14
Spudomene	S15
Kaersutite	S16
Biotite	S17
Jadeite	S18

Table 3.2: This table indicates the iron bearing compounds inside the Astimex standard and their relative denomination.

3.3.2 Measurements of K_β emission lines

It was then possible to measure the K_β line of each of these 18 iron bearing compounds contained inside the Astimex standard; for each mineral the emission spectrum was measured in the center because the materials were homogeneous and it was enough to consider what happens in just one point that is far enough from the edges to have a good description of the whole mineral. The incoming beam energy, as already said, was put equal to 7.2 keV in order to remove 1s electrons from the iron and create holes. The spectrometer scanned, with energy steps of 0.2 eV, the emission energies from 7.02 keV to 7.085 keV in order to measure the transitions of electrons from level 3 ($3p \rightarrow 1s$ in particular). The acquisition time was set equal to 2 seconds for each energy point. In particular it is possible to plot (see Figure 3.4) the intensity, that is the dead time corrected intensity at the detector, normalized to I02 (that is the intensity of the beam before exiting the tube) versus the emission energy at which the spectrometer was set. At this point, in order to have comparable X-ray emission spectra for different compounds, it is possible to normalize the dead time corrected intensity not only to the incoming flux I02 but also to the area below the spectrum (see Figure 3.5 where the K_β X-ray emission spectra of all 18 iron bearing compounds are plotted).

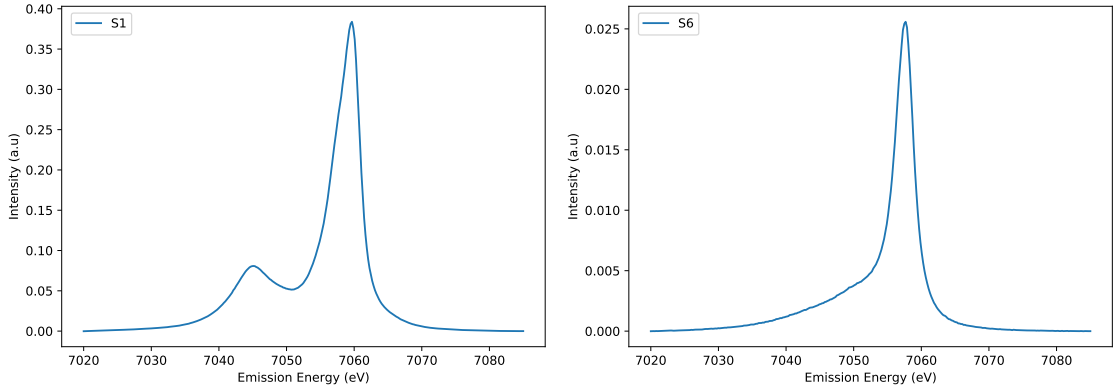

Figure 3.4: **Left**: K_β X-ray emission spectrum of a high spin compound, the intensity at the detector is normalized with respect to I02. **Right**: K_β X-ray emission spectrum of a low spin compound, the intensity at the detector is normalized with respect to I02.

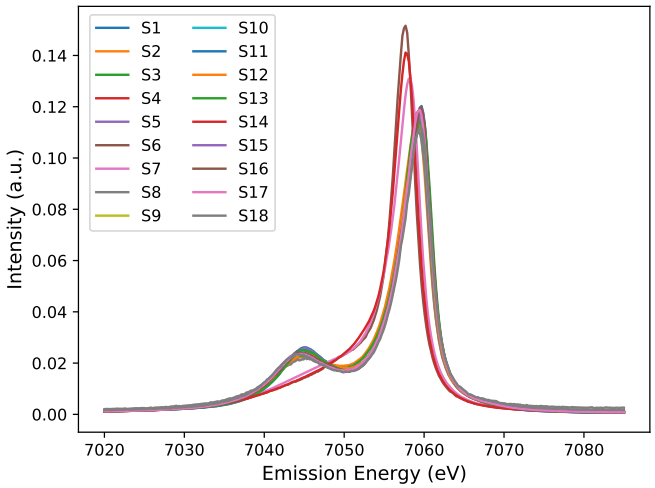

Figure 3.5: These are the K_β emission spectra of the 18 iron bearing minerals contained inside the Astimex standard. For each compound the dead time corrected intensity recorded at the detector is normalized with respect firstly to I02 and then to the area below the curve.

3.3.3 Measurements of K_α emission lines

It was also possible to measure the K_α X-ray emission spectra of the 18 iron bearing compounds. As for the measurement of the K_β lines, the K_α lines of the iron bearing compounds were measured in the center of each mineral. The incoming beam energy had to excite the iron 1s electrons and so it was set to 7.2 keV that, as previously said, is slightly above the iron Kedge binding energy (1.112 keV). The spectrometer scanned, with energy steps of 0.2 eV, the emission energies from 6.38 keV to 6.415 keV in order to measure the transitions of electrons from level 2 ($2p \rightarrow 1s$). The acquisition time was set equal to 2 seconds for each energy point.
Also in this case it is possible to plot (see Figure 3.6 **Left**) the dead time corrected intensity normalized to the incoming flux I02 versus the emission energy at which the spectrometer was set. In this case, as previously explained, the spectra of different compounds will not be comparable. In order to get comparable spectra it is necessary to normalize the detected intensity not only to the incoming flux I02 but also to the area below each curve; in Figure 3.6 **Right** the K_α X-rays emission spectra of all 18 iron bearing compounds are plotted, in this case the intensities are normalized to I02 and to the area below the corresponding spectrum.

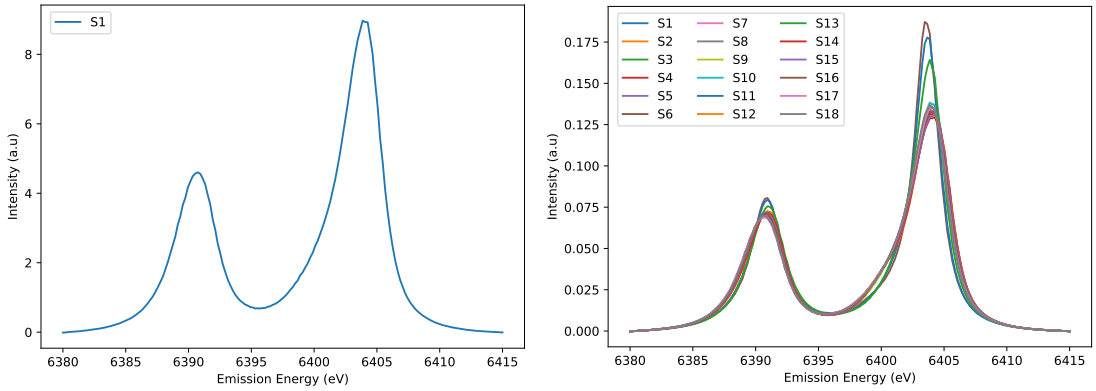

Figure 3.6: **Left**: K_α emission spectrum of the mineral denominated S1, the intensity is normalized to intensity I02. **Right**: K_α emission spectra of all 18 iron bearing minerals, the intensity is normalized to the intensity I02 and to the area below each curve.

3.4 Intensity ratios for two compounds

To proceed then with the main part of the experiment, that has been introduced in Chapter 2, a photodetector called Maxipix was installed in substitution to the APD. In particular the setup is showed in Figure 3.7 **Left**, around the detector is taped a lead foil in order to protect the detector surface from direct fluorescence and avoid in this way the presence of a background in the measurements. As already said, the Maxipix is a fast noise-free X-ray area detector and when the spectrometer is set to a fixed emission energy an intensity spot appears on the detector area 3.7 **Right**.

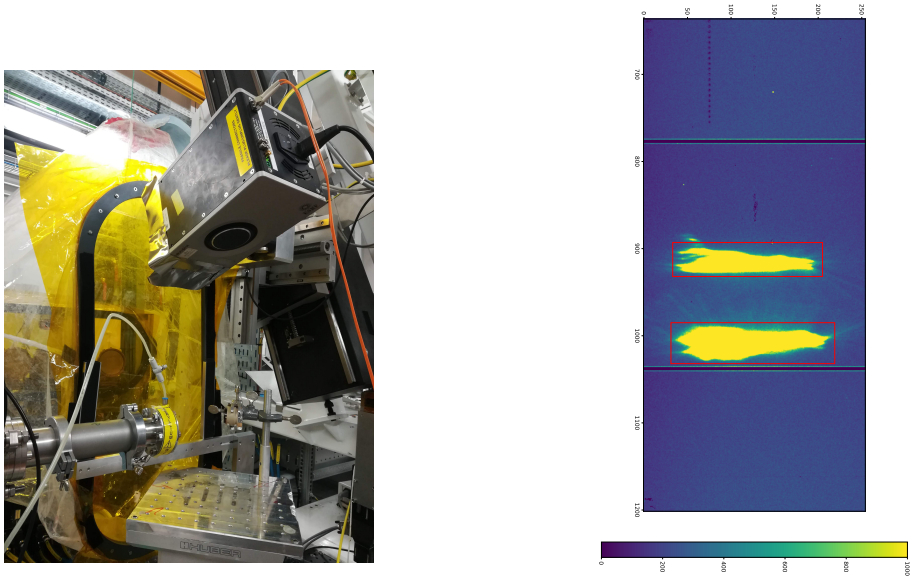

Figure 3.7: **Left**: This is the experimental setup, it is visible the tube from which the X-Rays exit, the sample, the helium bag, the analyzer crystals and the Maxipix. **Right**: The yellow spots indicate the intensities recorded by the detector when the spectrometer is set to two fixed emission energies. The red lines indicate the rectangles of integration and the so called roi1 and roi2 are the two respective recorded intensities (total number of photons). The intensity roi1 corresponds to the smaller emission energy while roi2 to the higher one.

In particular the aim of the experiment is to study if it is possible to discriminate between different iron bearing compounds just by comparing the ratio between two intensities (from the K_β or K_α lines) corresponding to two wisely chosen emission energies. It is possible to select the best two energies at which the spectrometer needs to be set thanks to the Python code presented in 2.2.2. For this section the analysis will be limited to the study of only two iron bearing compounds with iron in different chemical environments.

3.4.1 K_α versus K_β emission lines

As already said in 2.1 the K_β lines are more sensitive than the K_α lines to the spin state of the compound because of the strong interaction between 3p and 3d electrons (while the interaction between 2p and 3d electrons is weaker) [25]. On the other hand the K_α lines have a higher intensity with respect to the K_β and so it is possible to extract more or less the same amount of information from both lines.
But since there was not enough time to make a full analysis on both K_α and K_β spectra, before proceeding with the measurements it was necessary to choose which of these two emission lines analyze in order to obtain the emission energies compromise that gives the best intensity ratios contrast.
After having identified the two emission energies at which it is better to sample the spectra in order to have the maximum contrast between the intensity ratios, it is possible to calculate how many total counts are needed in order to get a signal to noise of at least 10 (the signal is the contrast between intensity ratios $RATIO1-RATIO2$ and the noise is the error associated to this contrast (see 2.2.2) and it inversely depends on the square root of the total counts). The best emission line between K_α and K_β is the one that provides a signal to noise of 10 with the lower total number of counts because in that case the acquisition time will be shorter.
If for example the XES spectra of a low and a high spin iron bearing compound (Pyrite (S14) and Kaersutite (S16)) are analyzed, it is clear that less counts are needed to have a signal to noise of 10 if K_β lines (see 3.8 **Top**) are compared; this happens because the spectra of the two iron bearing compounds are quite different (since they are really sensitive to the spin state) and so the signal to noise is higher. Indeed it is enough to have only around 600 counts on roi1 of S14 and around 300 counts on roi1 of S16 to have a signal to noise of 10. While if the K_α lines are compared (see 3.8 **Bottom**) it is necessary to have around 16000 counts on roi1 of S14 and around 17000 counts on roi1 of S16. From this analysis it seems that when two compounds containing an analyte with two different spin states must be recognized it is better to sample the K_β emission lines since less counts are needed in order to have a good contrast between intensity ratios.
It is then possible to analyze what happens when two similar iron bearing compounds (Magnetite (S2) and Haematite (S3)) are compared. In this situation the two K_β emission lines are quite similar (see 3.9 **Top right**) and the total counts needed to have a signal to noise of 10 is higher than in the case of low and high spin comparison; indeed to have such signal to noise the counts needed are around 17500 on roi1 of S2 and around 16000 on roi1 of S3. Instead when the K_α emission lines of these two compounds are compared the counts needed in order to have such signal to noise are around 15700 on roi1 of S2 and around 14800 on roi1 of S3; these total number of counts are still high since also the two K_α spectra are similar (see 3.9 **Bottom right**) but slightly less than the ones obtained by the K_β lines comparison. It seems that it would be better to analyze K_α emission lines when the iron bearing compounds are quite similar.
Depending on the compounds to recognize it is maybe better to use K_α or K_β lines but since the K_β lines are more sensitive to oxidation states, spin states and chemical environment, the measurements were mainly performed on the K_β energy range.

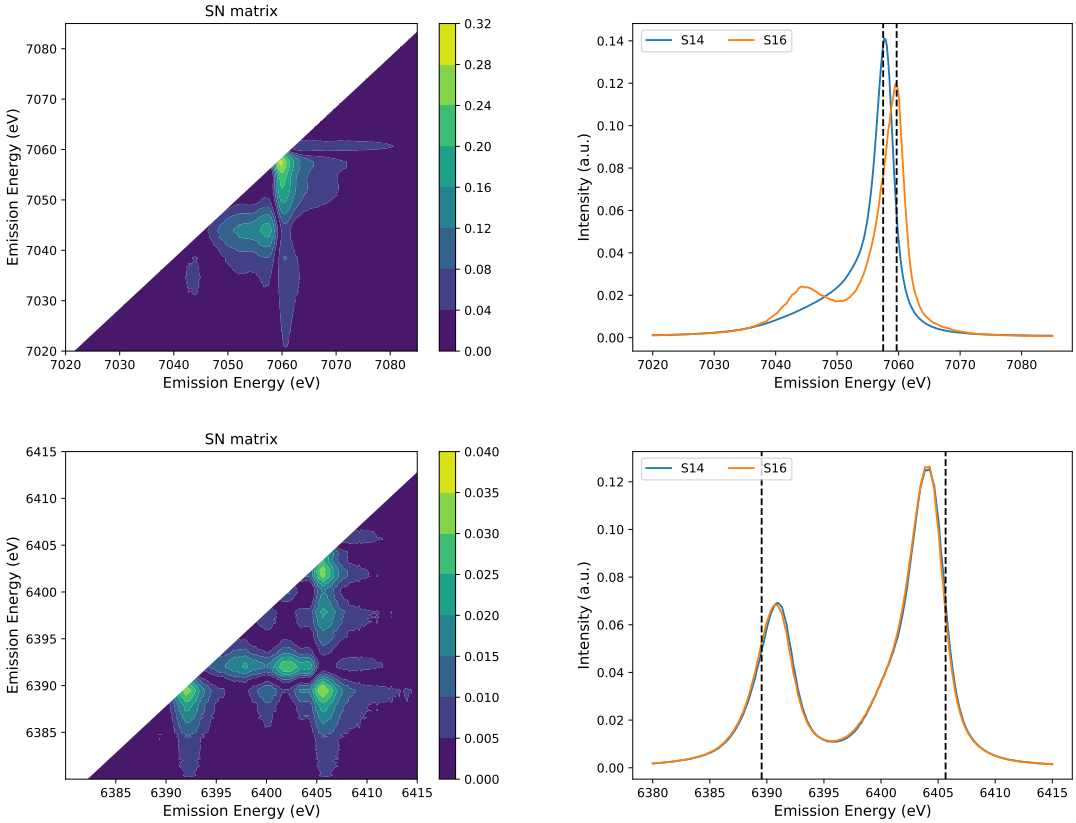

Figure 3.8: **Top Left**: The signal to noise matrix from which it is possible to identify the two emission energies at which the intensity ratios of S14 and S16 have the higher contrast (indicated in yellow). It is calculated from the comparison of the K_β XES spectra of the two minerals. **Top Right**: This is the plot of the K_β emission spectra of S14 (low spin) and S16 (high spin) with the identification of the two energies that give the maximum contrast: 7.0575 keV and 7.0597 keV. It is clearly visible that the two emission spectra are very different. **Bottom Left**: The signal to noise matrix from which it is possible to identify the two emission energies at which the intensity ratios of S14 and S16 have the higher contrast. It is calculated from the comparison of the K_α XES spectra of the two minerals. **Bottom Right**: This is the plot of the K_α emission spectra of S14 (low spin) and S16 (high spin) with the identification of the two energies that give the maximum contrast: 6.3895 keV and 6.4056 keV. The two emission spectra seem quite similar.

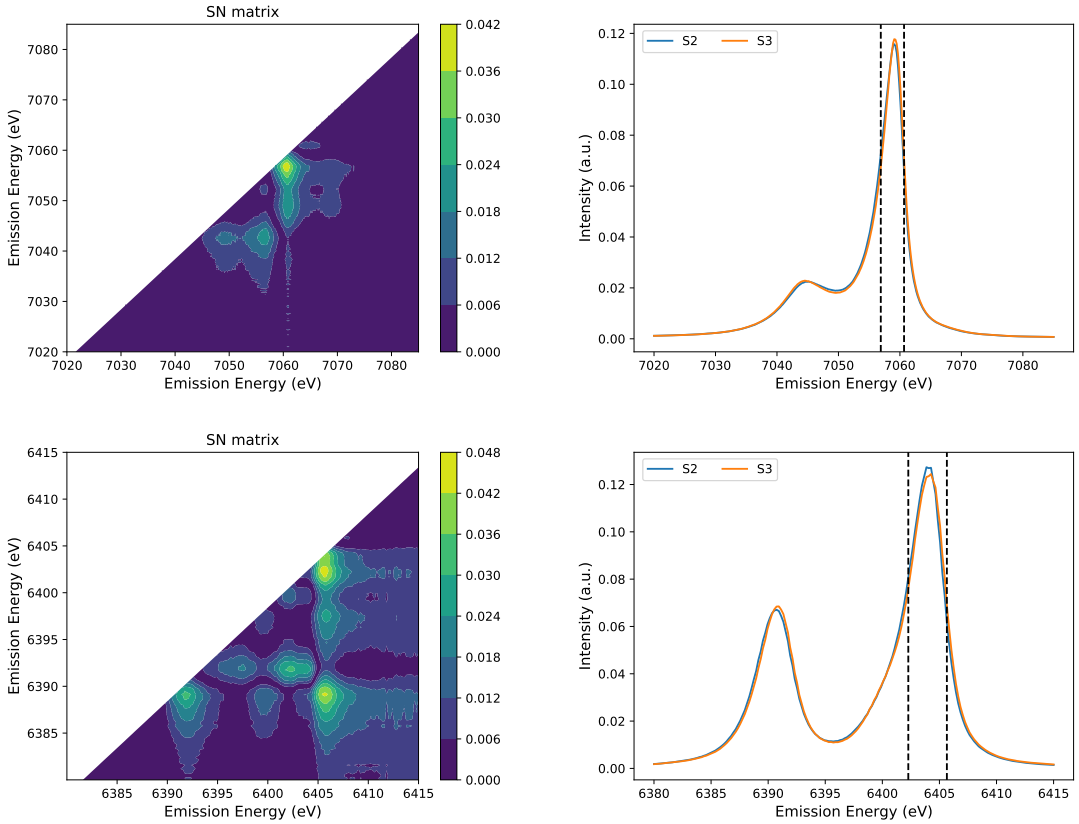

Figure 3.9: **Top Left**: The signal to noise matrix from which it is possible to identify the two emission energies at which the intensity ratios of S2 and S3 have the higher contrast (indicated in yellow). It is calculated from the comparison of the K_β XES spectra of the two minerals. **Top Right**: This is the plot of the K_β emission spectra of Magnetite (S2) and Haematite (S3) with the identification of the two energies that give the maximum contrast: 7.0569 keV and 7.0607 keV. In this case the two emission spectra seem quite similar. **Bottom Left**: The signal to noise matrix from which it is possible to identify the two emission energies at which the intensity ratios of S2 and S3 have the higher contrast. It is calculated from the comparison of the K_α XES spectra of the two minerals. **Bottom Right**: This is the plot of the K_α emission spectra of Magnetite (S2) and Haematite (S3) with the identification of the two energies that give the maximum contrast: 6.4023 keV and 6.4056 keV. It seems that the two emission spectra are quite similar but less than the K_β line case.

3.4.2 The intensity ratios measurement

In order to understand if the proposed method can be used to identify the presence of different iron bearing compounds, it is possible to scan the sample along certain directions, recording the intensities at the two chosen emission energies and in the end compute, for each point of the space, the ratio between these two intensities; to this intensity ratio it is associated an error that is inversely proportional to the square root of the count rate. So the aim is to verify if these intensity ratios are clearly distinguishable for two iron bearing minerals; if this is the case then the method can be used to differentiate and recognize the same analyte in different chemical environments (obviously if the chemical environment is the same, the intensity ratios will be the same).
To better understand practically this method it is possible to consider an example of a line scan through two iron bearing minerals, in particular in Figure 3.11 it is shown the scan through the compounds S7 (Pentlandite) and S5 (Pyrope Garnet). The energies at which the spectrometer was set during this measurement are 7.0577 keV and 7.0601 keV, that are found from the comparison of the K_β lines of the two compounds (see Figure 3.10 **Left** for the signal to noise matrix and 3.10 **Right** for the emission spectra of the two compounds); these are the two energies at which the intensity ratios relative to these two compounds have the best separation, these energies were calculated using the code explained in Chapter 2.

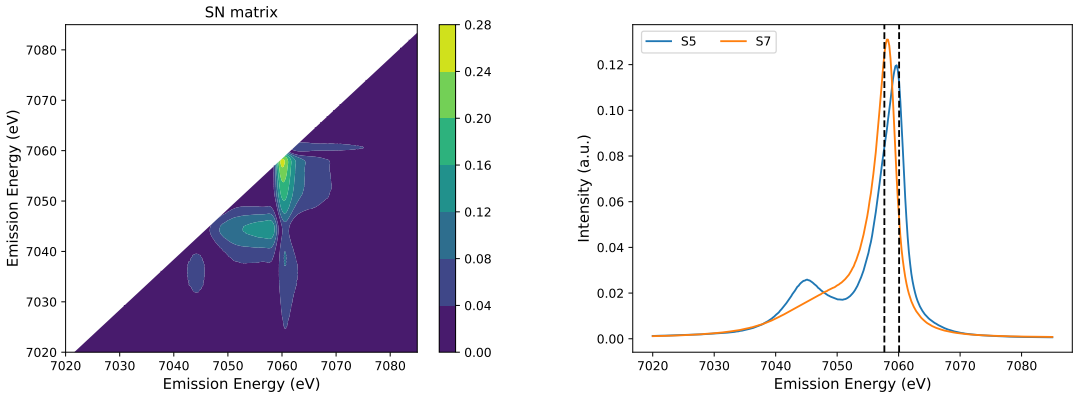

Figure 3.10: **Left**: The signal to noise matrix from which it is possible to identify the two emission energies at which the intensity ratios of S5 and S7 have the higher contrast (indicated in yellow). It is calculated from the comparison of the K_β XES spectra of the two minerals. **Right**: This is the plot of the two spectra of S5 and S7 with the identification of the two energies that give the maximum contrast: 7.0577 keV and 7.0601 keV (that is the yellow peak in the signal to noise matrix).

In particular a vertical line scan was done and each point was measured for 2 seconds. So by looking more specifically at Figure 3.11: on **Top Left** the intensities roi1 and roi2, corresponding one to the emission energy 7.0577 keV and the other to the emission energy 7.0601 keV, are plotted versus the position in the sample; on **Top Right** the ratio between the two intensities roi2/roi1 is plotted vs the position in the sample, notice that the ratio has a very large error bar in the resin since the total number of counts is low because the resin has no K_β emission line (the error on the ratio gets larger because it is inversely proportional to the square root of the

counts); on **Bottom Left** it is represented on the same plot both the ratio between the two recorded intensities roi2/roi1 (the part not relative to the minerals has been removed) and the intensity roi1; on **Bottom Right** it is plotted the ratio between the intensities roi2/roi1 removing the data corresponding to the parts inside the resin, this last kind of representation will be mainly used in the following plots.

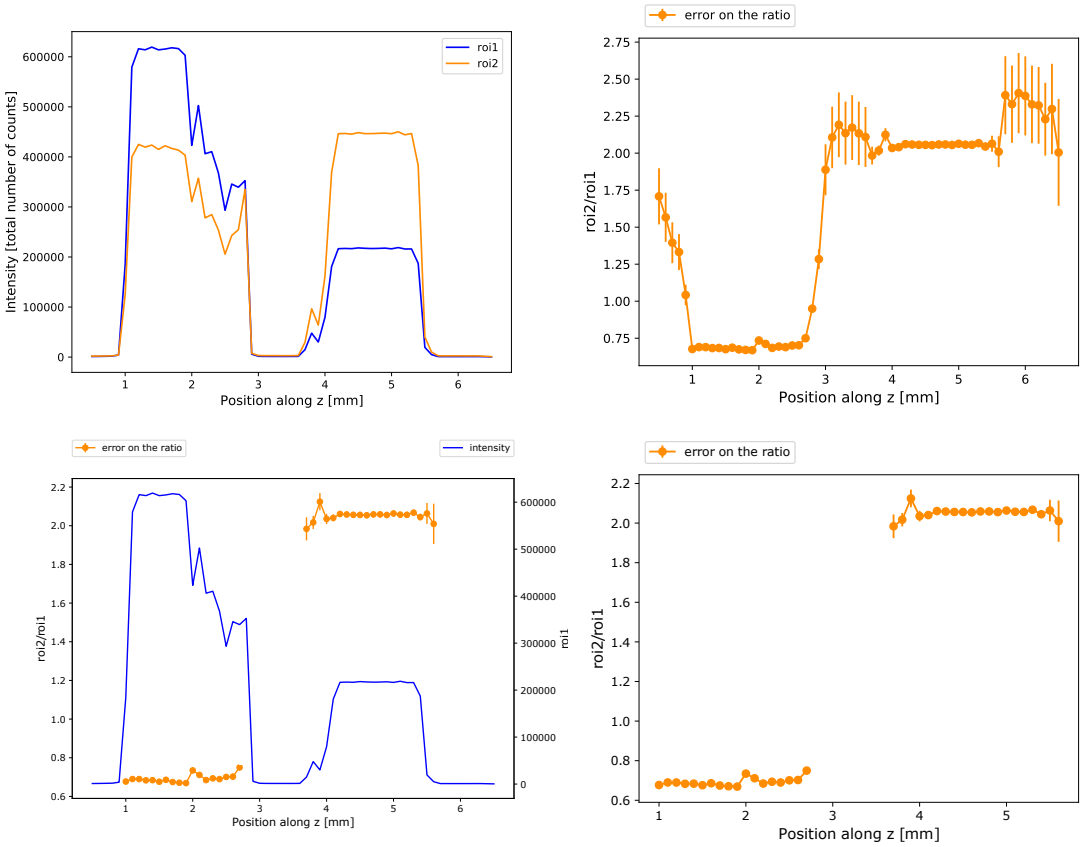

Figure 3.11: **Top Left**: Plot of the intensities roi1 and roi2, corresponding to the two energies 7.0577 keV and 7.0601 keV, versus position along z. The minerals that are scanned are S7 (Pentlandite) and S5 (Pyrope Garnet). **Top Right**: Plot of the ratio of the two intensities vs the position along z. **Bottom Left**: Plot of one of the two intensities (roi1) and of the ratio roi2/roi1, in this last plot the ratio in the resin is removed. **Bottom Right**: Plot of the ratio roi2/roi1 with removal of the part not concerning the minerals.

This method should eliminate every systematic error since the ratios between intensities are computed (many quantities get simplified), so the only error present should be the statistical one. For this reason the intensity ratio in a certain mineral should have a constant value (that at most varies within the error bar given by the statistics) but sometimes it is clear from the plots that the ratio assumes slightly different values than in the rest of the mineral (for example in the mineral S7 at z $\sim 2mm$). In particular the mineral S7 has a cubic symmetry and so no explanation to this behaviour has been found and further studies must be done. If instead a mineral has an hexagonal symmetry linear dichroism could be the reason of such jumps in the intensity ratio.

3.4.3 Effects on the intensity ratios when considering different emission energies

At this point it is possible to analyze what happens when different emission energies are chosen; in order to prove that the two emission energies that give the maximum contrast (at least for two compounds) are the ones found from the Python code showed in Chapter 2, different scans of the same minerals at different emission energies were measured. Again a scan through the same minerals S7 (Pentlandite) and S5 (Pyrope Garnet) were recorded, in particular emission energies corresponding to different values of the signal to noise were chosen by looking at the plot of the signal to noise matrix (see Figure 3.10 **Left**).
In Figure 3.12 the intensity ratios for different emission energies are plotted, it is clearly visible that, when two emission energies with a lower signal to noise are chosen, the contrast between the intensity ratios of the two compounds decreases. The worst case is the one in red for which the intensity ratios of two different compounds are almost equivalent while the best case is the one in blue where the contrast is quite large.

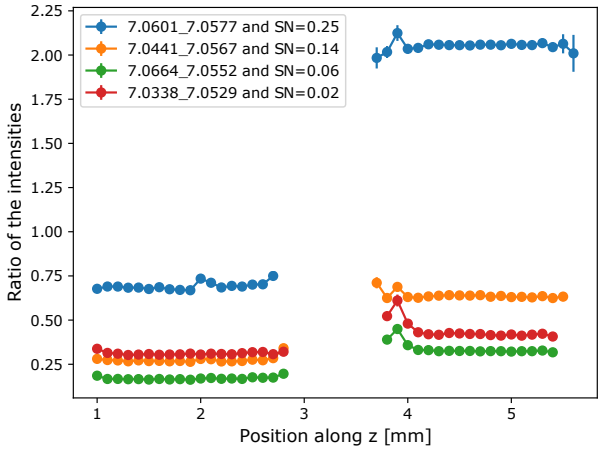

Figure 3.12: Representation of the intensity ratios vs position along z for different choices of emission energies when scanning through S7 and S5. It is clear that the best emission energy compromise is 7.0577 keV and 7.0601 keV while the worst is 7.0338 keV and 7.0529 keV.

3.4.4 Low and high spin iron bearing compounds

Another important measurement that was done regarded two iron bearing compounds, denominated as S14 (Pyrite) and S16 (Kaersutite), in which iron is present in two different spin states: low and high spin state. These compounds have quite different X-ray emission spectra since the analyte spin states are dissimilar. In Figure 3.13 **Left** it is represented the signal to noise matrix, that allows to identify the two emission energies that give the maximum contrast between the intensity ratios of the minerals S14 and S16, while on the **Right** the K_β X-ray emission spectra of the two compounds are plotted and the two emission energies used to make the

measurement are indicated: 7.0575 keV and 7.0597 keV.

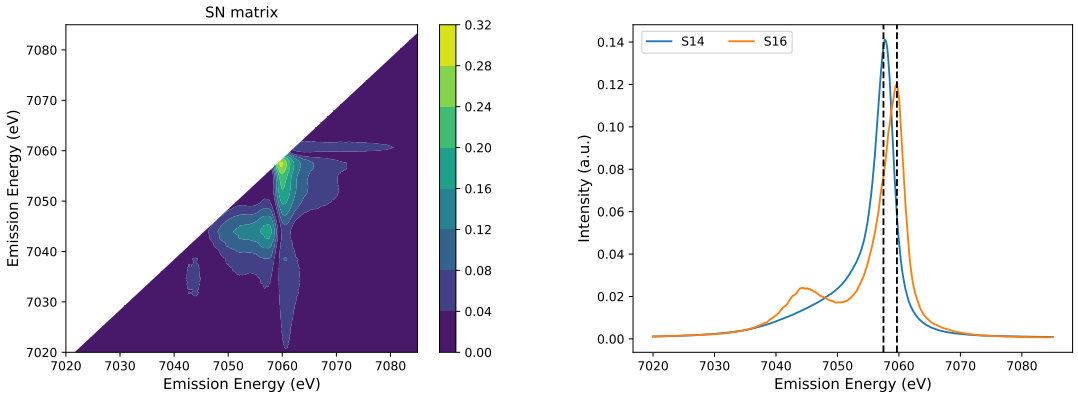

Figure 3.13: **Left**: The signal to noise matrix from which it is possible to identify the two emission energies at which the intensity ratios of S14 and S16 have the higher contrast (indicated in yellow). It is calculated from a comparison of the K_β XES spectra of the two minerals. **Right**: This is the plot of the two spectra of S14 and S16 with the identification of the two energies that give the maximum contrast: 7.0575 keV and 7.0597 keV. It is clearly visible from the XES spectra that the compound S14 has low spin while S16 has high spin and so the two emission spectra are obviously very different.

In such situation the contrast between intensity ratios is so high (high signal to noise) that it is possible to obtain distinguishable ratios (still by using the two best emission energies) even when having very low count rates. In order to show this interesting behaviour, multiple vertical lines that crossed the minerals S14 and S16 were scanned for different intensities of the incoming beam, in particular the first scan was taken without attenuating the incoming beam flux and then different attenuators were put in until the beam was attenuated of fifteen times (att(15)). As it can be seen in Figure 3.14 when the count rate is extremely low the ratios of the two iron bearing compounds are still quite distinguishable even though the error bar starts getting quite large. This happens because, as already said, the error on the ratio is inversely proportional to the square root of the counting rate and so when the counting rate decreases the error increases. In this case the two compounds have two quite different intensity ratios and for this reason they are still distinguishable for a while when the error on the ratio increases. It is also possible to retrieve for the two cases the signal to noise (that is the contrast between the two intensity ratios divided by the noise associated to this contrast 2.2.2; when changing the total number of counts the signal remains contant while the noise changes): if no attenuator (att(0)) is inserted the signal to noise is around 100 while when the flux is attenuated by fifteen times (att(15)) the signal to noise is around 10, that is still a pretty high value that allow to clearly distinguish the two intensity ratios.

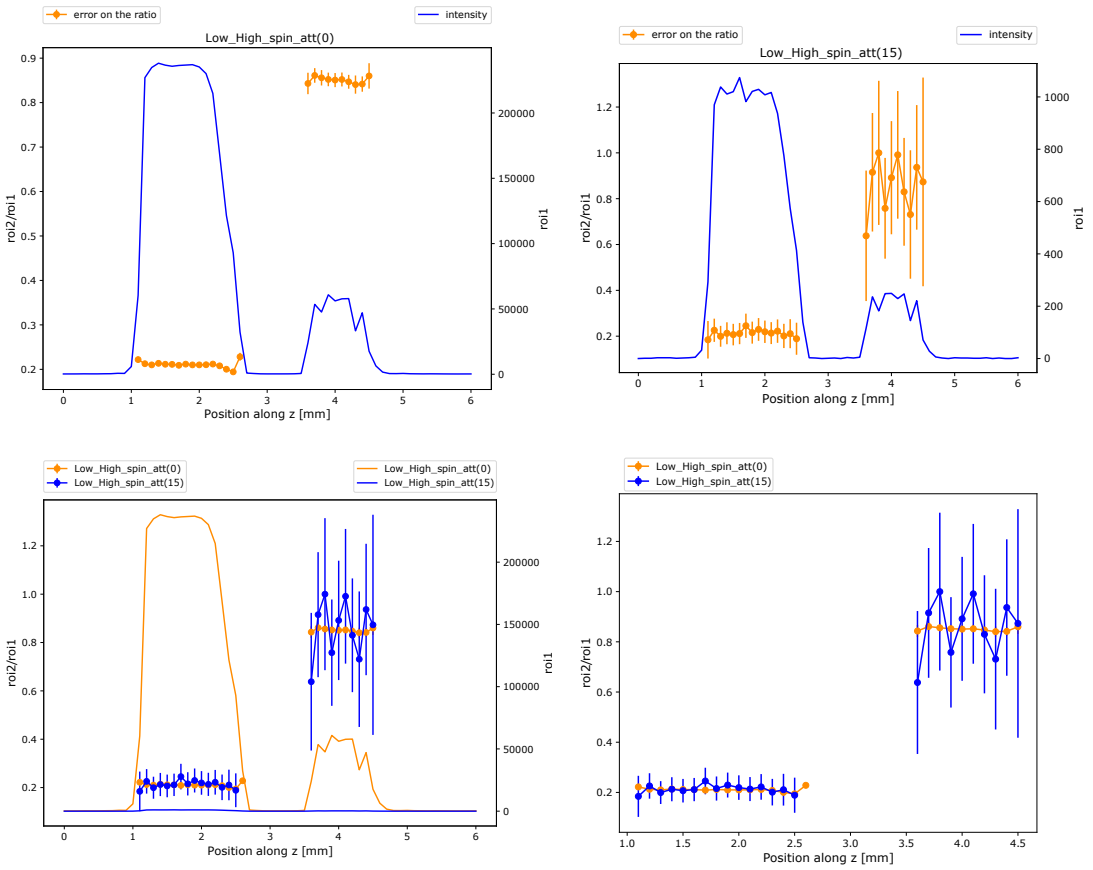

Figure 3.14: In this case a low (S14) and a high (S16) spin iron bearing compound are scanned. **Top Left**: Plot of the ratio roi2/roi1 and of the total counts roi1 in the case in which the flux is not attenuated (att(0)). The signal to noise is around 100. **Top Right**: Plot of the ratio roi2/roi1 and of the total counts roi1 in the case in which the flux is attenuated by fifteen times (att(15)). The signal to noise is around 10. **Bottom Left**: It is plotted the ratio roi2/roi1 and the intensity roi1, the orange indicates the case in which the beam intensity is not attenuated while the blue indicates the case when the intensity of the beam is very attenuated. It is quite clear that even with very low count rates the intensity ratios are very distinguishable even though the error bar in the second case gets very large. **Bottom Right**: This is a closer view of the roi2/roi1 plot.

3.4.5 Haematite and Magnetite

It is now time to observe the case of Magnetite (S2) and Haematite (S3) that are two very similar iron bearing compounds with similar K_β lines. By using the Python code previously presented it is possible to find the two emission energies that give the maximum contrast between the intensity ratios: 7.0569 keV and 7.0601 keV (see Figure 3.15 for the plot (on **Left**) of the signal to noise matrix useful to identify the best two emission energies and the plot (on **Right**) of the identification of the best two energies in the XES spectra of the S2 and S3). In this case, since the two compounds have very similar chemical composition, the contrast between their intensity ratios (signal to noise) is quite small and in order to reduce the error on the ratio as much as possible it is necessary to count for a longer time.

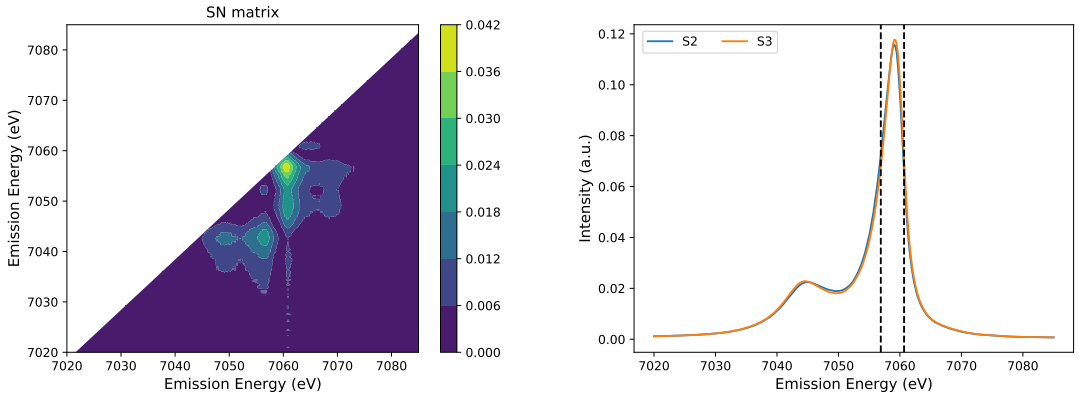

Figure 3.15: **Left**: The signal to noise matrix due to the comparison of the K_β XES spectra of the minerals S2 and S3. It is useful to identify the two emission energies for which there is the best contrast between intensity ratios. **Right**: This is the plot of the two K_β lines with the identification of the two best emission energies: 7.0569 keV and 7.0607 keV.

As already done for the case of high and low spin iron compounds, also in this case it is possible to make different line scans through Haematite (S3) and Magnetite (S2) and study what happens to the intensity ratios and to the associated error bar when the intensity of the incoming beam is decreased (attenuators are used). In Figure 3.16 in each single plot it is showed the comparison between the case in which there are no attenuators inserted (orange lines) and cases in which there are different kinds of attenuators (blue lines). In particular the intensity ratios and also the intensity roi1 are plotted. It is clear that when the intensity of the incoming beam is quite attenuated (there is a lower number of photons) the two intensity ratios start being indistinguishable. This happens because the error increases when the counting rate decreases. In Figure 3.17 other plots, that show the effect of the insertion of different attenuators on the intensity ratio roi2/roi1 and on the intensity roi1, are plotted. In the case of Haematite and Magnetite the two intensity ratios are not too different and so the increasing of the error implies the fact that the two ratios get indistinguishable. This means that when two really similar iron compounds must be identified it is necessary to count longer in order to distinguish between them.

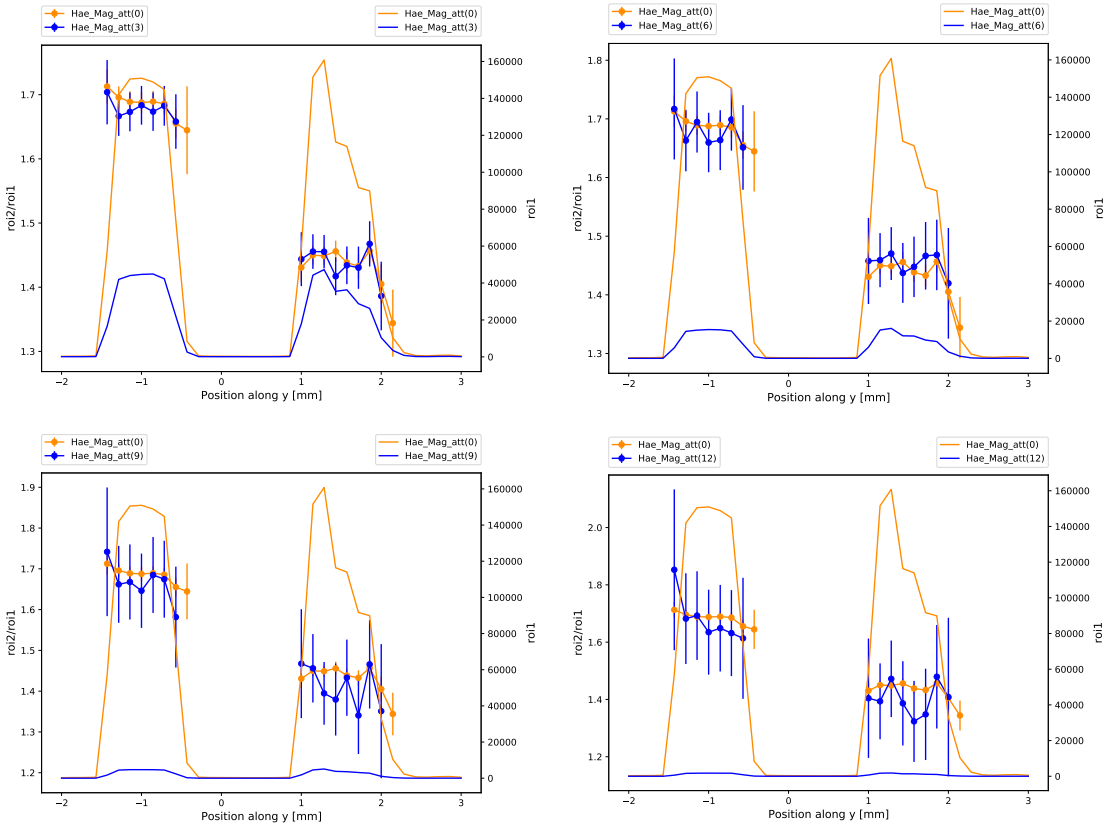

Figure 3.16: Comparison between the case where the intensity of the incoming beam is not attenuated (in orange) and the case where it is attenuated (in blue). The ratio roi2/roi1 and the intensity roi1 are plotted. **Top Left**: Comparison between att(0) (the incoming flux is not attenuated) and att(3) (the incoming flux is attenuated by three times). The error is not too large compared to the case of no attenuators. The signal to noise in the case att(0) is around 30 while in the case att(3) is around 20. **Top Right**: Comparison between att(0) and att(6) (the incoming flux is attenuated by six times). The error starts increasing. The signal to noise in the case of att(6) is around 10. **Bottom Left**: Comparison between att(0) and att(9) (the incoming flux is attenuated by nine times). The error becomes quite large and it starts to become difficult to distinguish between the two ratios. The signal to noise in the case of att(9) is around 6. **Bottom Right**: Comparison between att(0) and att(12) (the incoming flux is attenuated by twelve times). In this case the two ratios are clearly indistinguishable, the error is very large. The signal to noise in the case of att(12) is around 4.

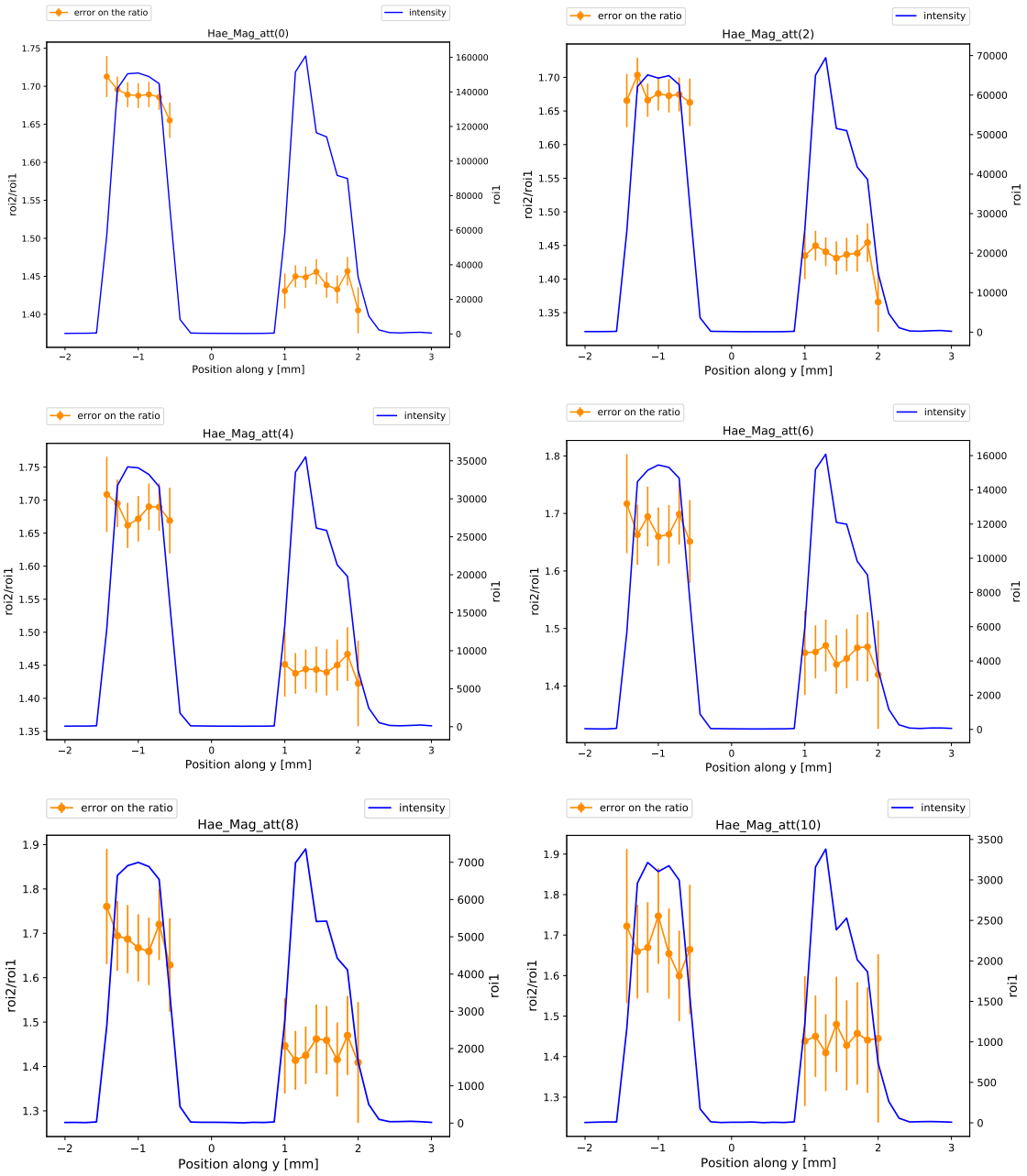

Figure 3.17: In this Figure it is plotted the ratio roi2/roi1 and the intensity roi1 for a different incoming flux. In this way it is possible to better observe the intensity ratios and the corresponding number of counts. **Top Left**: att(0) (the incoming flux is not attenuated). Here the error is the smallest possible and the two ratios are distinguishable. The signal to noise is around 30. **Top Right**: att(2) (the incoming flux is attenuated by twice). The error starts increasing. The signal to noise is around 20. **Middle Left**: att(4) (the incoming flux is attenuated by four times). The error continues increasing. The signal to noise is around 15. **Middle Right**: att(6) (the incoming flux is attenuated by six times). The two ratios start becoming less distinguishable. The signal to noise is around 10. **Bottom Left**: att(8) (the incoming flux is attenuated by eight times). The error becomes quite large and it is more and more difficult to distinguish between the two ratios. The signal to noise is around 6. **Bottom Right** att(10) (the incoming flux is attenuated by ten times). In this case the two ratios are clearly indistinguishable, the error is very large. The signal to noise is around 5.

3.5 Intensity ratios for more than two compounds

At this point the experimental analysis was devoted to see if the energy compromise found with the method explained in Chapter 2 was effectively allowing to recognize the presence of the same analyte in more than two chemical environments. In order to see if this method was valid for more than two compounds the Astimex standard was ideally divided in 4 regions:

- the first region comprehended the minerals denominated S1, S2, S3;
- the second region comprehended the minerals denominated S5, S6, S7;
- the third region comprehended the minerals denominated S8, S9, S10, S11;
- the fourth region comprehended the minerals denominated S14, S15, S16, S17, S18.

For each region it was possible to calculate the best two emission energies allowing to differentiate all the iron bearing compounds contained in that region.

3.5.1 First region

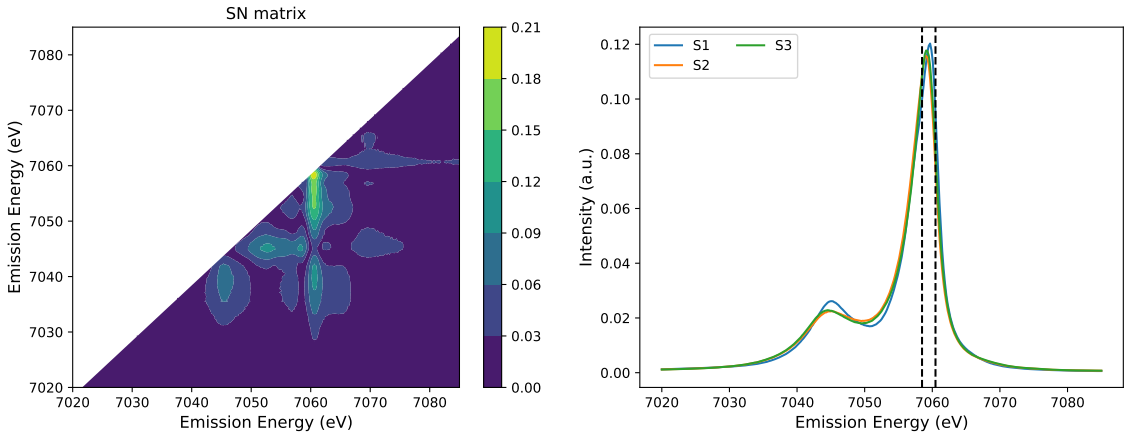

Figure 3.18: **Left**: Signal to noise matrix useful to identify the two emission energies that give the better contrast of the intensity ratios. **Right**: This is the plot of the emission spectra of the iron bearing compounds contained in the first region, moreover there is the identification of the two best emission energies that give the maximum contrast of intensity ratios: 7.0585 keV and 7.0605 keV.

The first region is the one that contains the minerals denominated S1, S2 and S3; the two emission energies at which the spectrometer should be set and for which the intensity ratios of the three iron bearing minerals should be distinguishable are 7.0585 keV and 7.0605 keV. In particular in Figure 3.18 it is plotted (on the **Left**) the signal to noise matrix useful to identify the two emission energies that give the better contrast of the intensity ratios (recall that the signal to noise matrix for more than two compounds is given by the summation of the signal to noise matrices of each pair of compounds 2.2.3) and (on the **Right**) it is plotted the K_β XES spectra of the iron bearing minerals contained in the first region, the two dashed black lines

identify the two emission energies that should give the best contrast between all the intensity ratios. To check if effectively these two emission energies allow to obtain three distinguishable intensity ratios it is possible to make some line scans through the region; in the plot in Figure 3.19 there is a vertical scan through the minerals denominated S2 and S1 and an horizontal scan through S3 and S2, in both cases the intensity ratios are distinguishable. This means that by setting the spectrometer to the two emission energies computed with the Python code, it is possible to clearly differentiate the iron bearing compounds in the first region.

In this case it is interesting to make a two dimensional scan of the region and plot an image where the color indicates the value of the intensity ratio roi2/roi1. It is clearly visible that the three compounds have three different colors and so different and distinguishable intensity ratios (see Figure 3.20).

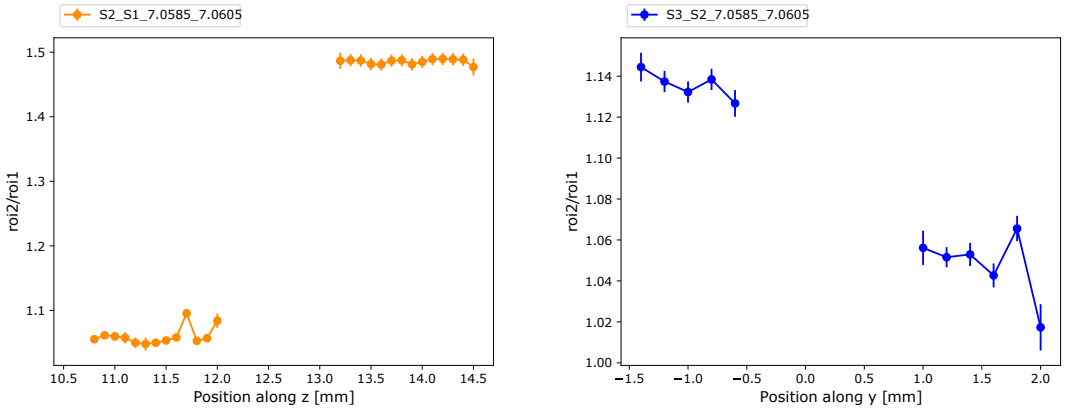

Figure 3.19: **Left**: This is the plot of the ratio of the intensities roi2/roi1 recorded by scanning a vertical line that passed through the minerals S2 and S1. **Right**: This is the plot of the ratio of the intensities roi2/roi1 recorded by scanning a horizontal line that passed through the minerals S3 and S2.

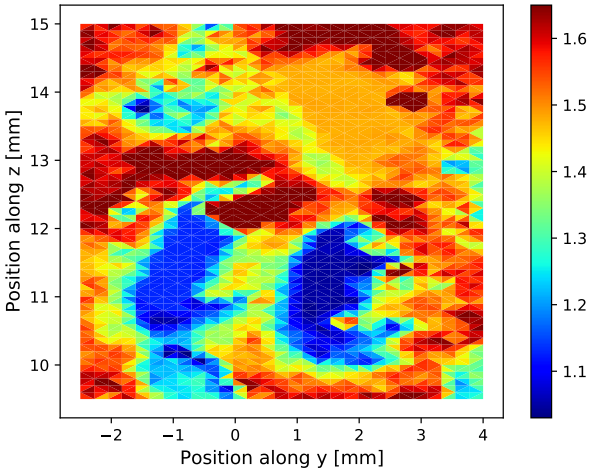

Figure 3.20: Two dimensional image of the first region, the intensity ratio roi2/roi1 is indicated with different colors depending on the value. S1 is in orange, S2 in blue and S3 in light blue.

3.5.2 Second region

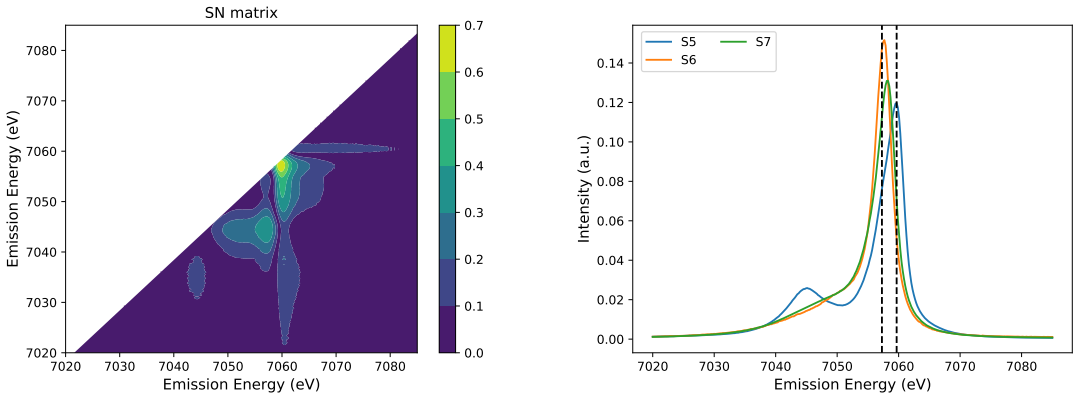

Figure 3.21: **Left**: Signal to noise matrix useful to identify the two emission energies that give the better contrast of the intensity ratios. **Right**: This is the plot of the emission spectra of the iron bearing compounds contained in the second region, moreover there is the identification of the two best emission energies that give the maximum contrast of intensity ratios: 7.0573 keV and 7.0597 keV.

The second region contains the minerals denominated S5, S6 and S7 and the best two emission energies that should allow to distinguish the three iron bearing minerals are 7.0573 keV and 7.0597 keV (see Figure 3.21 for the signal to noise matrix and the K_β XES spectra of the iron bearing compounds, where the two best emission energies are indicated). Then, in order to check if these two emission

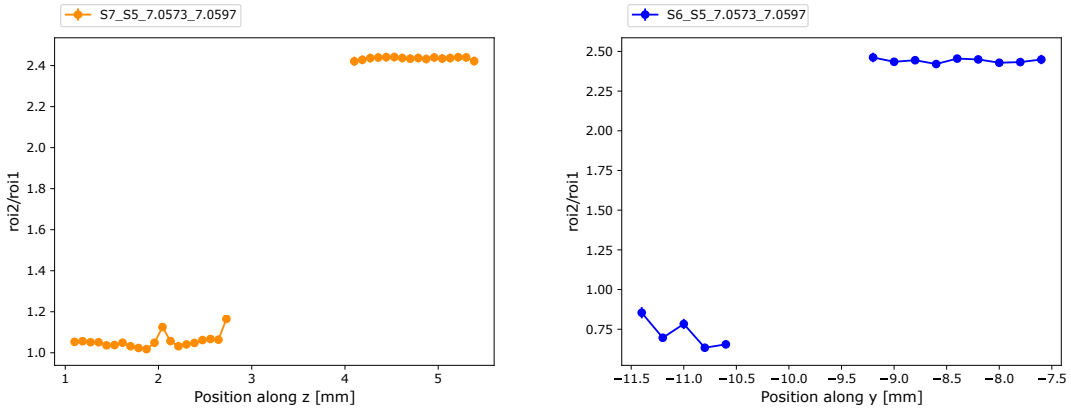

Figure 3.22: **Left**: This is the plot of the ratio of the intensities roi2/roi1 recorded by scanning a vertical line that passed through the minerals S7 and S5. **Right**: This is the plot of the ratio of the intensities roi2/roi1 recorded by scanning a horizontal line that passed through the minerals S6 and S5.

energies effectively allow to obtain intensity ratios distinguishable from compound to compound, a vertical (containing S7 and S5) and a horizontal (containing S6 and S5) line were scanned. It is clear that also in this case the iron bearing compounds are distinguishable since their intensity ratios are quite different at those emission energies found with the Python code.

It is interesting to plot the two dimensional image representing the scan through the second region, also in this case the different colors indicate the different values of intensity ratios roi2/roi1. The three compounds have clearly three different colors.

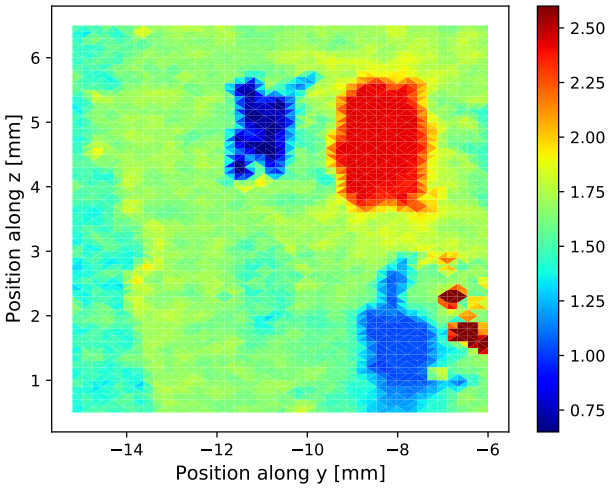

Figure 3.23: Two dimensional image of the second region, the intensity ratio roi2/roi1 is indicated with different colors depending on the value. S5 is in red, S6 in blue and S7 in light blue.

3.5.3 Third region

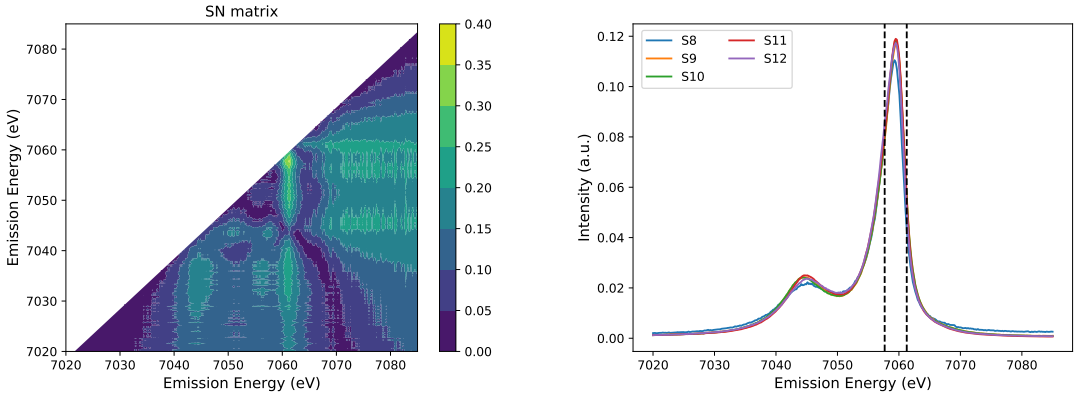

Figure 3.24: **Left**: Signal to noise matrix useful to identify the two emission energies that give the better contrast of the intensity ratios. **Right**: This is the plot of the emission spectra of the iron bearing compounds contained in the third region, moreover there is the identification of the two best emission energies that give the maximum contrast of intensity ratios: 7.0577 keV and 7.0613 keV.

In the third region there are the minerals denominated from S8 to S12, the two best emission energies are 7.0577 keV and 7.0613 keV (see Figure 3.24 for signal to noise matrix and emission spectra of the minerals). In order to verify if these two emission energies allow to have intensity ratios that are distinguishable for the

different iron bearing compounds of this region, a vertical and a horizontal line scan are made through the region. In this case the intensity ratios, as it can be seen in Figure 3.25, are not all distinguishable. Since it seems that the two emission energies are not able to give distinguishable intensity ratios for all iron bearing compounds inside the region (in particular for the compounds S9, S10 and S11), it is necessary to study in more detail if at least there exist two emission energies that can differentiate between those iron bearing compounds with similar intensity ratio.

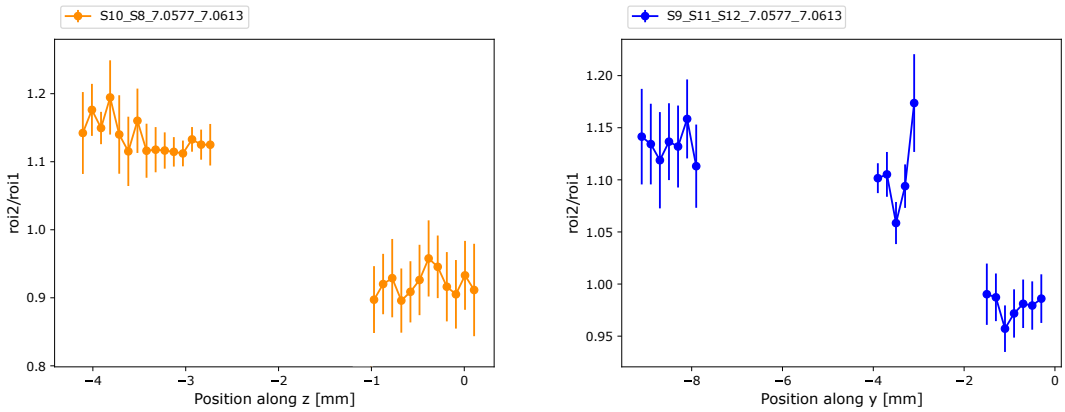

Figure 3.25: **Left**: This is the plot of the ratio of the intensities roi2/roi1 recorded by scanning a vertical line that passed through the minerals S10 and S8. **Right**: This is the plot of the ratio of the intensities roi2/roi1 recorded by scanning a horizontal line that passed through the minerals S9, S11 and S12.

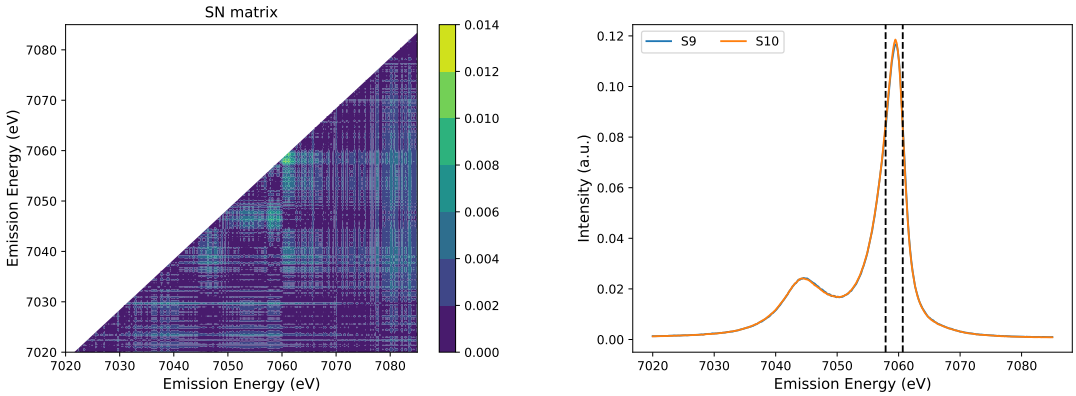

Figure 3.26: **Left**: Signal to noise matrix useful to identify the two emission energies that give the better contrast of the intensity ratios for compounds S9 and S10. **Right**: This is the plot of the emission spectra of the iron bearing compounds S9 and S10, there is the identification of the two best emission energies that give the maximum contrast of intensity ratios: 7.0579 keV and 7.0607 keV.

In particular it is possible to analyze the compounds S9 and S10 (both have an intensity ratio of about 1.15 at the emission energies of the third region). In Figure 3.26 it is showed the signal to noise matrix and the K_β emission lines of the two iron bearing compounds, it can be noticed that these compounds have very similar

emission lines (these minerals do not properly contain iron but they contain traces of iron that may have similar chemical environment, spin and oxidation state). In any case it is possible to identify two emission energies (7.0579 keV and 7.0607 keV) in the signal to noise matrix but in the image it seems not to exist a pronounced unique peak and its value is quite small, this is due to the fact that the two lines are almost equal. In principle it should be possible to differentiate between these compounds using these new emission energies and by counting for a long time (in order to have a signal to noise of 10 it is necessary to have around 210000 counts on roi1 of S9 and 215000 counts on roi1 of S10. If instead the K_α emission lines are compared less counts are needed in order to get such signal to noise: around 27000 counts on roi1 of S9 and around 25000 counts on roi1 of S10). It was not performed such measurement but from the recorded spectra it was possible to calculate the intensity ratios at these two emission energies: the intensity ratio of S9 is 1.02 and the intensity ratio of S10 is 0.97, these intensity ratios have a very small contrast and unless the measurement is performed at the right energies and with enough counts it will be impossible to distinguish between these compounds.

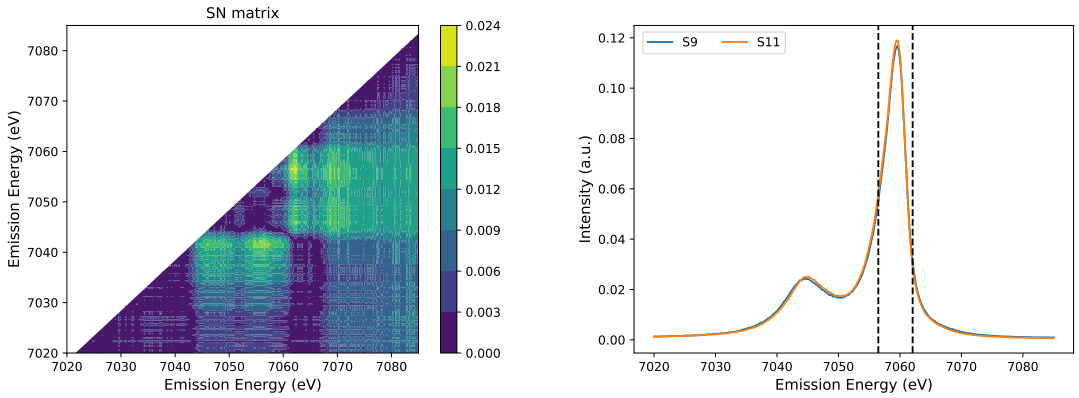

Figure 3.27: **Left**: Signal to noise matrix useful to identify the two emission energies that give the better contrast of the intensity ratios for compounds S9 and S11. **Right**: This is the plot of the emission spectra of the iron bearing compounds S9 and S11, there is the identification of the two best emission energies that give the maximum contrast of intensity ratios: 7.0565 keV and 7.0621 keV.

At this point it is necessary to analyze in more detail also the iron bearing compounds S9 (that contains traces of iron) and S11 (Olivine) because the presence of a big error bar on the intensity ratio of the compound S9 makes these two minerals indistinguishable. It is needed a more detailed analysis of these two compounds: in Figure 3.27 it is plotted the signal to noise matrix and the K_β emission lines of S9 and S11. Also in this case the two emission lines are quite similar but it is possible to find two emission energies for which the intensity ratios of the two compounds are distinguishable: 7.0565 keV and 7.0621 keV. The signal to noise matrix does not show a pronounced unique peak and its value is quite small (but higher than the case S9 and S10). Since no measurement was performed at these two energies, it is possible to calculate from the spectra of the two compounds the intensity ratios that would be obtained: the intensity ratio of is S9 is 2.78 and the intensity ratio of S11 is 2.01. These intensity ratios are not as close as the intensity ratios of the compounds

S9 and S10, but in any case a long counting at the right emission energies is needed in order to differentiate between the two compounds (in order to have a signal to noise of 10 it is necessary to have around 390000 counts on roi1 of S9 and 420000 counts on roi1 of S11. If instead the K_α emission lines are compared less counts are needed in order to get such signal to noise: around 1800 counts on roi1 of S9 and around 2400 counts on roi1 of S11).

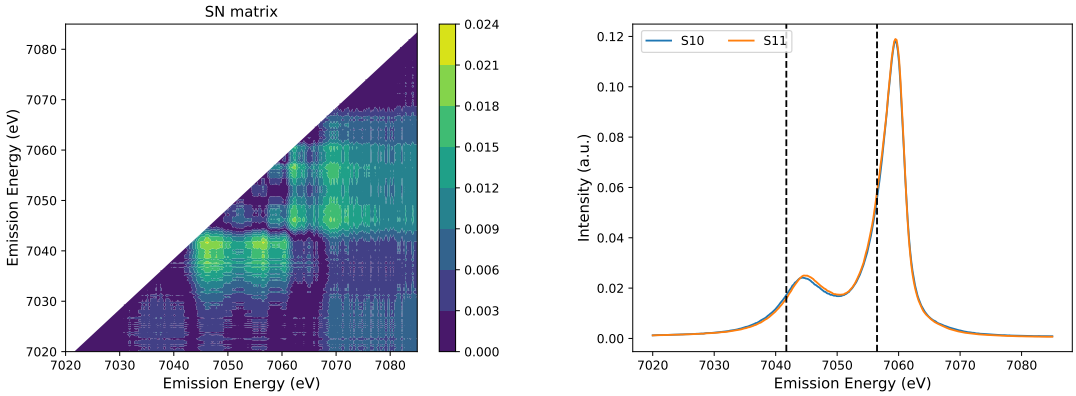

Figure 3.28: **Left**: Signal to noise matrix useful to identify the two emission energies that give the better contrast of the intensity ratios for compounds S10 and S11. **Right**: This is the plot of the emission spectra of the iron bearing compounds S10 and S11, there is the identification of the two best emission energies that give the maximum contrast of intensity ratios: 7.0417 keV and 7.0565 keV.

The last pair of minerals that is necessary to analyze in more detail is composed by the iron bearing compounds S10 (that contains traces of iron) and S11 (Olivine). In particular in Figure 3.28 it is plotted the signal to noise matrix and the K_β emission lines of S10 and S11. Also in this case the two emission lines are quite similar but it is possible to find two emission energies for which the intensity ratios of the two compounds are distinguishable: 7.0417 keV and 7.0565 keV. Also in this case the signal to noise matrix does not show a pronounced unique peak and its value is quite small (but higher than the case s9 and S10). No measurement was performed at these two energies, but it is possible to calculate from the spectra of the two compounds the intensity ratios that would be obtained: the intensity ratio of is S10 is 3.21 and the intensity ratio of S11 is 3.68. These intensity ratios are not as close as the intensity ratios of the compounds S9 and S10, but in any case a long counting at the right emission energies is needed in order to differentiate between the two compounds (in order to have a signal to noise of 10 it is necessary to have around 14700 counts on roi1 of S10 and 13500 counts on roi1 of S11. If instead the K_α emission lines are compared less counts are needed in order to get such signal to noise: around 2000 counts on roi1 of S10 and around 2600 counts on roi1 of S11).

At this point it is possible to plot the two dimensional image that represents the scan through the third region (see Figure 3.29) when the emission energies calculated for that region are used. The colors indicate the values of the intensity ratios, S9 and S10 have the same color because they have indistinguishable intensity ratios at the two emission energies used for the scan (the intensity ratio is also quite similar to S11 even though the color is slightly different, it is necessary to take into account

the fact that there is an error bar on the intensity ratios that in this two dimensional plot is not showed).

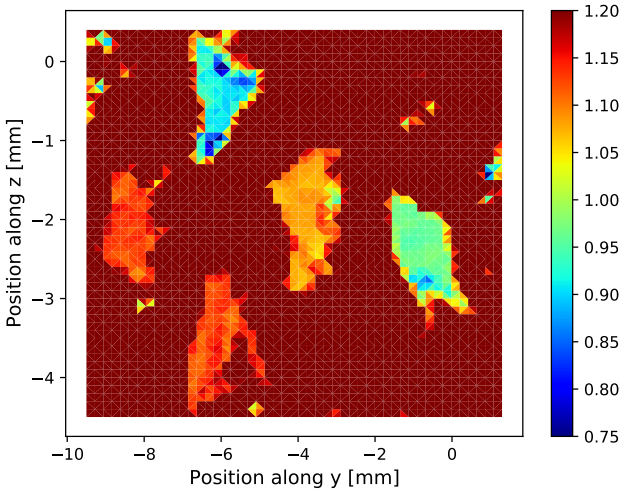

Figure 3.29: Two dimensional image of the third region, the intensity ratio roi2/roi1 is indicated with different colors depending on the value. It is possible to see that S9 and S10, that contain just traces of iron, have the same intensity ratio (in dark orange) since it is probable that they have the same iron concentration, oxidation and spin states. S8 is in light blue, S11 in orange and S12 in green.

3.5.4 Fourth region

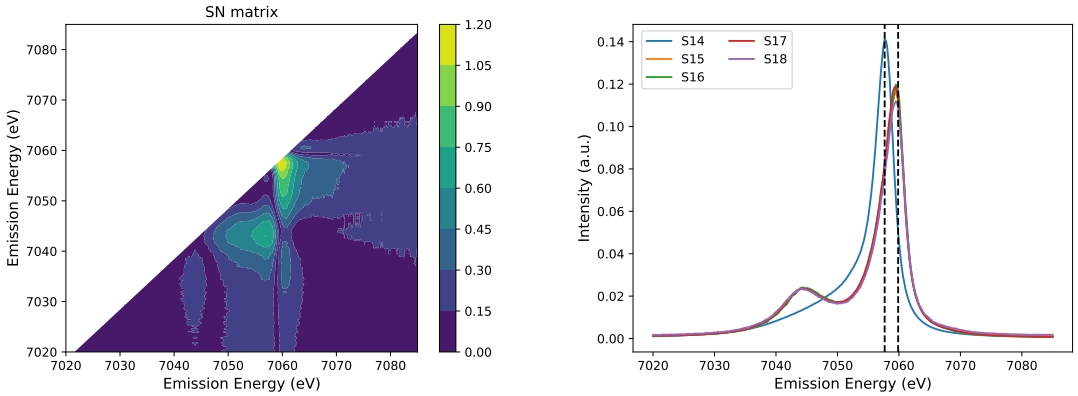

Figure 3.30: **Left**: Signal to noise matrix useful to identify the two emission energies that give the better contrast of the intensity ratios. **Right**: This is the plot of the emission spectra of the iron bearing compounds contained in the fourth region, moreover there is the identification of the two best emission energies that give the maximum contrast of intensity ratios: 7.0577 keV and 7.0599 keV.

In the fourth and last region of the Astimex standard there are the minerals denominated from S14 to S18, the two best emission energies identified thanks to the Python code are: 7.0577 keV and 7.0599 keV (see Figure 3.30 for the signal to noise

matrix and the plot of the K_β emission lines). A vertical and horizontal scan through this region are done in order to understand if these two emission energies allow to have distinguishable intensity ratios for the iron bearing compounds contained inside the region (see Figure 3.31).

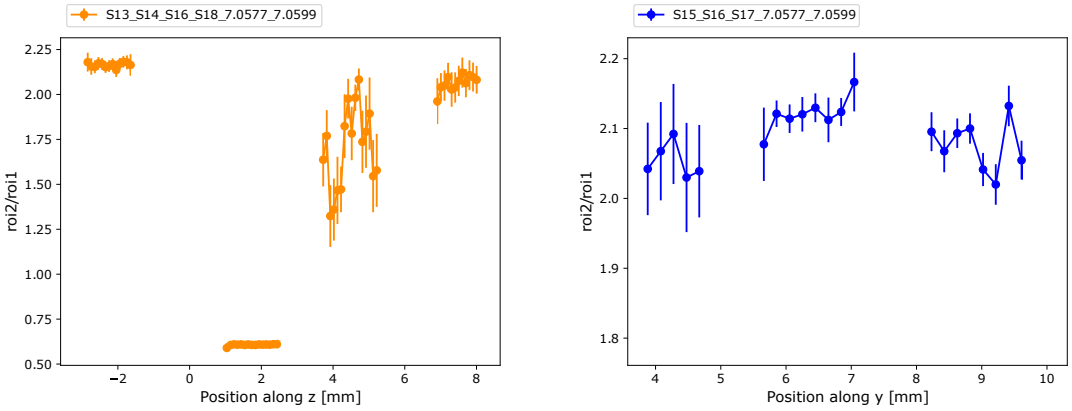

Figure 3.31: **Left**: This is the plot of the ratio of the intensities roi2/roi1 recorded by scanning a vertical line that passed through the minerals S13, S14, S16 (the line scan did not exactly centered this mineral) and S18. **Right**: This is the plot of the ratio of the intensities roi2/roi1 recorded by scanning a horizontal line that passed through the minerals S15, S16 and S17.

It is quite clear that by setting the spectrometer to the two emission energies found with the Python code it is not possible to obtain all distinguishable intensity ratios. In particular the iron bearing compounds S15 (that contains traces of iron), S16 (Kaersutite) and S18 (that contains traces of iron) seem to have the same intensity ratios that is around 1.1. Since their intensity ratios cannot be distinguished using the previously calculated emission energies, it is necessary to study each pair of these iron bearing compounds separately. From the comparison of S15 with S16 (see Figure 3.32), S15 with S18 (see Figure 3.33) and S16 with S18 (see Figure 3.34) it is possible to see that the K_β emission lines of these three compounds are very similar and the signal to noise matrix does not give a pronounced unequivocal peak and its value is very small (the emission lines are too similar to show a high enough contrast). So in principle it is possible to distinguish between these three compounds by measuring them in pair at the right energies and for a long time in order to decrease the error on the ratio. If S15 and S16 are compared it is necessary to have around 9000 counts on roi1 of S15 and around 8000 counts on roi1 of S16 in order to have a signal to noise of 10 (if the K_α lines are compared the counts needed are around 80000 on roi1 of S15 and around 81000 on roi1 of S16); if S15 and S18 are compared it is necessary to have around 58000 counts on roi1 of S15 and around 55500 counts on roi1 of S18 in order to have a signal to noise of 10 (if the K_α lines are compared the counts needed are around 11000 on roi1 of S15 and around 12000 on roi1 of S18); if S16 and S18 are compared it is necessary to have around 8000 counts on roi1 of S16 and around 7000 counts on roi1 of S18 in order to have a signal to noise of 10 (if the K_α lines are compared the counts needed are around 24600 on roi1 of S16 and around 25800 on roi1 of S18).

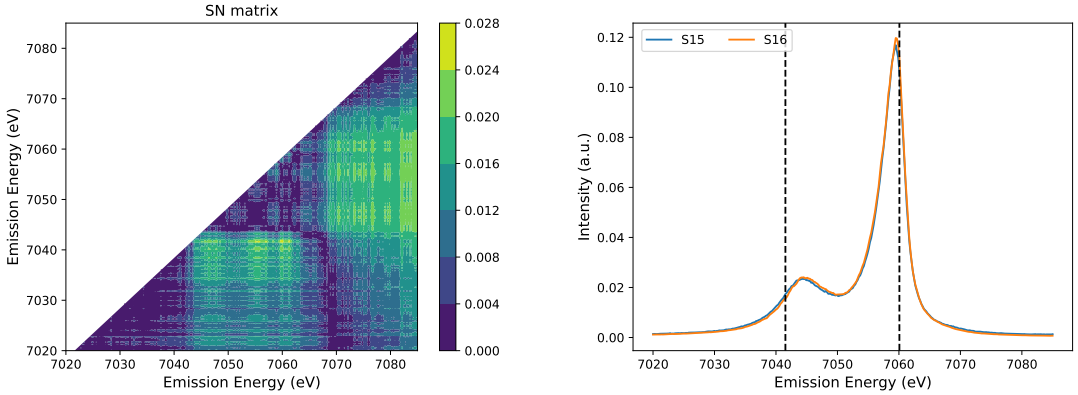

Figure 3.32: **Left**: Signal to noise matrix useful to identify the two emission energies that give the better contrast of the intensity ratios. **Right**: This is the plot of the emission spectra of the iron bearing compounds S15 and S16, there is the identification of the two best emission energies that give the maximum contrast of intensity ratios: 7.0415 keV and 7.0601 keV.

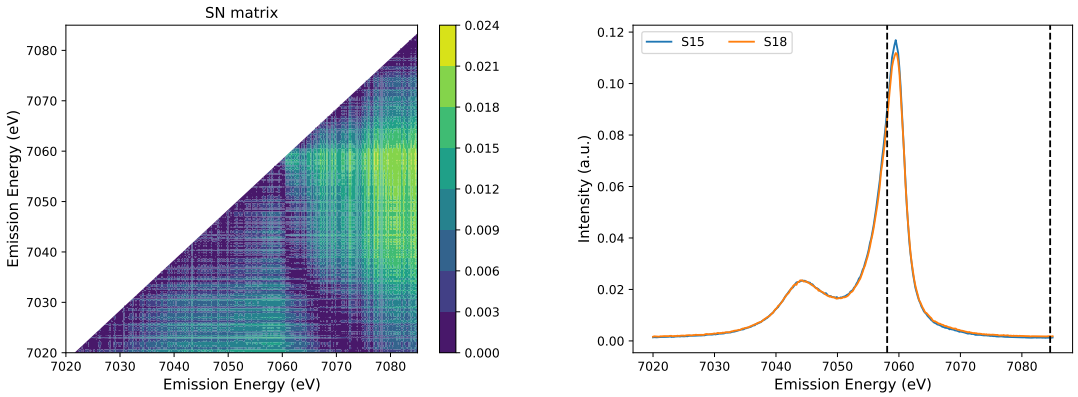

Figure 3.33: **Left**: Signal to noise matrix useful to identify the two emission energies that give the better contrast of the intensity ratios. **Right**: This is the plot of the emission spectra of the iron bearing compounds S15 and S18, there is the identification of the two best emission energies that give the maximum contrast of intensity ratios: 7.0581 keV and 7.0846 keV .

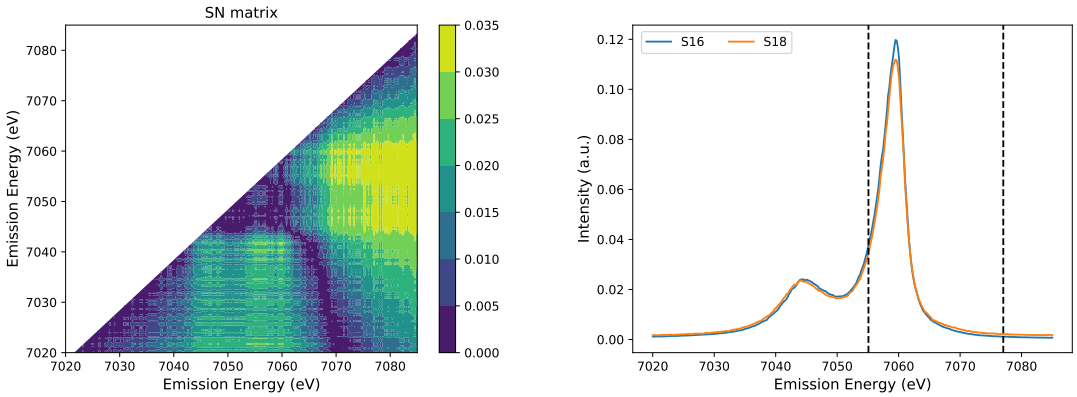

Figure 3.34: **Left**: Signal to noise matrix useful to identify the two emission energies that give the better contrast of the intensity ratios. **Right**: This is the plot of the emission spectra of the iron bearing compounds S16 and S18, there is the identification of the two best emission energies that give the maximum contrast of intensity ratios: 7.0569 keV and 7.0692 keV.

Note: while scanning the two dimensional plot of the fourth region the front end closed and some data were missing so for this reason the two dimensional image is not reported in this thesis since it cannot give a useful visualization of the data.

3.5.5 Scan of the whole sample

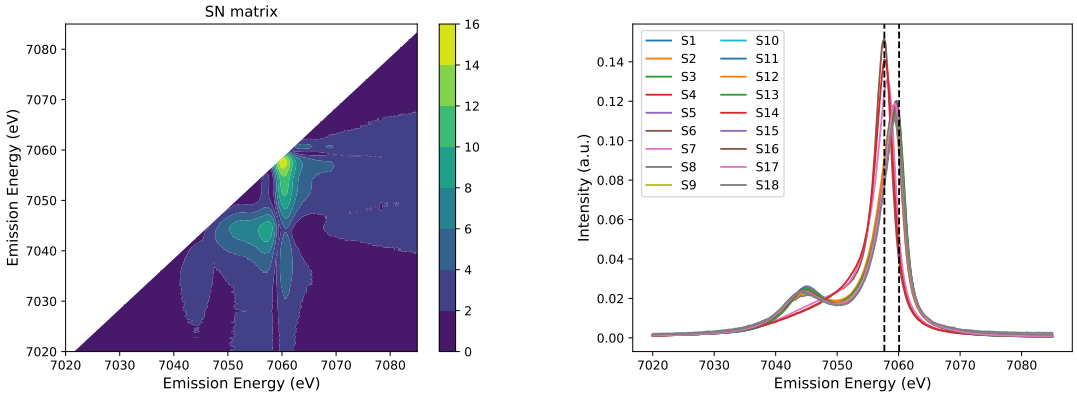

Figure 3.35: **Left**: The signal to noise matrix due to the comparison of the K_β XES spectra of all the 18 iron bearing minerals. **Right**: This is the plot of the K_β lines of all the iron bearing minerals in the Astimex with the identification of the two energies that give the maximum contrast between the intensity ratios: 7.0577 keV and 7.0601 keV.

For completeness the whole Astimex sample was scanned even though it was quite clear from the previous analysis that it is impossible to find two emission energies that allow to distinguish between all the iron bearing compounds in the resin. But in any case a full scan was performed at the following emission energies: 7.0577 keV and 7.0601 keV (computed thanks to the Python code). In Figure 3.35 the final signal to noise matrix and the K_β emission lines of all 18 iron bearing minerals

inside the sample are plotted.
As it has been seen previously, the third and the fourth region are the most difficult to differentiate since the iron bearing compounds present have similar K_β lines; for this reason some vertical and horizontal line scans (see Figure 3.36) through these two regions were measured in order to understand if it was possible to distinguish between at least between some of these compounds. The iron bearing compounds of the third region S9, S10 and S11 seem indistinguishable because their intensity ratio roi2/roi1 is around 2.05 and the same for the compounds of the fourth region S15, S16, S17 and S18, that have an intensity ratio around 2.

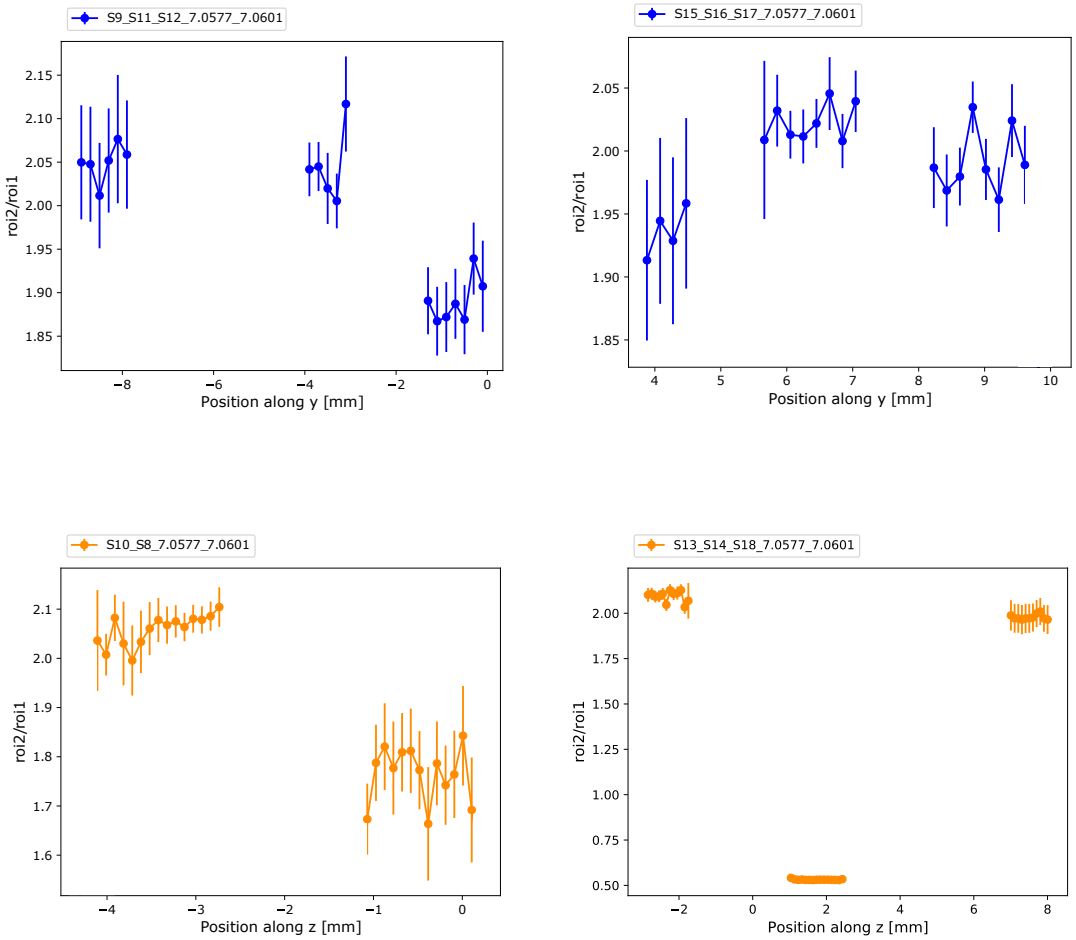

Figure 3.36: **Left Top**: This is the plot of the ratio of the intensities roi2/roi1 recorded by scanning a horizontal line that passed through the minerals S9, S11 and S12. **Right Top**: This is the plot of the ratio of the intensities roi2/roi1 recorded by scanning a vertical line that passed through the minerals S15, S16 and S17. **Left Bottom**: This is the plot of the ratio of the intensities roi2/roi1 recorded by scanning a vertical line that passed through the minerals S10 and S18. **Right Bottom**: This is the plot of the ratio of the intensities roi2/roi1 recorded by scanning a vertical line that passed through the minerals S13, S14, S16 and S18 (S16 is missing because the scan did not pass through it).

The whole Astimex sample was then scanned by recording the intensities at the two emission energies calculated with the Python code. In particular in Figure 3.37 **Left** the value of the intensity roi1 is represented as a function of the position inside the sample; while in Figure 3.37 **Right** the ratio roi2/roi1 is represented as a function of the position in the sample. In this case only the minerals with roi1 above a certain threshold have been plotted. This last plot shows the chemical contrast of the iron bearing minerals and, as foreseen, the compounds S9, S10 and S11 are indistinguishable and the same happens for the compounds S15, S16, S17 and S18. At these two emission energies it is possible to clearly distinguish between Haematite and Magnetite (in yellow and in green in the figure on the **Right**) and between low and high spin compounds (blue and orange in figure on the **Right**).
The two emission energies that were used are obviously not ideal to distinguish every pair of compounds but in any case it is clear that this method can be an additional evaluation tool to discriminate the different chemical states of a certain analyte (in this case iron).

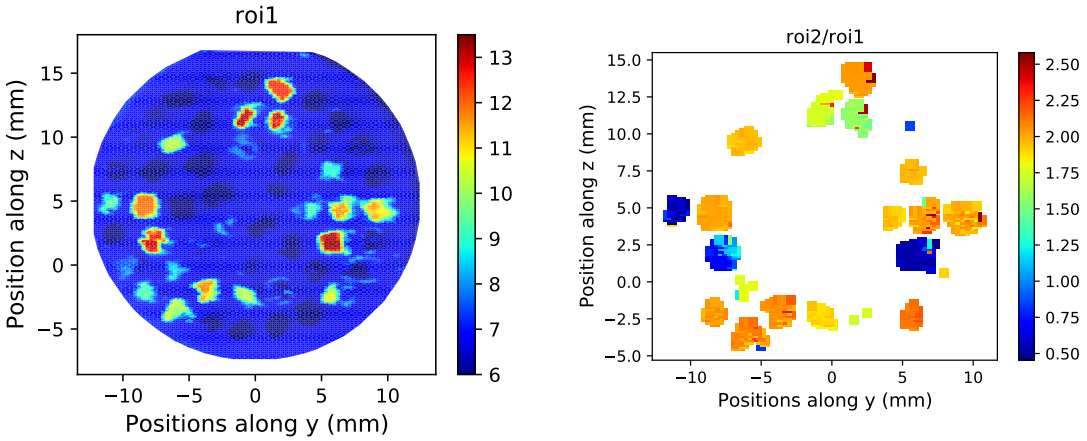

Figure 3.37: **Left**: Full scan of the Astimex standard where the colors indicate the value of the intensity roi1 (in logaritmic scale). This plot shows the position of the minerals. **Right**: Full scan of the sample, the colors indicate the value of the intensity ratio roi2/roi1 and in particular only the ratios given by intensities that are over a certain threshold are plotted in order to highlight the iron bearing minerals and have a clearer colorbar. This plot shows the chemical contrast.

Conclusion

The method presented in this thesis has the aim to help quickly recognize the presence of a certain analyte (in this case iron) in different chemical environments without recording the whole X-ray emission spectrum, but just by looking at the intensity ratios corresponding to two wisely chosen emission energies.
In particular, the former objective was to find two emission energies at which the highest number of iron bearing compounds had distinguishable intensity ratios. If this had been possible, it would have been enough to sample the emission spectra of all iron bearing compounds at those two energies in order to recognize in which chemical state the iron is, since each value of the intensity ratio would be characteristic only of a certain compound. But in the end it appears that it is not possible to find two emission energies that allow to obtain distinguishable intensity ratios for all the iron bearing compounds. The reason why this is not feasible is because the Python code (see Chapter 2) used to identify the best energy compromise for more than two compounds does not necessarily give the maximum contrast between intensity ratios for all the combinations of different iron bearing compounds but just for the majority of them. Improvements to the code or maybe a better way to identify the two best emission energies, at which sampling the spectra when more of two compounds are considered, could be implemented.
Since it is not possible to use the same two emission energies to distinguish between all iron bearing compounds, it is necessary to know which compounds could be present in the sample under analysis in order to compare their tabulated emission spectra and find the best energy compromise. In general this method could be used to study those systems where the possible iron bearing compounds that could be present are already known as for example inside a catalytic reactor (that can contain metallic iron, iron oxide or iron with other ligands as carbon or nitrogen) where it could be interesting to analyze the distribution of the compounds. Another interesting application could involve the study of cultural heritage and in particular the colour degradation of paintings, that is mainly due to oxidation processes; also in this case the possible iron species are mostly known.
This method is an additional tool to study the system under consideration, it is a very fast technique and moreover allows to obtain meaningful chemical information by shining a lower dose of X-rays on the sample with respect to a full spectrum. This last characteristic is very important for radiation sensitive sample since radiation damage could be prevented. In conclusion, further studies could be performed to optimize this innovative technique that has many advantages and a broad range of possible applications.

Acknowledgements

I would like to thank my thesis advisor, Professor Giacomo Claudio Ghiringhelli, who gave me the opportunity to go abroad and work in an international and stimulating environment as the ESRF. Moreover my gratitude extends to my research supervisor Doctor Pieter Glatzel, who accepted me in his team at ID26 and introduced me to research.

Ringrazio la mia famiglia che ha creduto in me e mi ha spronato nei momenti di sconforto. Ringrazio gli amici di sempre e quelli incontrati sul percorso, che riescono sempre a farmi ritrovare un po' di leggerezza. Ma il più importante ringraziamento va ad Andrea che mi ha sempre sostenuta in questo percorso di studi e mi ha aiutata particolarmente nella stesura di questa tesi. Grazie per aver condiviso con me ogni giorno di questo percorso universitario!

Appendix A

All experimentally measured spectra

All the spectra that have been measured at the beamline ID26 are plotted.

A.1 K_β energy range

A.1.1 Valence to Core

It was possible to measure the valence to core emission spectrum that considers the relaxation of electrons close to the Fermi level (valence electrons) into 1s core holes. It is an emission spectroscopy (where the incoming beam is again at 7.2 keV) but at higher energies with respect to K_β lines; since the signal is very weak it is necessary to measure for a longer time. The measurement of this spectrum is quite complex because the number of points and the acquisition time must be different between the parts of the spectrum in order to retrieve most of the information. In particular the valence to core spectrum is divided in three parts:

- from 7.065 to 7.085 keV there is the final part of K_β line. In this part few points are taken and each point is theoretically counted for 1.5 seconds;
- from 7.085 to 7.114 keV there is the valence to core peak (elastic peak), many points are taken and each point is counted for long, theoretically 5 seconds. This because it is a weak signal;
- from 7.114 to 7.120 keV there is the background. Few points are taken but very long counts (theoretically 10 seconds) to reduce the background.

Moreover for the samples for which the intensity of the K_β line is low, these are the compounds that have a low concentration of iron, it is necessary to count longer (time per point is multiplied by a factor that increases with the decreasing of iron concentration) in order to have a detectable intensity. It is possible to plot the dead time corrected intensity, normalized to I02, with respect to the emission energy (see Figure A.1).

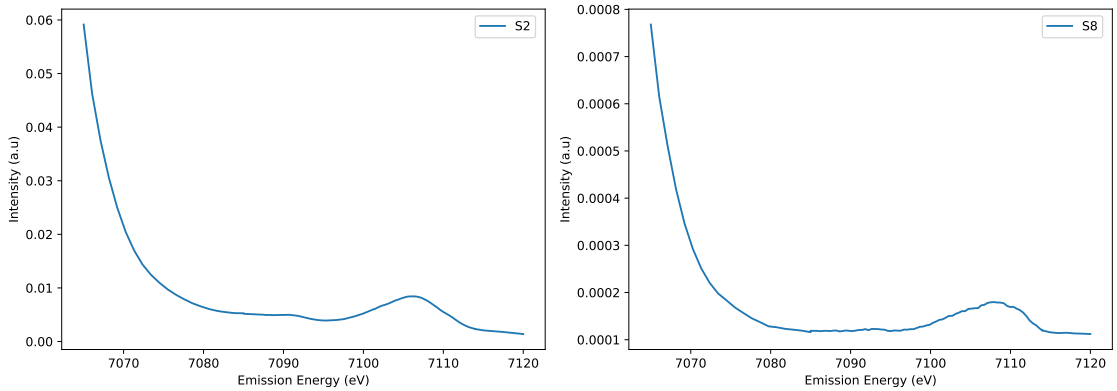

Figure A.1: **Left**: Valence to core X-ray emission spectrum of a compound with high intensity of the K_β peak, the intensity at the detector is normalized with respect to I02 in each point. **Right**: Valence to core X-ray emission spectrum of a compound with low intensity of the K_β peak, in this case it is necessary to count each point for a longer time in order to retrieve information because the intensity is very small.

A.1.2 X-rays Absorption Near Edge Spectroscopy (XANES) at the emission energy of the K_β peak

In XANES 1s electrons (Kedge) are excited above the Fermi level with a energy variable incoming beam and there will be relaxation processes with emission of photons that will be analyzed by the spectrometer. XANES spectra for the 18 iron bearing minerals inside the Astimex are computed, for each mineral the spectrometer sits at the energy of the peak of its K_β line retrieved from the previous XES spectra (see Table A.1).

Compound	Energy of the K_β XES peak [eV]
S1	7059.68
S2	7059.08
S3	7059.08
S4	7059.68
S5	7059.68
S6	7057.68
S7	7058.08
S8	7059.28
S9	7059.68
S10	7059.48
S11	7059.48
S12	7059.48
S13	7059.68
S14	7057.68
S15	7059.48
S16	7059.48
S17	7059.48
S18	7059.48

Table A.1: Energy at which there is the peak of the K_β X-rays emission line for each compound, when recording the XANES of a certain compound the spectrometer sits at this energy.

The intensity of each K_β peak will be different depending on the Fe concentration of the sample and if the mineral has an high concentration of iron it is enough to scan for few seconds (30 seconds) while it is needed a longer time to scan low Fe concentrated minerals in order to get a quality of the spectra comparable to the highly concentrated ones. As already said the ring was working in 16 bunch mode and so the photons arriving on the detector saturated it and so a dead time correction of the intensity is needed to retrieve the good intensity. Moreover it is necessary to put an attenuator (it's an Al foil) that will attenuate the beam before it reaches the sample, in this way the detector saturation can be avoided (for low concentrated samples it is not necessary to insert the attenuator since the intensity is already low). It is possible to plot (see Figure A.2) the dead time corrected intensity reaching the detector, normalized in each point to the value I02, versus the incoming energy, in particular in figure it is plotted the average intensity between three different measurements.

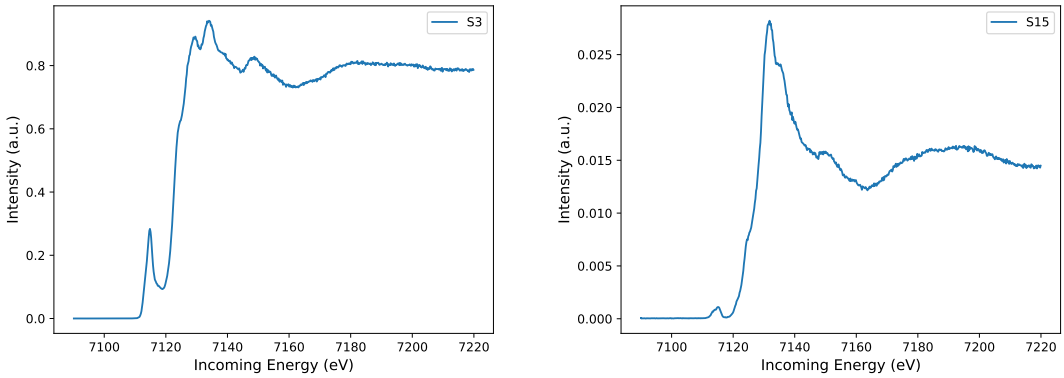

Figure A.2: **Left**: XANES spectrum for a high iron concentrated mineral. **Right**: XANES spectrum for a low iron concentrated mineral.

A.1.3 Spectra of the 18 iron bearing compounds

In particular from A.3 to A.20 the plots represent the K_β merged with valence to core spectra and XANES spectra with the spectrometer sitting at the energy of the K_β peak of that specific compound.

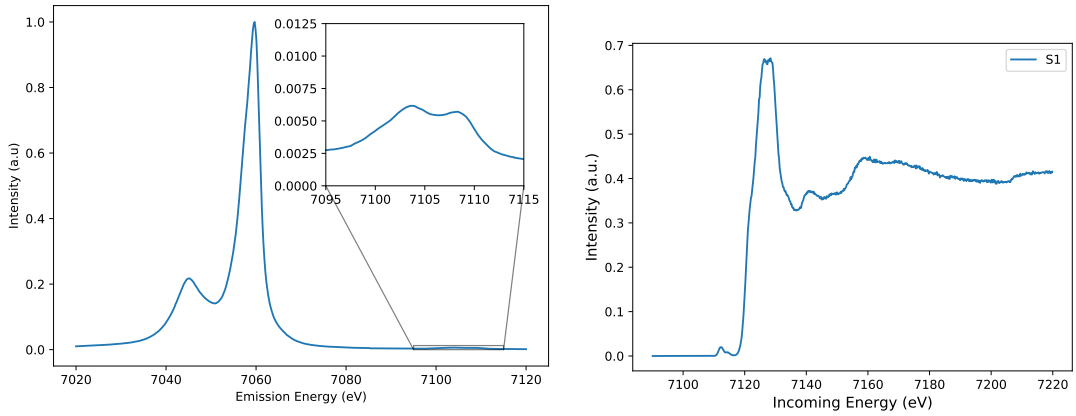

Figure A.3: **Left**: K_β and valence to core emission spectrum of mineral denominated S1, the intensity is normalized first to intensity I02 and than to the area below the curve. **Right**: XANES spectrum of mineral denominate S1, the intensity is just normalized to the intensity I02.

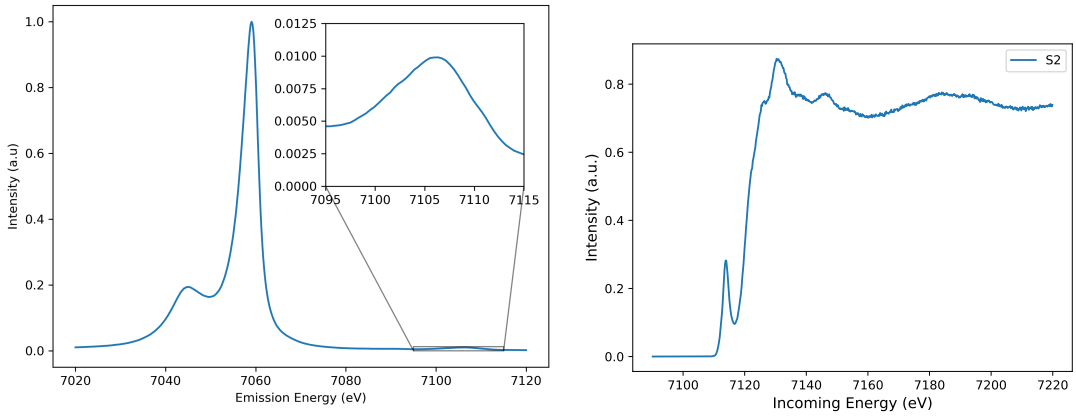

Figure A.4: **Left**: K_β and valence to core emission spectrum of mineral denominated S2, the intensity is normalized first to intensity I02 and than to the area below the curve. **Right**: XANES spectrum of mineral denominate S2, the intensity is just normalized to the intensity I02.

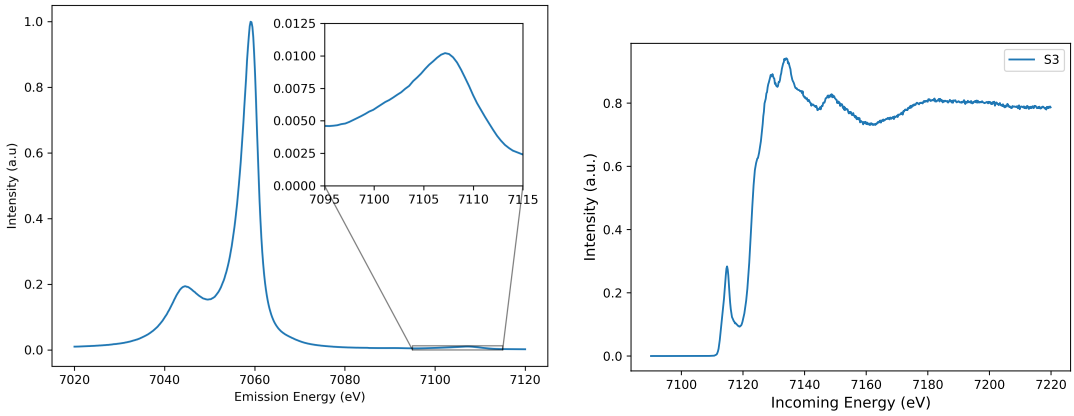

Figure A.5: **Left**: K_β and valence to core emission spectrum of mineral denominated S3, the intensity is normalized first to intensity I02 and than to the area below the curve. **Right**: XANES spectrum of mineral denominate S3, the intensity is just normalized to the intensity I02.

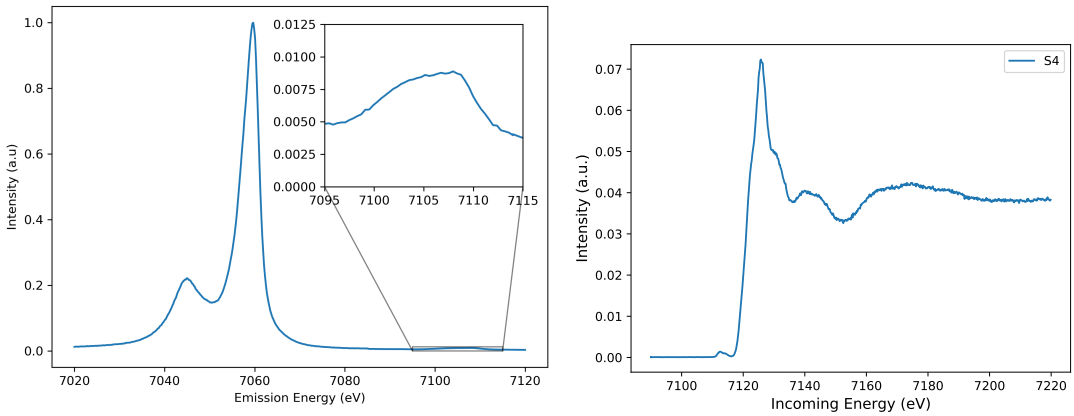

Figure A.6: **Left**: K_β and valence to core emission spectrum of mineral denominated S4, the intensity is normalized first to intensity I02 and than to the area below the curve. **Right**: XANES spectrum of mineral denominate S4, the intensity is just normalized to the intensity I02.

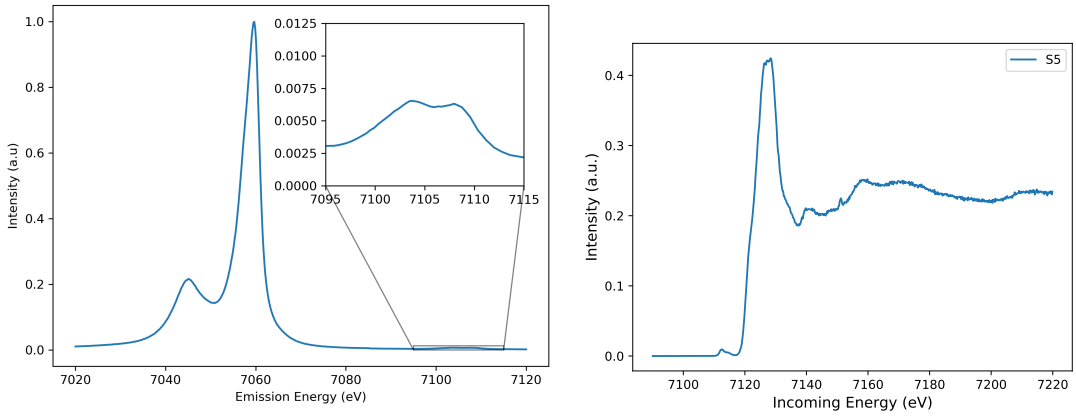

Figure A.7: **Left**: K_β and valence to core emission spectrum of mineral denominated S5, the intensity is normalized first to intensity I02 and than to the area below the curve. **Right**: XANES spectrum of mineral denominate S5, the intensity is just normalized to the intensity I02.

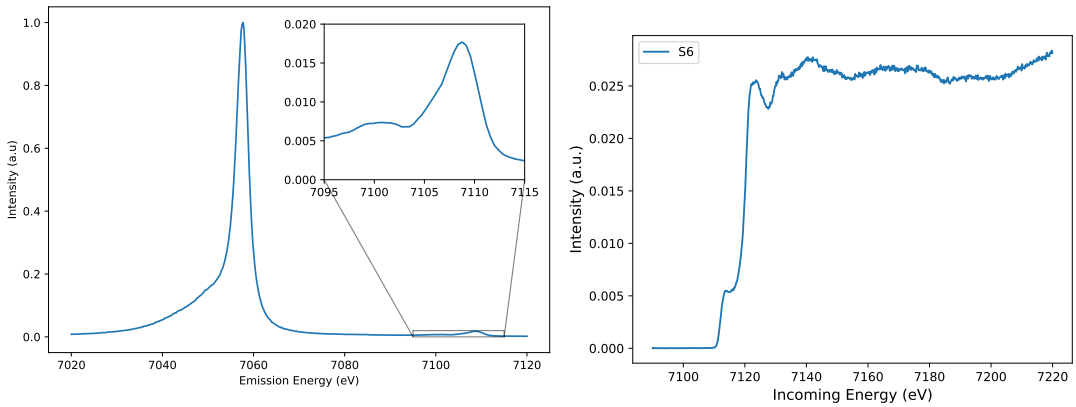

Figure A.8: **Left**: K_β and valence to core emission spectrum of mineral denominated S6, the intensity is normalized first to intensity I02 and than to the area below the curve. **Right**: XANES spectrum of mineral denominate S6, the intensity is just normalized to the intensity I02.

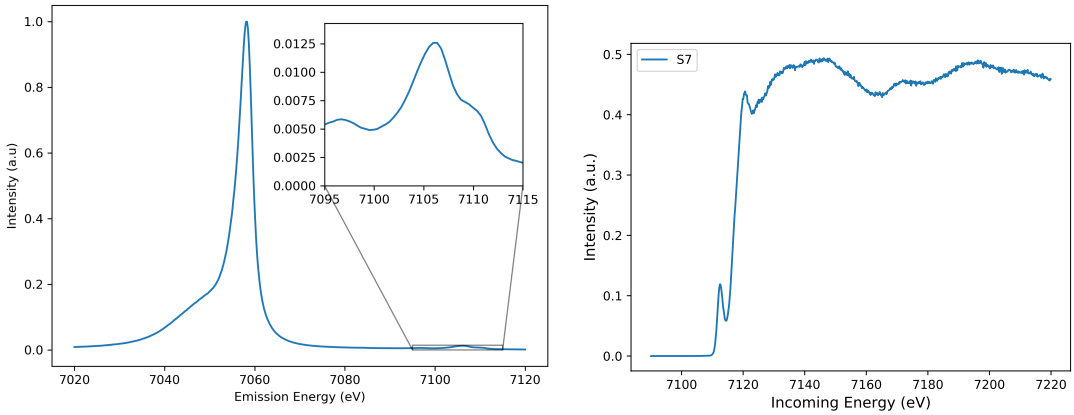

Figure A.9: **Left**: K_β and valence to core emission spectrum of mineral denominated S7, the intensity is normalized first to intensity I02 and than to the area below the curve. **Right**: XANES spectrum of mineral denominate S7, the intensity is just normalized to the intensity I02.

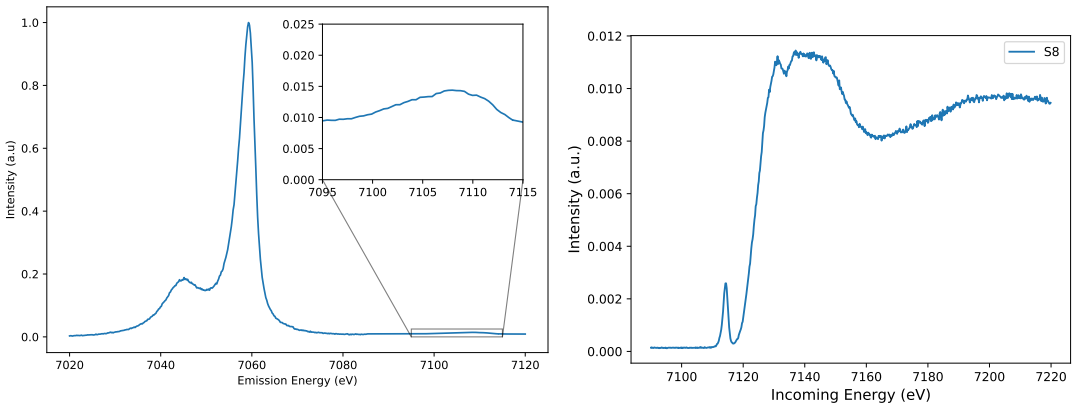

Figure A.10: **Left**: K_β and valence to core emission spectrum of mineral denominated S8, the intensity is normalized first to intensity I02 and than to the area below the curve. **Right**: XANES spectrum of mineral denominate S8, the intensity is just normalized to the intensity I02.

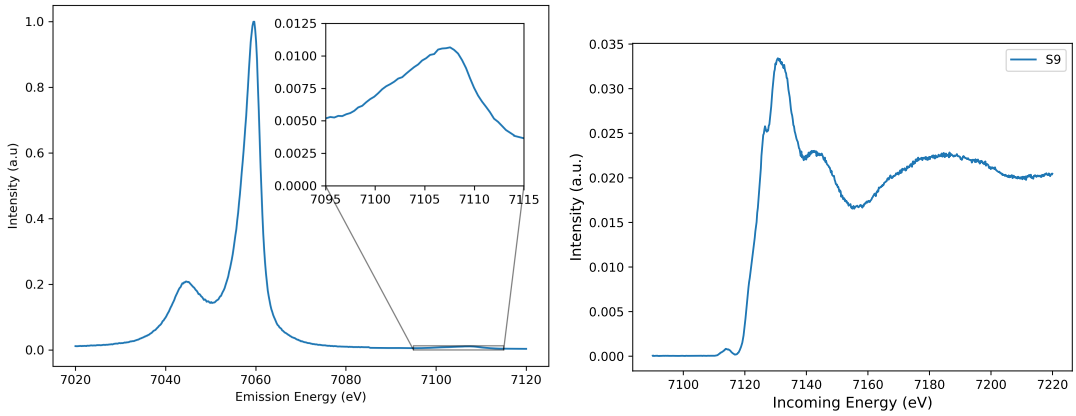

Figure A.11: **Left**: K_β and valence to core emission spectrum of mineral denominated S9, the intensity is normalized first to intensity I02 and than to the area below the curve. **Right**: XANES spectrum of mineral denominate S9, the intensity is just normalized to the intensity I02.

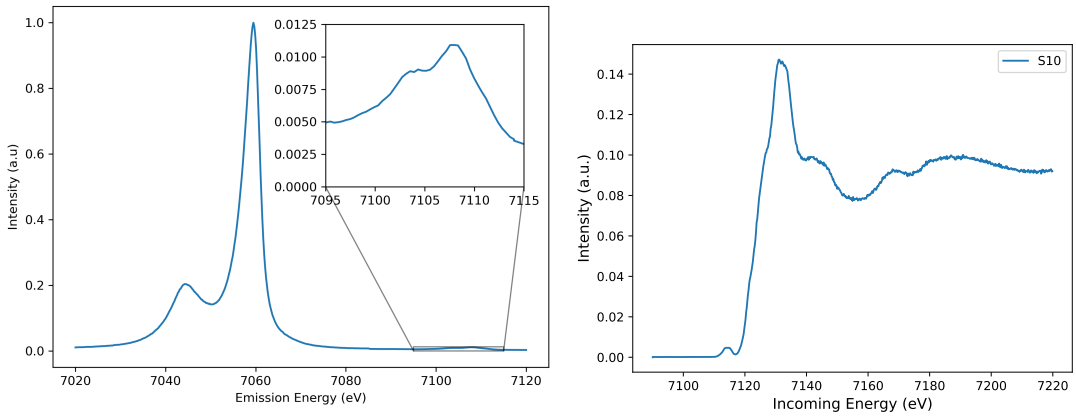

Figure A.12: **Left**: K_β and valence to core emission spectrum of mineral denominated S10, the intensity is normalized first to intensity I02 and than to the area below the curve. **Right**: XANES spectrum of mineral denominate S10, the intensity is just normalized to the intensity I02.

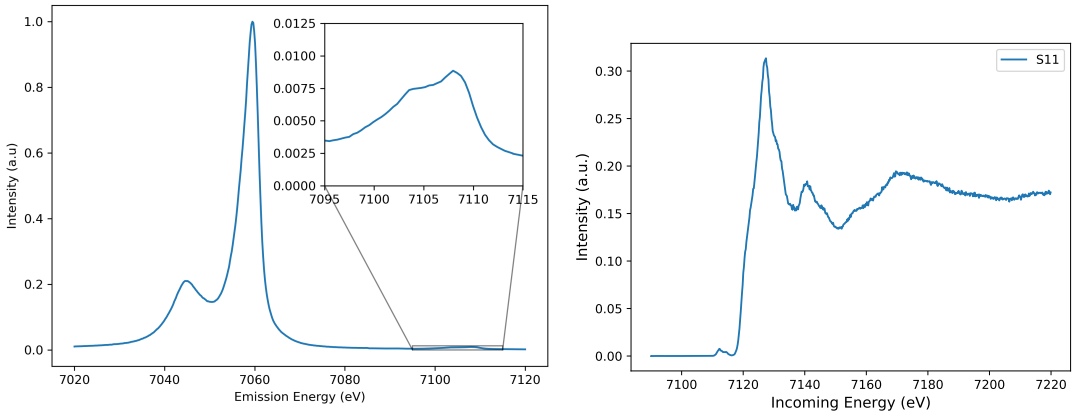

Figure A.13: **Left**: K_β and valence to core emission spectrum of mineral denominated S11, the intensity is normalized first to intensity I02 and than to the area below the curve. **Right**: XANES spectrum of mineral denominate S11, the intensity is just normalized to the intensity I02.

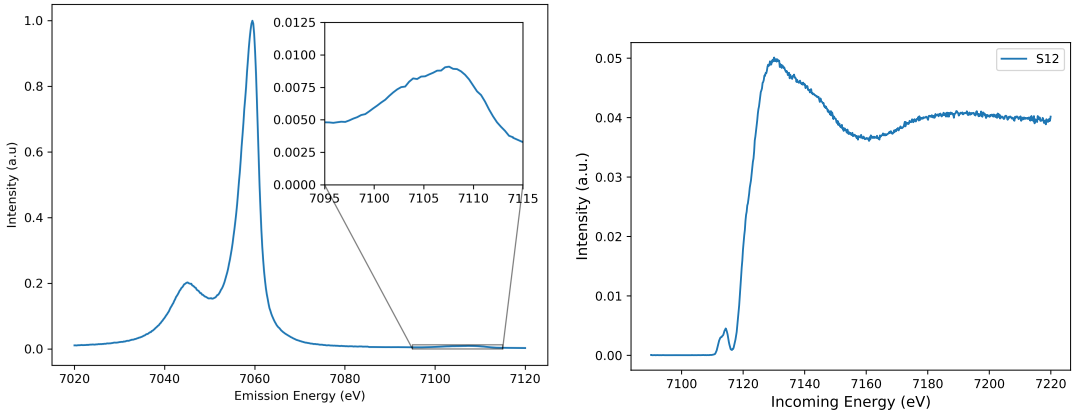

Figure A.14: **Left**: K_β and valence to core emission spectrum of mineral denominated S12, the intensity is normalized first to intensity I02 and than to the area below the curve. **Right**: XANES spectrum of mineral denominate S12, the intensity is just normalized to the intensity I02.

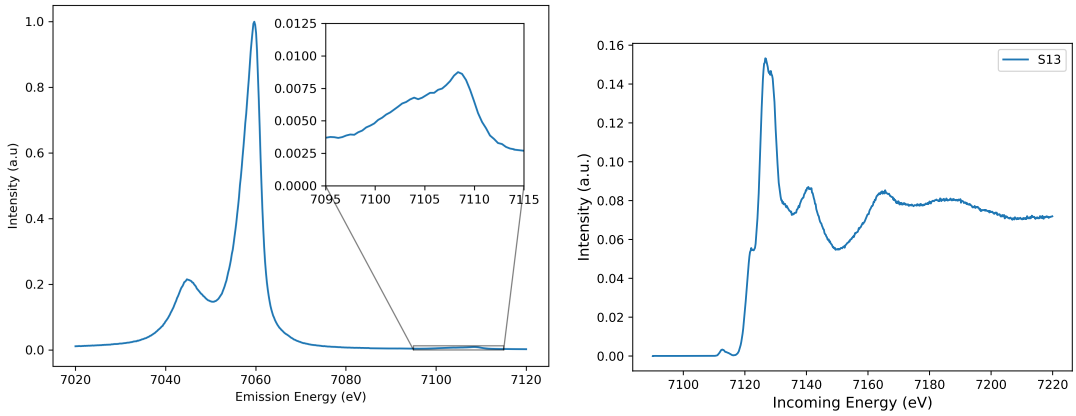

Figure A.15: **Left**: K_β and valence to core emission spectrum of mineral denominated S13, the intensity is normalized first to intensity I02 and than to the area below the curve. **Right**: XANES spectrum of mineral denominate S13, the intensity is just normalized to the intensity I02.

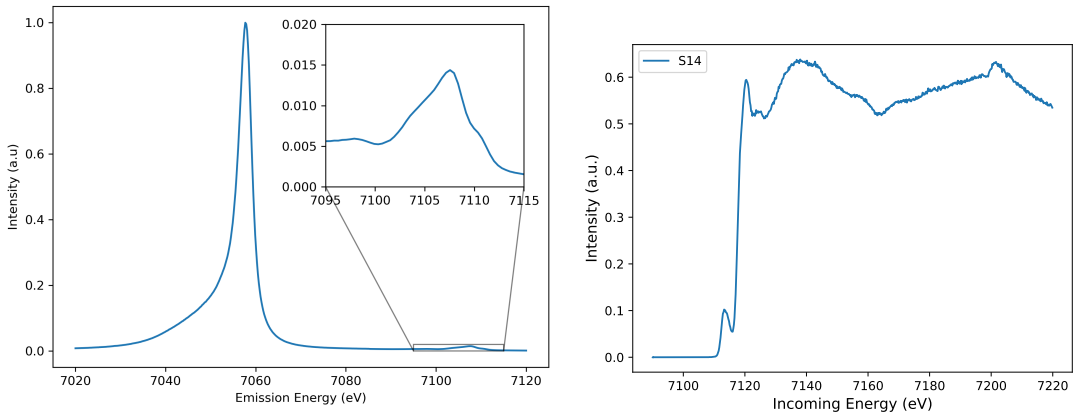

Figure A.16: **Left**: K_β and valence to core emission spectrum of mineral denominated S14, the intensity is normalized first to intensity I02 and than to the area below the curve. **Right**: XANES spectrum of mineral denominate S14, the intensity is just normalized to the intensity I02.

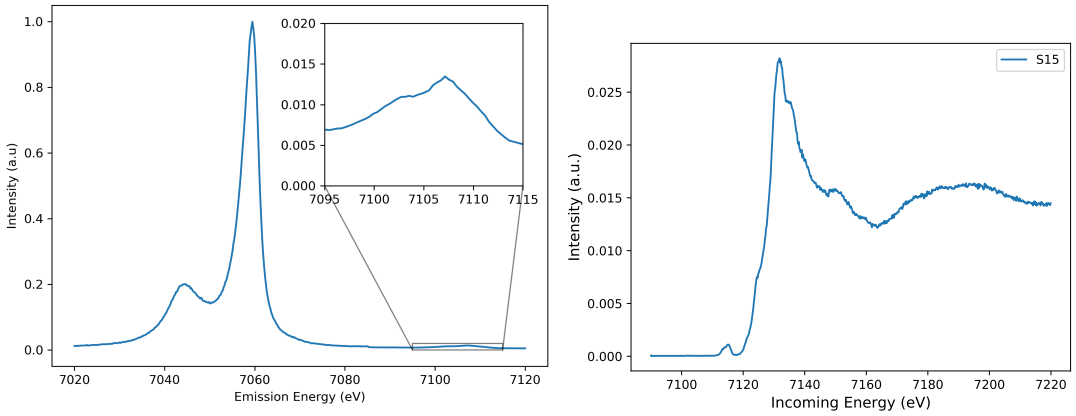

Figure A.17: **Left**: K_β and valence to core emission spectrum of mineral denominated S15, the intensity is normalized first to intensity I02 and than to the area below the curve. **Right**: XANES spectrum of mineral denominate S15, the intensity is just normalized to the intensity I02.

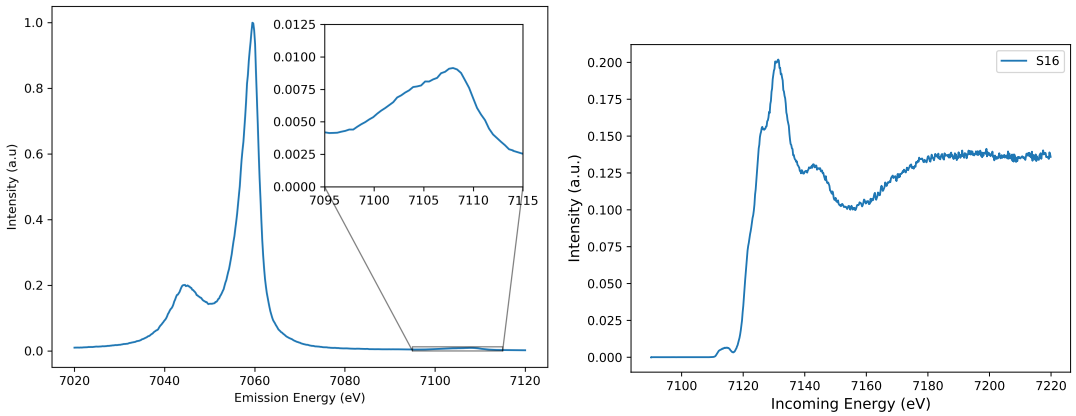

Figure A.18: **Left**: K_β and valence to core emission spectrum of mineral denominated S16, the intensity is normalized first to intensity I02 and than to the area below the curve. **Right**: XANES spectrum of mineral denominate S16, the intensity is just normalized to the intensity I02.

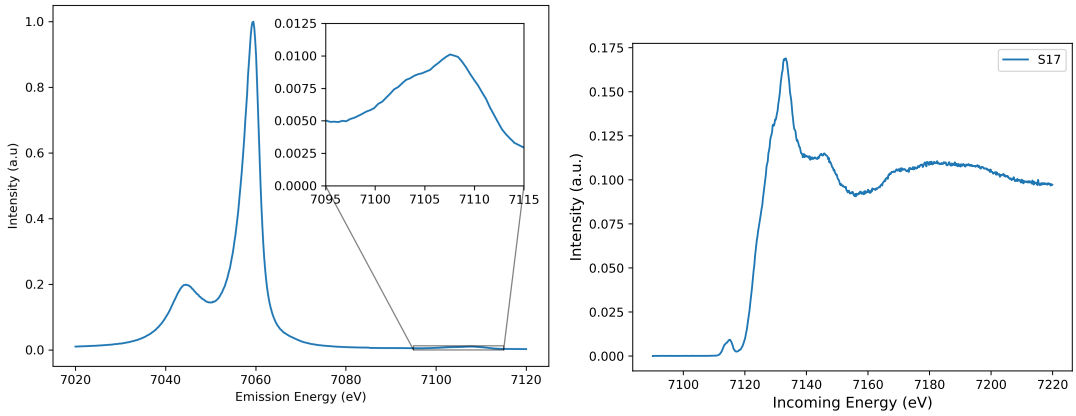

Figure A.19: **Left**: K_β and valence to core emission spectrum of mineral denominated S17, the intensity is normalized first to intensity I02 and than to the area below the curve. **Right**: XANES spectrum of mineral denominate S17, the intensity is just normalized to the intensity I02.

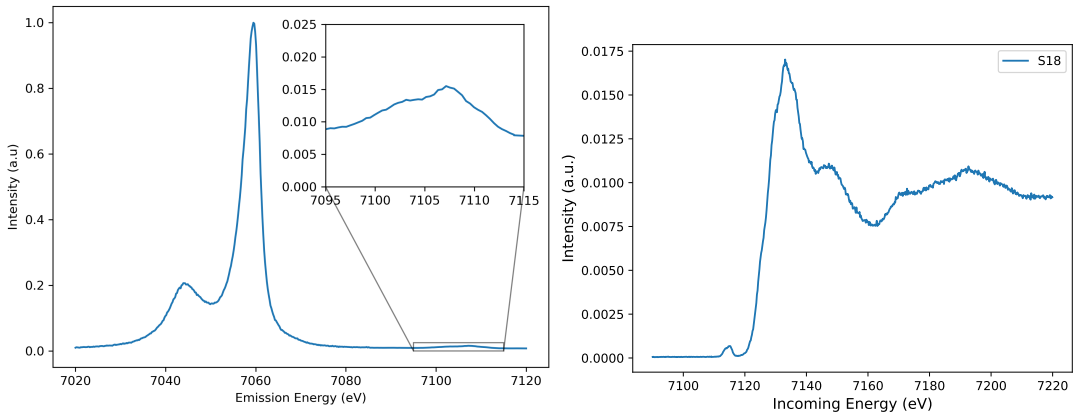

Figure A.20: **Left**: K_β and valence to core emission spectrum of mineral denominated S18, the intensity is normalized first to intensity I02 and than to the area below the curve. **Right**: XANES spectrum of mineral denominate S18, the intensity is just normalized to the intensity I02.

A.2 K_α energy range

A.2.1 X-rays Absorption Near Edge Spectroscopy (XANES) at the emission energy of the K_α peak

In XANES 1s electrons (Kedge) are excited above the Fermi level with a energy variable incoming beam and there will be relaxation processes with emission of photons that will be analyzed by the spectrometer. XANES spectra for the 18 iron bearing minerals inside the Astimex are computed, for each mineral the spectrometer sits at the energy of the peak of its K_α line retrieved from the previous XES spectra (see Table A.2). Each maximum is measured for 120 seconds.

Compound	Energy of the K_α XES peak [eV]
S1	6403.86
S2	6403.86
S3	6404.26
S4	6404.26
S5	6403.86
S6	6403.47
S7	6404.26
S8	6403.86
S9	6403.86
S10	6403.86
S11	6403.66
S12	6404.26
S13	6403.86
S14	6404.26
S15	6404.26
S16	6404.26
S17	6403.86
S18	6403.86

Table A.2: Energy at which there is the peak of the K_β X-rays emission line for each compound, when recording the XANES of a certain compound the spectrometer sits at this energy.

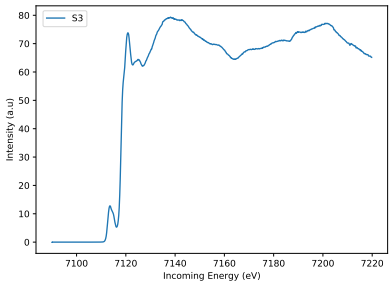

Figure A.21: **Left**: XANES at the compound denominated S3, the intensity is normalized to the intensity I02.

It is possible to plot (see Figure A.21) the dead time corrected intensity, normalized to the incoming flux I02, versus the incoming energy; in particular in figure it is plotted the average intensity between three different measurements.

A.2.2 Spectra of the 18 iron bearing compounds

In particular from A.22 to A.39 the spectra represent the K_α emission lines and XANES spectra with the spectrometer sitting at the energy of the K_α peak of that specific compound.

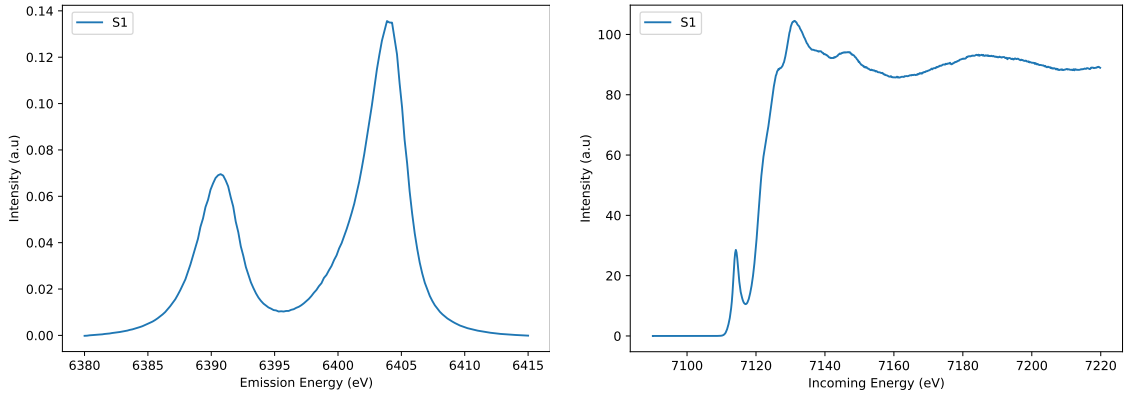

Figure A.22: **Left**: K_α emission spectrum of mineral denominated S1, the intensity is normalized first to intensity I02 and than to the area below the curve. **Right**: XANES spectrum of mineral denominate S1, the intensity is just normalized to the intensity I02.

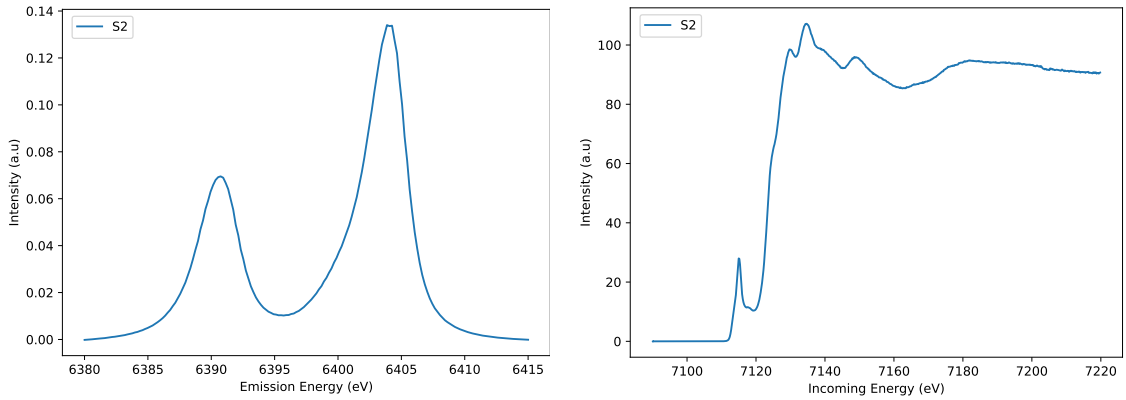

Figure A.23: **Left**: K_α emission spectrum of mineral denominated S2, the intensity is normalized first to intensity I02 and than to the area below the curve. **Right**: XANES spectrum of mineral denominate S2, the intensity is just normalized to the intensity I02.

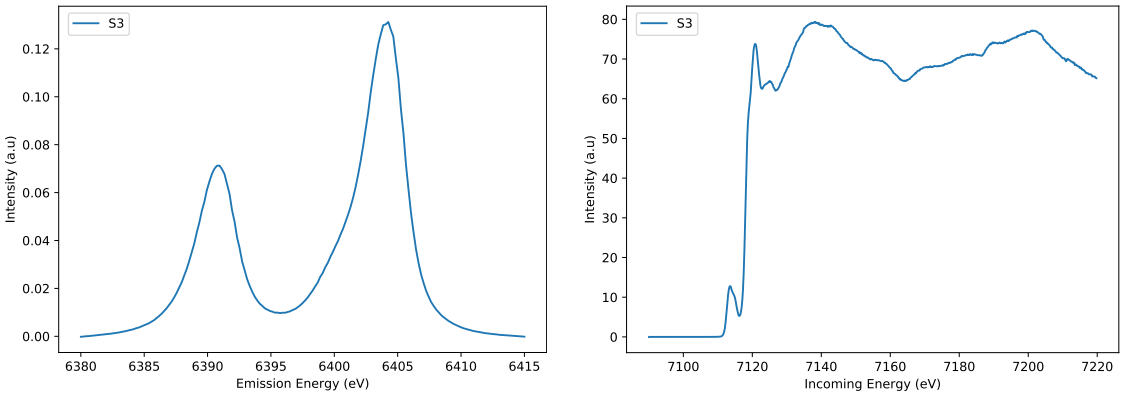

Figure A.24: **Left**: K_α emission spectrum of mineral denominated S3, the intensity is normalized first to intensity I02 and than to the area below the curve. **Right**: XANES spectrum of mineral denominate S3, the intensity is just normalized to the intensity I02.

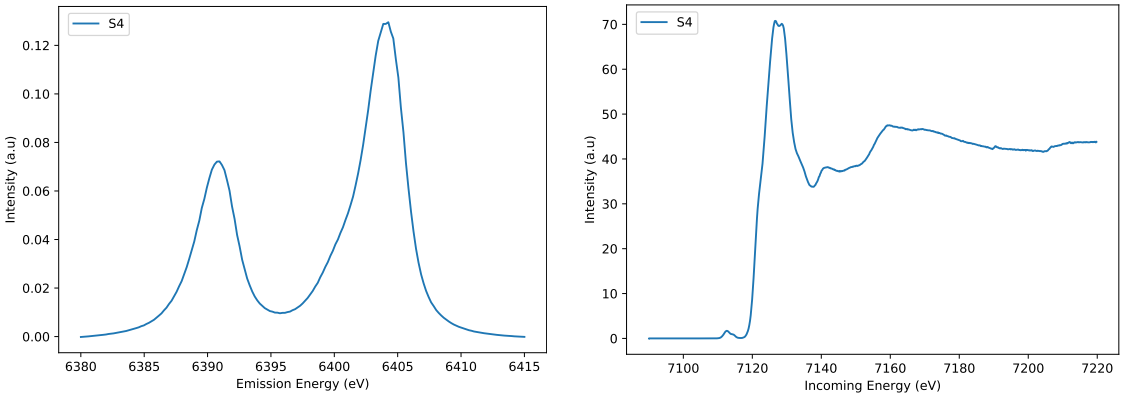

Figure A.25: **Left**: K_α emission spectrum of mineral denominated S4, the intensity is normalized first to intensity I02 and than to the area below the curve. **Right**: XANES spectrum of mineral denominate S4, the intensity is just normalized to the intensity I02.

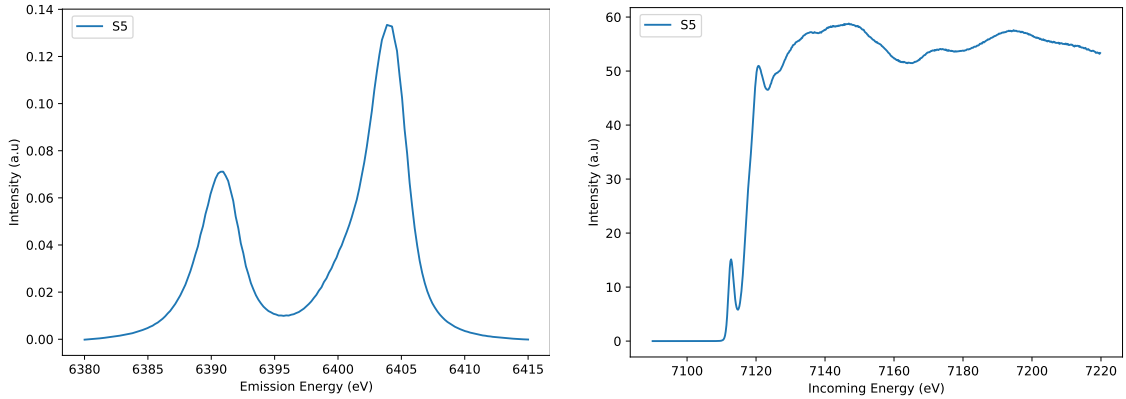

Figure A.26: **Left**: K_α emission spectrum of mineral denominated S5, the intensity is normalized first to intensity I02 and than to the area below the curve. **Right**: XANES spectrum of mineral denominate S5, the intensity is just normalized to the intensity I02.

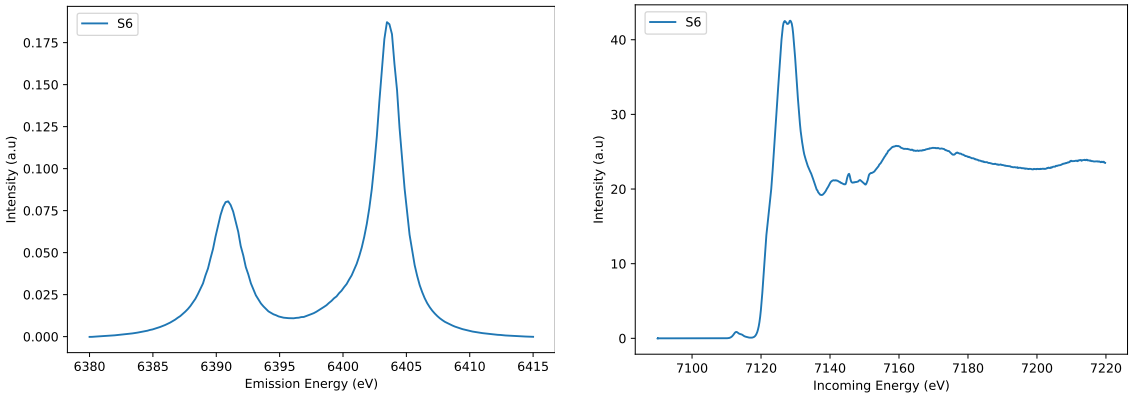

Figure A.27: **Left**: K_α emission spectrum of mineral denominated S6, the intensity is normalized first to intensity I02 and than to the area below the curve. **Right**: XANES spectrum of mineral denominate S6, the intensity is just normalized to the intensity I02.

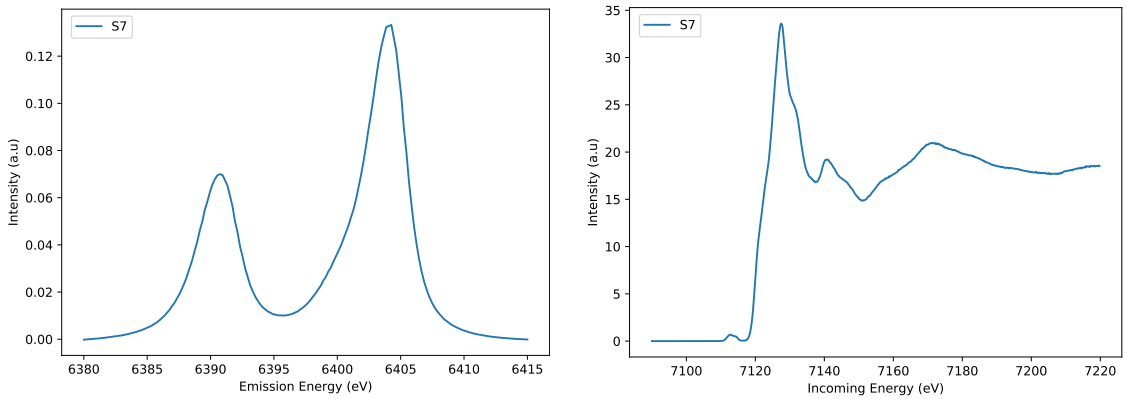

Figure A.28: **Left**: K_α emission spectrum of mineral denominated S7, the intensity is normalized first to intensity I02 and than to the area below the curve. **Right**: XANES spectrum of mineral denominate S7, the intensity is just normalized to the intensity I02.

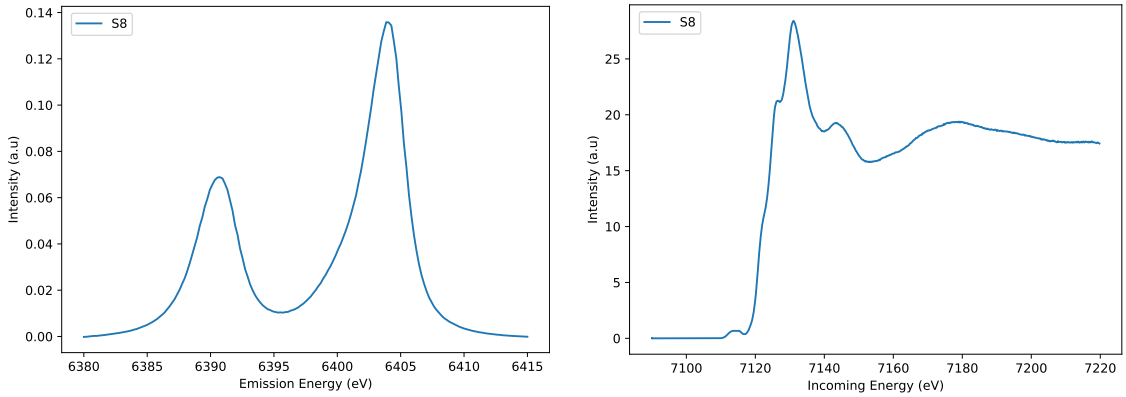

Figure A.29: **Left**: K_α emission spectrum of mineral denominated S8, the intensity is normalized first to intensity I02 and than to the area below the curve. **Right**: XANES spectrum of mineral denominate S8, the intensity is just normalized to the intensity I02.

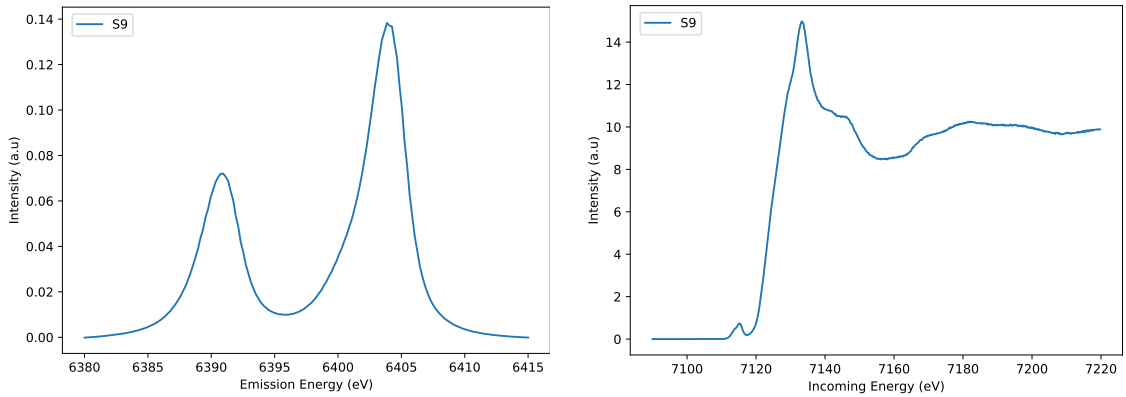

Figure A.30: **Left**: K_α emission spectrum of mineral denominated S9, the intensity is normalized first to intensity I02 and than to the area below the curve. **Right**: XANES spectrum of mineral denominate S9, the intensity is just normalized to the intensity I02.

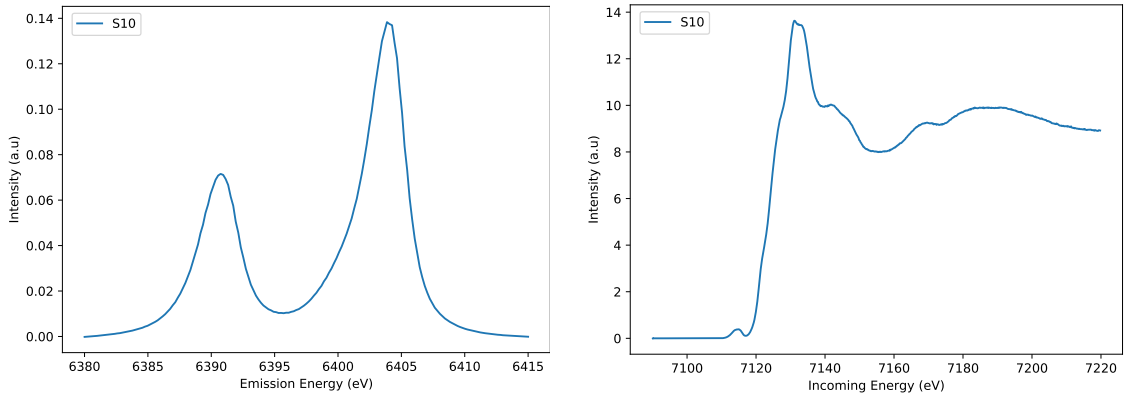

Figure A.31: **Left**: K_α emission spectrum of mineral denominated S10, the intensity is normalized first to intensity I02 and than to the area below the curve. **Right**: XANES spectrum of mineral denominate S10, the intensity is just normalized to the intensity I02.

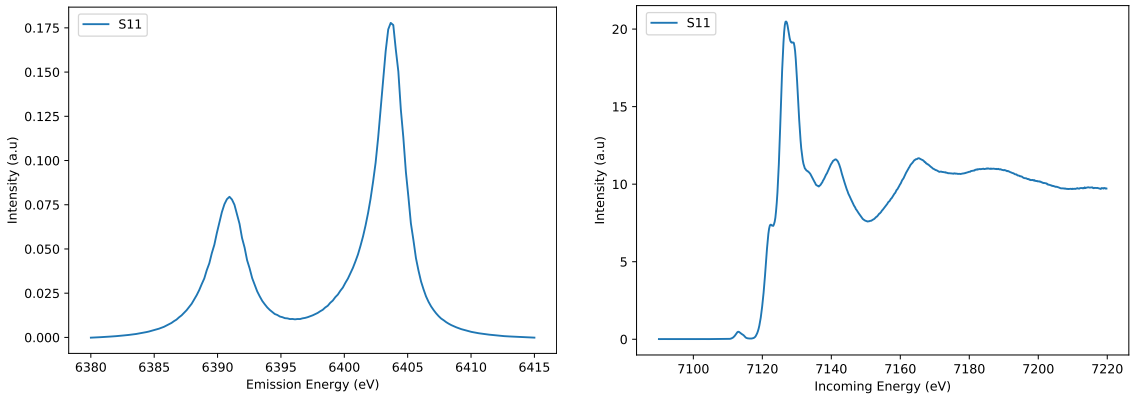

Figure A.32: **Left**: K_α emission spectrum of mineral denominated S11, the intensity is normalized first to intensity I02 and than to the area below the curve. **Right**: XANES spectrum of mineral denominate S11, the intensity is just normalized to the intensity I02.

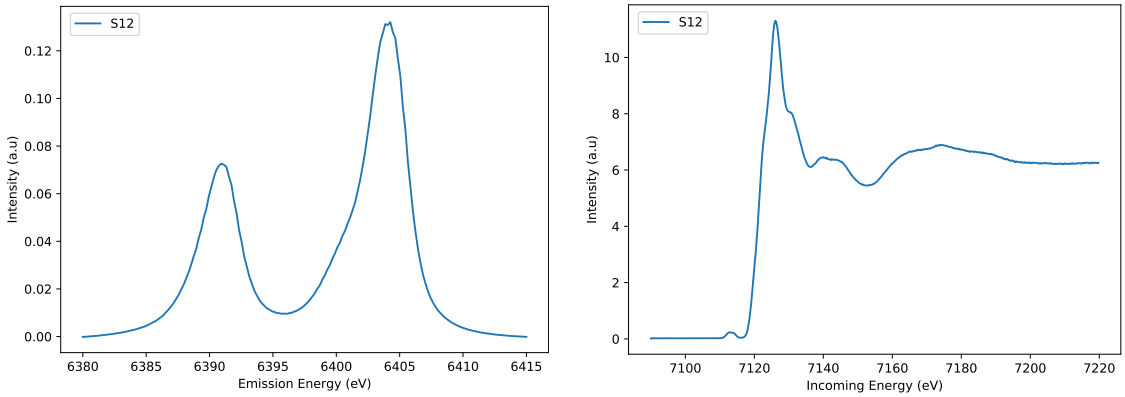

Figure A.33: **Left**: K_α emission spectrum of mineral denominated S12, the intensity is normalized first to intensity I02 and than to the area below the curve. **Right**: XANES spectrum of mineral denominate S12, the intensity is just normalized to the intensity I02.

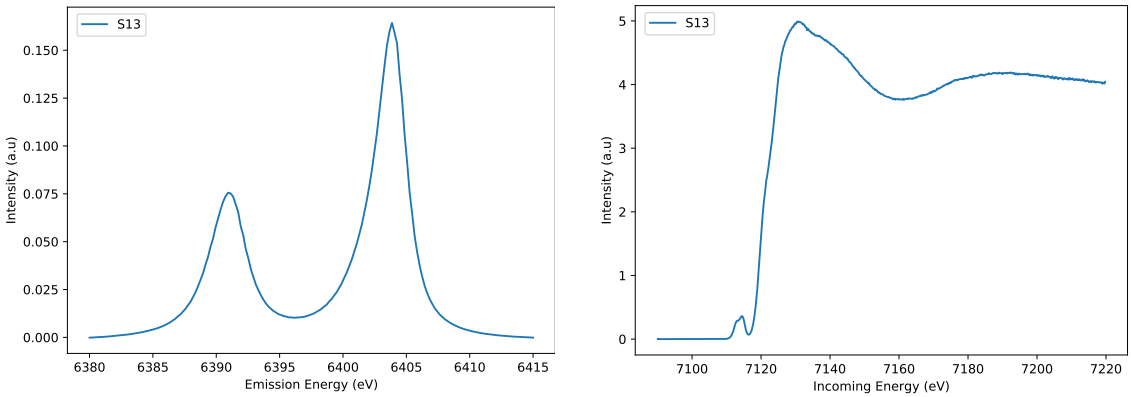

Figure A.34: **Left**: K_α emission spectrum of mineral denominated S13, the intensity is normalized first to intensity I02 and than to the area below the curve. **Right**: XANES spectrum of mineral denominate S13, the intensity is just normalized to the intensity I02.

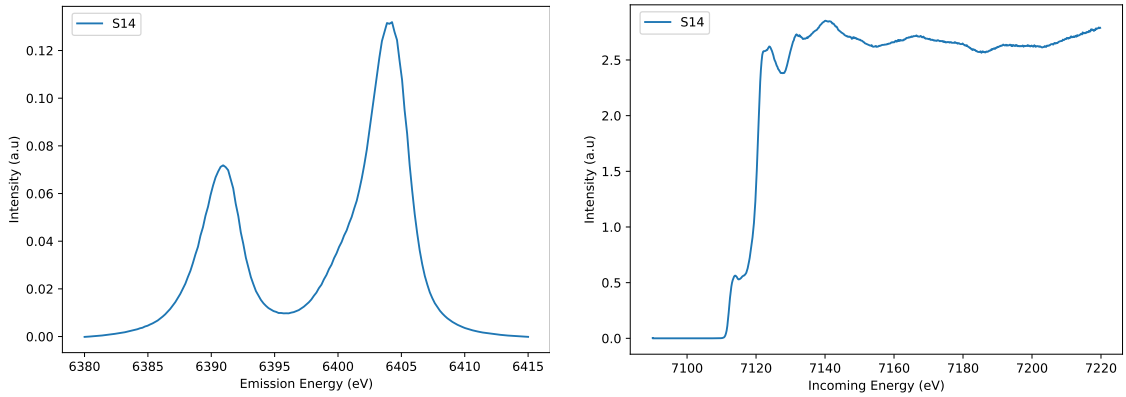

Figure A.35: **Left**: K_α emission spectrum of mineral denominated S14, the intensity is normalized first to intensity I02 and than to the area below the curve. **Right**: XANES spectrum of mineral denominate S14, the intensity is just normalized to the intensity I02.

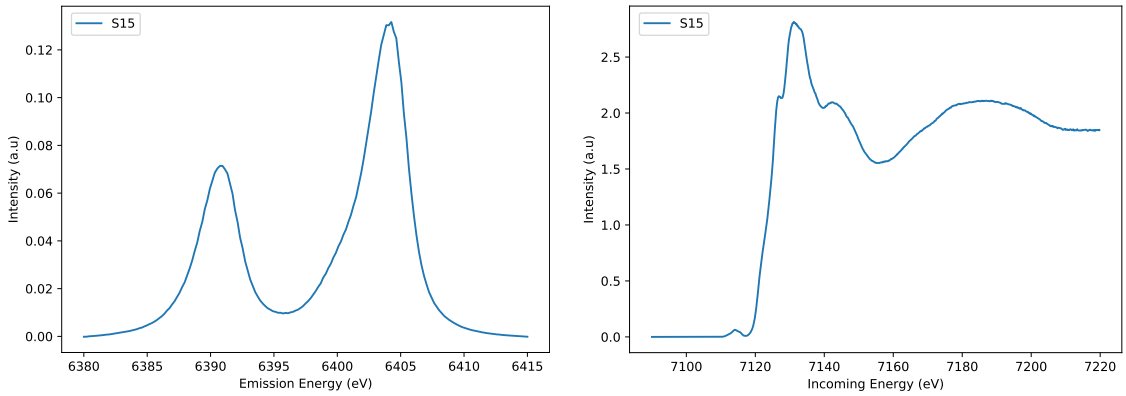

Figure A.36: **Left**: K_α emission spectrum of mineral denominated S15, the intensity is normalized first to intensity I02 and than to the area below the curve. **Right**: XANES spectrum of mineral denominate S15, the intensity is just normalized to the intensity I02.

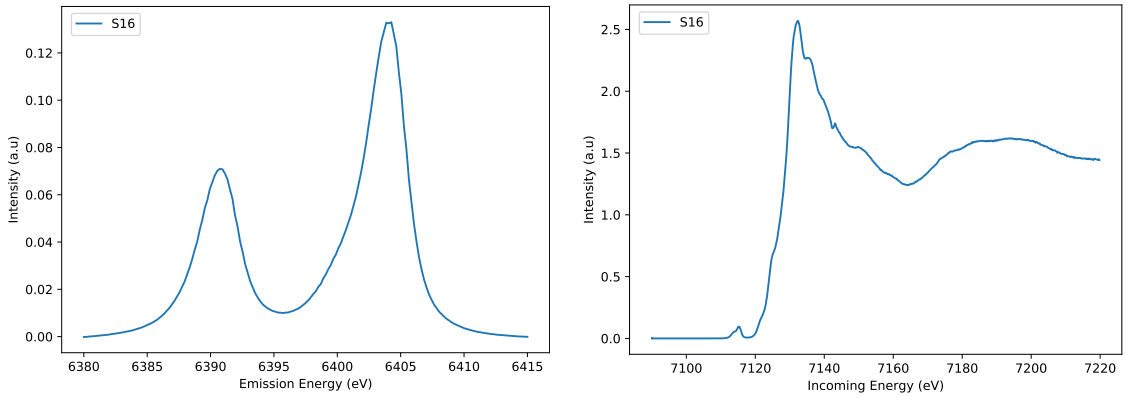

Figure A.37: **Left**: K_α emission spectrum of mineral denominated S16, the intensity is normalized first to intensity I02 and than to the area below the curve. **Right**: XANES spectrum of mineral denominate S16, the intensity is just normalized to the intensity I02.

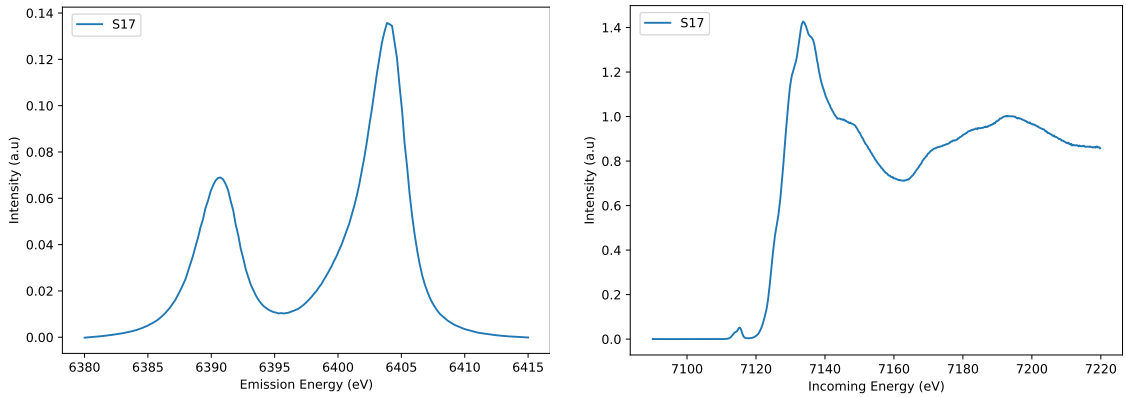

Figure A.38: **Left**: K_α emission spectrum of mineral denominated S17, the intensity is normalized first to intensity I02 and than to the area below the curve. **Right**: XANES spectrum of mineral denominate S17, the intensity is just normalized to the intensity I02.

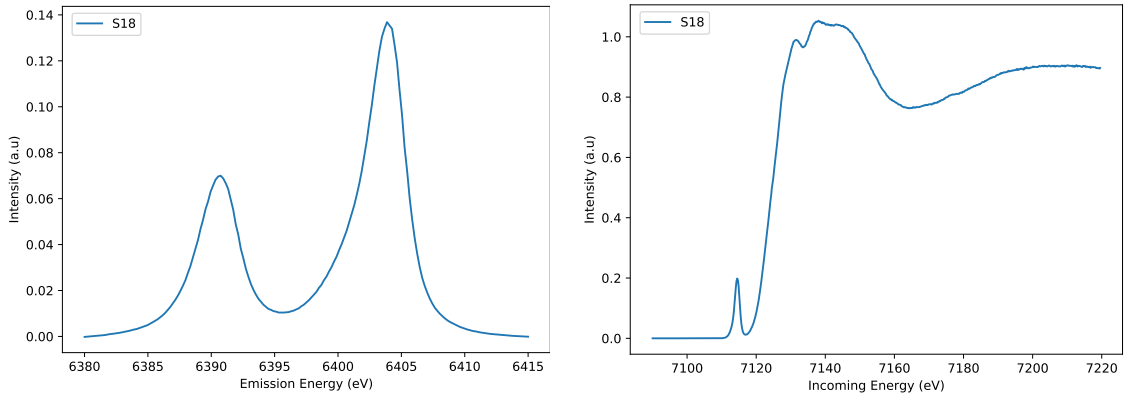

Figure A.39: **Left**: K_α emission spectrum of mineral denominated S18, the intensity is normalized first to intensity I02 and than to the area below the curve. **Right**: XANES spectrum of mineral denominate S18, the intensity is just normalized to the intensity I02.

List of Figures

List of Tables

Bibliography

[1] Joseph J. Larmor. 'On a dynamical theory of the electric and luminiferous medium'. In: *Philosophical Transactions of the Royal Society* 190 (1897), pp. 205–300.

[2] Helmut Wiedemann. 'Synchrotron radiation'. In: *Particle Accelerator Physics*. Springer, 2003, pp. 647–686.

[3] Jens Als-Nielsen and Des McMorrow. *Elements of modern X-ray physics*. John Wiley & Sons, 2011.

[4] K Codling. 'Atomic and Molecular Physics Using Synchrotron Radiation–the Early Years'. In: *Journal of synchrotron radiation* 4.6 (1997), pp. 316–333.

[5] Pantaleo Raimondi. 'ESRF-EBS: The extremely brilliant source project'. In: *Synchrotron Radiation News* 29.6 (2016), pp. 8–15.

[6] *ESRF website*. URL: `http://www.esrf.eu`.

[7] *SOLEIL website*. URL: `http://www.synchrotron-soleil.fr`.

[8] *RF cavities*. URL: `https://ebs.esrf.fr/`.

[9] Alberto Cereser. 'Nanofocused X-ray analysis of semiconductor nanowires'. PhD thesis. June 2011. DOI: `10.13140/2.1.2837.0728`.

[10] *ID26 Private Space*. URL: `https://confluence.esrf.fr/`.

[11] Pieter Glatzel et al. 'The five-analyzer point-to-point scanning crystal spectrometer at ESRF ID26'. In: *Journal of Synchrotron Radiation* 28.1 (2021).

[12] Jan Kern et al. 'Simultaneous femtosecond X-ray spectroscopy and diffraction of photosystem II at room temperature'. In: *Science* 340.6131 (2013), pp. 491–495.

[13] Sara Lafuerza et al. 'New reflections on hard X-ray photon-in/photon-out spectroscopy'. In: *Nanoscale* 12.30 (2020), pp. 16270–16284.

[14] Jean-Pascal Rueff and Abhay Shukla. 'Inelastic x-ray scattering by electronic excitations under high pressure'. In: *Reviews of Modern Physics* 82.1 (2010), p. 847.

[15] L Ducotté et al. 'Mechanical aspects of the ID26 emission spectrometer II: improving stability for a large instrument by the use of multiple air pad supports'. In: *Diamond Light Source Proceedings* 1.MEDSI-6 (2010).

[16] *Avalanche Photodiodes at ESRF*. URL: `https://www.esrf.fr/Apache_files/Conferences/APDWorkshop/Jean-Marie_Rigal.PDF`.

[17] R Ballabriga et al. 'The Medipix3 prototype, a pixel readout chip working in single photon counting mode with improved spectrometric performance'. In: *IEEE Transactions on Nuclear Science* 54.5 (2007), pp. 1824–1829.

[18] Uwe Bergmann and Pieter Glatzel. 'X-ray emission spectroscopy'. In: *Photosynthesis research* 102.2 (2009), pp. 255–266.

[19] *ALS. X-ray data booklet*. URL: `http://xdb.lbl.gov/`.

[20] Chikashi Suzuki et al. 'Electronic structures of 3d transition metal (Ti–Cu) oxides probed by a core hole'. In: *Chemical physics* 247.3 (1999), pp. 453–470.

[21] Kenjiro Tsutsumi and Hiroo Nakamori. 'X-ray K emission spectra of chromium in various chromium compounds'. In: *Journal of the Physical Society of Japan* 25.5 (1968), pp. 1418–1423.

[22] Xin Wang, Frank MF de Groot and Stephen P Cramer. 'Spin-polarized x-ray emission of 3 d transition-metal ions: a comparison via K α and K β detection'. In: *Physical Review B* 56.8 (1997), p. 4553.

[23] Pieter Glatzel, Roberto Alonso-Mori and Dimosthenis Sokaras. 'Hard x-ray photon-in/photon-out spectroscopy: instrumentation, theory and applications'. In: *X-Ray Absorption and X-Ray Emission Spectroscopy: Theory and Applications* 1 (2016).

[24] FMF De Groot et al. 'Charge transfer multiplet calculations of the K beta X-ray emission spectra of divalent nickel compounds'. In: *Journal of Physics: Condensed Matter* 6.34 (1994), p. 6875.

[25] Sara Lafuerza et al. 'Chemical Sensitivity of Kβ and Kα X-ray Emission from a Systematic Investigation of Iron Compounds'. In: *Inorganic Chemistry* 59.17 (2020), pp. 12518–12535.

[26] Andrea Carlantuono. 'X-ray Emission Spectroscopy to retrieve the local spin moment in 3d transition metal compounds'. 2016.

[27] Matteo Bianchini. 'Resonant X-Ray spectroscopy of fractal TiO_2 structures for photovoltaic applications'. 2012.